Universidad Autónoma de Madrid

Facultad de Ciencias

Departamento de Biología Molecular

"Control of genomic stability by APC/C-Cdh1 and therapeutic implications"

Manuel Eguren Fernández

Degree in Biology

Thesis Director:

Dr. Marcos Malumbres

Centro Nacional de Investigaciones Oncológicas (CNIO)

Madrid

Marcos Malumbres, Jefe de Grupo del laboratorio de División Celular y Cáncer del Centro Nacional de Investigaciones Oncológicas

CERTIFICA:

Que la tesis doctoral titulada “Control of genomic stability by APC/C-Cdh1 and therapeutic implications”, ha sido realizada en el Centro Nacional de Investigaciones Oncológicas y tutelada en el Departamento de Biología Molecular de la Universidad Autónoma de Madrid.

La tesis realizada por Manuel Eguren Fernández reúne todas las condiciones requeridas por la legislación vigente y la originalidad y calidad científica para poder ser presentada y defendida con el fin de optar al grado de Doctor.

Y para que conste donde proceda, firmo el presente certificado.

Madrid, a 29 de Agosto de 2013

Dr. Marcos Malumbres

A mis padres, a Lucía y a Sil

Summary

The E3-ubiquitin ligase APC/C-Cdh1 is essential for embryonic endoreduplication but its relevance in the mammalian mitotic cell cycle is still unclear. We show here that genetic ablation of Cdh1 in the developing nervous system results in hypoplastic brain, abnormal development of ependymal cells and hydrocephalus. These defects correlate with increased levels of multiple cell cycle regulators and increased entry into S-phase in neural progenitors, resulting in replicative stress. However, cell division is prevented in the absence of Cdh1 due to the activation the DNA damage response, induction of p53, G2 arrest and apoptotic death. Concomitant ablation of p53 rescues apoptosis but not replicative stress, resulting in premature death due to the presence of damaged neurons throughout the adult brain. Interestingly, partial inhibition of cyclin-dependent kinases (Cdks) rescues the replicative stress and the defective proliferation suggesting that Cdh1 loss results in DNA-damage-like response due to Cdk hyperactivation. In addition, by using a proteomic approach in Cdh1-null cells and mouse tissues, we have identified the kinesin Eg5 and topoisomerase 2α as APC/C-Cdh1 targets involved in the maintenance of genomic stability. The high levels of Eg5 in Cdh1-null cells are accompanied by partial resistance to Eg5 inhibitors such as monastrol. In contrast, Cdh1-null cells display a dramatic sensitivity to Top2α poisons currently used in cancer therapy as a consequence of increased levels of trapped Top2α-DNA complexes. Treatment of human cancer cells with APC/C inhibitors results in increased sensitivity to Top2α poisons revealing a new synthetic lethal interaction that could be used for the optimization of anticancer treatments. These data indicate that a) Inactivation of Cdh1 *in vivo* results in replicative stress, cell cycle arrest and cell death; and b) APC/C inhibition may have therapeutic use, not only by inhibiting Cdc20 leading to mitotic arrest, but also by altering the levels of Cdh1 substrates (such as Eg5 and Top2α). Thus, targeting the APC/C may result in differential responses (increased resistance or susceptibility) to specific therapeutic agents.

Resumen

La E3-ubiquitina ligasa APC/C-Cdh1 es esencial para la endoreduplicación durante el desarrollo embrionario, pero su relevancia en el ciclo celular mitótico de mamíferos todavía no está clara. La eliminación genética de Cdh1 específicamente en el sistema nervioso resulta en hipoplasia, desarrollo anormal de las células ependimarias e hidrocefalia. Estos defectos correlacionan con un incremento en niveles de reguladores del ciclo celular y en entrada en fase S en los progenitores neurales, que da lugar a estrés replicativo. En ausencia de Cdh1 estas células progenitoras no progresan en el ciclo debido a la activación de la respuesta a daño en el DNA, la inducción de p53, la parada en la fase G2 y la muerte celular programada (apoptosis). La eliminación de p53 previene la apoptosis de las células deficientes para Cdh1, pero no el estrés replicativo. Sin embargo, la inhibición parcial de la actividad de quinasas dependientes de ciclinas (Cdks) rescata el estrés replicativo y los problemas en proliferación, lo que sugiere que la acumulación de daño en el DNA en ausencia de Cdh1 se debe a la hiperactivación de las Cdks. Además, mediante técnicas proteómicas en células y tejidos deficientes para Cdh1, hemos identificado a la kinesina Eg5 y la topoisomerasa 2α como nuevos sustratos de APC/C-Cdh1 implicados en el mantenimiento de la estabilidad genómica. La acumulación de Eg5 en células donde se ha eliminado Cdh1 provoca una resistencia parcial al inhibidor de Eg5 monastrol. Por otro lado, las células deficientes para Cdh1 son especialmente sensibles al inhibidor de topoisomerasa etopósido, actualmente utilizado en tratamientos antitumorales. De hecho, el tratamiento de líneas tumorales humanas con un inhibidor de APC/C incrementa la sensibilidad a inhibidores de topoisomerasa 2. Estos datos muestran que: a) La inactivación de Cdh1 *in vivo* provoca estrés replicativo, parada del ciclo y muerte celular; and b) La inhibición de APC/C puede tener aplicaciones terapéuticas, no sólo a través de la inducción de parada en mitosis por bloqueo de la actividad de cdc20, sino también mediante el aumento de niveles de sustratos de Cdh1 (tales como Eg5 o Top2α) que modulan la respuesta a distintos tratamientos contra el cancer.

Contents

Summary 7

Resumen 11

Contents 15

List of Abbreviations 21

Introduction 25

1. APC/C: Composition, mechanism of action and regulation 28
2. APC/C functions in the cell cycle 32
   2.1. Exiting from mitosis 32
   2.2. Preventing unscheduled DNA replication and genomic instability 33
   2.3. APC/C-Cdh1 function in endocycles 39
3. APC/C beyond the cell cycle 41
   3.1. Coupling metabolic requirements with cell proliferation 41
   3.2. Cell-type specific functions of the APC/C 42
4. Relevance of the APC/C in cancer 46

Aim of the work 49

Material and Methods 53

1. Generation and Characterization of Mutant Mice 55
   1.1. Genotyping of the mutant mice 55
   1.2. Object recognition test 56
   1.3. Histology and immunohistochemistry (IHC) 56
   1.4. Molecular imaging 58
      1.4.1. Computerized axial tomography (CT Scan) 58
      1.4.2. Nuclear magnetic resonance (NMR) 58

Contents

2. Cell culture 58

2.1. Neural progenitor culture 58

2.1.1. Isolation and culture of neural progenitors 59

2.1.2. Self-renewal assay 59

2.1.3. Differentiation assay and immunofluorescence 60

2.1.4. Biochemical analyses of neural progenitors 60

2.2. Cortical neurons culture 61

2.3. Flow cytometry 61

2.4. MEFs isolation 61

2.5. Viral infections 62

2.6. Transfection / Nucleofection 62

2.7. Drugs 62

3. Biochemical procedures and Microscopy 62

3.1. Degradation and ubiquitination assays 62

3.2. Real-time reverse-transcription PCR (qRT-PCR) 63

3.3. Immunoblot (WB) 63

3.4. Cells and tissue immunofluorescence (IF) 64

3.5. Wholemount staining 64

3.6. High-throughput microscopy (HTM) 65

3.7. Videomicroscopy 66

4. Proteomic analysis 66

4.1. Stable isotope labeling by amino acids in cell culture (SILAC) 66

4.2. Isobaric tags for relative and absolute quantitation (iTRAQ) 67

5. Statistical analysis 68

Results 69

1. Physiological relevance of Cdh1 in the nervous system 71
1.1. Generation of mouse knockout for Cdh1 in the nervous system 71
1.2. Specific ablation of Cdh1 in the developing nervous system results in reduced cortical neurogenesis 72
1.3. Cdh1 ensures proper DNA replication in neural progenitors 79
1.4. Cdh1 modulates Cdk activity in neural progenitors preventing replicative stress 82
1.5. Cdh1 deficiency causes a DNA damage response leading to G2 arrest 87
1.6. The accumulation of DNA damage in Cdh1-null cells is p53-independent, but results in p53-dependent cell death 89
1.7. Hydrocephalus is accompanied by a cellular response to Cdh1 deficiency in ependymal cells 95

2. A search for new APC/C-Cdh1 substrates 101
2.1. Quantitative proteomics screens in Cdh1-null cells 101
2.2. Cdh1 controls the protein levels of Eg5 and Top2α in mouse and human cells 106

3. New therapeutic implications of inhibiting APC/C-Cdh1 111
3.1. Cdh1-dependent degradation of Eg5 modulates the response to Eg5 inhibitors 111
3.2. Genetic ablation of Cdh1 leads to increased susceptibility to topoisomerase poisons 115
3.3. Chemical inhibition of the APC/C sensitizes cells to topoisomerase poisons 119

Discussion 123

1. Relevance of Cdh1 in the cell cycle 125

2. Identification of new Cdh1 targets 129

3. Therapeutic implications of APC/C-Cdh1 inhibition 134

Conclusions 139

References 143

Annex 161

List of abbreviations

3M	Triple mutant
3v	Third ventricle
ActD	Actinomycin D
AMPAR	AMPA receptor
APC/C	Anaphase Promoting Complex/Cyclosome
AraC	β-D-arabinofuranoside
C3A	Active-Caspase 3
Cdh1^{ALA}	Cdh1 hyperactive/non phosphorylatable mutant
Cdk	Cyclin-dependent kinase
Cre	Cre Recombinase
CSF	Cerebrospinal fluid
CSF extract	Xenopus cytostatic factor-arrested egg extract
CT Scan	Computerized axial tomography
CHX	Cycloheximide
DOM	Duration of mitosis
DSB	Double Strand Break
E	Embryonic day
EdU	5-ethynyl-2'-deoxyuridine
EV	Empty vector
FDR	False discovery rate
γH2AX	Phosphorylated histone H2AX
Hdac6	Histone deacetylase 6
HTM	High-throughput microscopy
IF	Immunofluorescence
IHC	Immunohistochemistry
IP	Immunoprecipitation
iTRAQ	Isobaric tag for relative and absolute quantitation
lge	Lateral ganglionic eminence
lv	Lateral ventricle
LSL	Lox-STOP-Lox
MEFs	Mouse Embryonic Fibroblasts
MBP	Myelin basic protein
MCC	Mitotic Checkpoint Complex
MS	Mass spectrometry
nctx	Neocortex
P	Postnatal day
PBS+	PBS with 0.1% Triton X-100

pH3	Phosphorylated histone H3
pRb	Retinoblastoma protein
preRC	Pre-replicative complex
RT	Room temperature
SAC	Spindle Assembly Checkpoint
SCF	Skp1/Cullin/F-box protein complex
Scr	Scramble
SILAC	Stable isotope labeling by amino acids in cell culture
Top2	DNA topoisomerase 2
WB	Western Blot

Introduction

The eukaryotic cell cycle is tightly regulated through the control of the protein level and activity of critical enzymes. Whereas the expression of cell cycle regulators is controlled at the transcriptional level during early phases, proper progression throughout the cell division cycle also depends on the timely phosphorylation-dephosphorylation and ubiquitin-dependent degradation of critical proteins at specific stages, which ensure the proper and unidirectional transition between the different phases.

Within the proteolytic machinery, major E3 ubiquitin ligases that target proteins for proteasome-dependent degradation during the cell cycle include the SCF (Skp1/Cullin/F-box) protein complex and the Anaphase-promoting Complex/Cyclosome (APC/C) (Harper *et al.*, 2002; Cardozo and Pagano, 2004; Acquaviva and Pines, 2006; Peters, 2006). These complexes are responsible, in conjunction with other ubiquitination enzymes, of the addition of a polyubiquitin chain to substrate proteins that are then recognized by the 26S proteasome and degraded (Peters, 2006; Skaar and Pagano, 2009; Bassermann *et al.*, 2013). Whereas the SCF controls G1/S through G2/M transitions, the APC/C is responsible for targeting critical regulators for degradation during mitosis and G1 until its activity is inhibited at the G1/S transition.

1. APC/C: Composition, mechanism of action and regulation

The APC/C was identified in pioneer biochemical and genetic studies in 1995 as a catalytic activity required for degradation of cyclins, the activator subunits of the Cyclin-dependent kinases or Cdks, major kinases involved in progression through the different phases of the cell cycle. This large multimeric complex is composed by at least 13 different core subunits in addition to the regulatory coactivators (Figure 1; Table 1). Many of these proteins are present in two copies per complex and, therefore, the total number of subunits is close to 20 with a combined molecular mass of 1.2 MDa (Schreiber *et al.*, 2011).

Figure 1

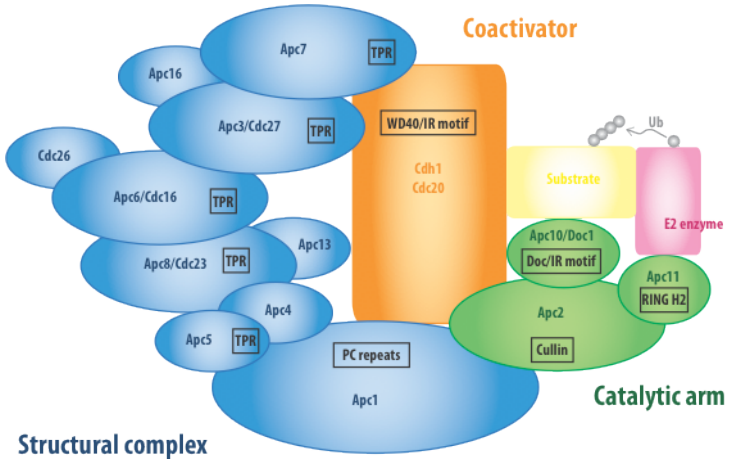

Schematic representation of the mammalian APC/C. The structural motifs of each subunit are shown in black boxes.

Substrate recognition by APC/C is based on complex mechanisms that determine its capability to ubiquitinate a large number of different substrates at specific phases of the cell cycle. Coactivators function as adaptors to recruit substrates to the APC/C by their capacity to recognize conserved APC/C degrons present in its substrates, such as D (destruction) box (Glotzer *et al.*, 1991; King *et al.*, 1996) and KEN box (Pfleger and Kirschner, 2000) motifs.

Table 1

S. cerevisiae	*H. sapiens*	Structural motif	Function
Structural subunits			
Apc1*	APC1	PC repeats	Scaffolding subunit
Cdc16*	APC6	TPR	Scaffolding subunit
Cdc27*	APC3	TPR	Cdh1/Apc10 binding
–	APC7	TPR	Cdh1/Apc10 binding
Apc4*	APC4	Unknown	Scaffolding subunit
Apc5*	APC5	Extended TPR	Scaffolding subunit
Cdc23*	APC8	TPR	Scaffolding subunit
Mnd2	–	Unknown	Ama1 inhibitor
Apc9	–	Unstructured	Cdc27 stabilising
Apc13/Swm1	APC13	Unstructured	Cdc23 stabilising
Cdc26	CDC26	Unstructured	Cdc16 stabilising
–	APC16	Unknown	Unknown
Catalytic arm			
Apc2*	APC2	Cullin homology	Scaffolding subunit
Apc10/Doc1*	APC10	Doc homology/IR motif	Substrate recognition
Apc11*	APC11	RING H2	E2-binding
Coactivators			
Cdc20*	CDC20	WD40/IR motif	
Cdh1*	CDH1	WD40/IR motif	
Ama1	–	WD40/IR motif	

Core and Regulatory Subunits of the APC/C. *Essential subunits.

Although, coactivators are solely responsible for KEN box recognition (Chao *et al.*, 2012), the D box degron is engaged by a bipartite co-receptor composed of both the cofactor and the APC/C subunit Doc1 (also known as Apc10) (Figure 2). Doc1 cooperates with the coactivator subunits to confer high-affinity D box binding and it is also implicated in processive substrate ubiquitination (Passmore *et al.*, 2003; Carroll *et al.*, 2005; Buschhorn *et al.*, 2011; da Fonseca *et al.*, 2011). The C-terminal WD40 domain in the coactivator mediates its interaction with the D box and KEN box degrons (Kraft *et al.*, 2005; Chao *et al.*,

2012), whereas its N-terminal C box stimulates APC/C catalytic activity (Kimata *et al.*, 2008; Labit *et al.*, 2012).

Figure 2

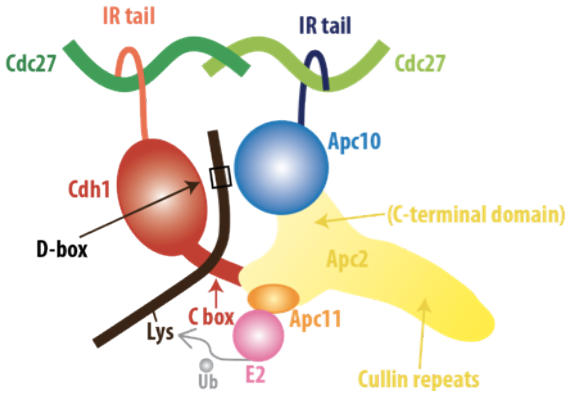

Substrate recognition by APC/C. Adapted from (da Fonseca *et al.*, 2011).

Apc11, a RING domain subunit tightly associated with the cullin subunit Apc2, binds the E2 enzymes and confers the catalytic activity to the APC/C. Toghether with the coactivtator, Apc2, Apc11 and Doc1 subunits constitute the catalytic and substrate recognition module of the complex, which account for less than 20% of the overall APC/C mass. The other components of the complex, provide scaffolding functions, coordinating the organization of the subunits that form the catalytic and substrate recognition module and also mediating interactions with other proteins and complexes such as the mitotic checkpoint complex (Herzog *et al.*, 2009).

APC/C activity is tightly controlled through the cell cycle and the processes underlying its regulation are exerted mostly through its coactivators, either Cdc20 or Cdh1, which interact only transiently with the APC/C and recruit specific substrates to the complex. Therefore, the regulation of these interactions is a key event that defines the timing of APC/C activation.

Cdc20 is expressed during DNA synthesis (S-phase), G2 and mitosis; however, it can only bind to the APC/C when several subunits of this complex have been phosphorylated by mitotic kinases. APC/C-Cdc20 is essential for anaphase onset driving mitotic exit by targeting cyclin B and securin for destruction thus promoting the activation of separase and sister chromatid segregation and resulting in decreased Cdk activity (Peters, 2006). On the contrary, Cdh1 phosphorylation by Cyclin-dependent kinases (Cdks) during S-phase, G2 and mitosis impairs its binding to the APC/C. During mitotic exit, the inactivation of Cdks and subsequent activation of mitotic exit phosphatases allows Cdh1 dephosphorylation and binding to the APC/C, thereby replacing Cdc20. APC/C-Cdh1 complexes complete Cdk1 inactivation through targeting mitotic cyclins for destruction and triggers the ubiquitination of many other cell cycle regulators such as mitotic kinases or some of their regulators (Plk1, Aurora A, B, Tpx2, etc.), thus preventing the accumulation of these proteins during the following G1 phase and the subsequent unscheduled entry into S-phase (Peters, 2006; Garcia-Higuera *et al.*, 2008; Eguren *et al.*, 2011). Finally, APC/C-Cdh1 also targets Cdc20 for degradation favoring the complete switch from APC/C-Cdc20 to APC/C-Cdh1 during the exit from mitosis (Peters, 2006; Thornton and Toczyski, 2006; Yu, 2007; Manchado *et al.*, 2010a). Thus, Cdks and the APC/C regulate each other during cell cycle progression, and the reciprocal control between them modulates protein levels and activity of major regulators of the cell division cycle allowing the proper transitions between DNA replication and mitosis.

In addition, regulation of APC/C activity is also associated with inhibition of substrate recognition by Cdc20 and Cdh1 through regulatory proteins or complexes with pseudosubstrate inhibitory motifs that interact with degron recognition sites on coactivators. One of these inhibitors, is the effector of the spindle assembly checkpoint, a complex composed of Cdc20, Mad2, Mad3/BubR1, and Bub3 and referred as the mitotic

checkpoint complex (MCC) (Musacchio and Salmon, 2007; Kim and Yu, 2011). This complex prevents KEN box dependent substrate recognition by blocking the KEN box recognition site of Cdc20 with a KEN box motif in Mad3/BubR1 (Burton and Solomon, 2007; King *et al.*, 2007; Sczaniecka *et al.*, 2008; Malureanu *et al.*, 2009; Chao *et al.*, 2012). The formation of the D box co-receptor is also disrupted by displacing Cdc20, and consequently preventing D box recognition (Herzog *et al.*, 2009; Chao *et al.*, 2012). Moreover, the vertebrate protein Emi1 inhibits the APC/C by means of its conserved D box and a zinc-binding region. These domains provide strong APC/C-binding affinity and antagonize APC/C E3 ligase activity by blocking substrate binding (Miller *et al.*, 2006).

2. APC/C functions in the cell cycle

2.1. Exiting from mitosis

In multicellular organisms such as mammals, most adult cells do not divide and are maintained in a state known as quiescence. When these cells re-enter into the cell cycle, they need to synthesize most of the proteins required for cell cycle progression; i.e. the factories involved in DNA replication and the structures and regulators involved in chromosome segregation. Most of the control of the cell cycle during these early phases therefore relies on the regulation of transcription. Entry into the cell cycle depends on the activation of Cdks and the subsequent inactivation of the retinoblastoma protein (pRb), a general repressor of the transcription of many cell cycle genes (Malumbres and Barbacid, 2001).

To be able to decide whether to continue cycling or to exit to quiescence, cells need to eliminate the cell cycle machinery synthesized during G1/S/G2. APC/C-Cdc20 first drives the exit from mitosis by targeting securin and mitotic cyclins for degradation, thus resulting in

the necessary inactivation of mitotic Cdk (Figure 3) (Peters, 2006). Cdh1 also contributes to mitotic exit by targeting mitotic cyclins, although this cofactor is not essential at this stage (Garcia-Higuera *et al.*, 2008; Li *et al.*, 2008). In addition, Cdh1 targets many other cell cycle regulators for degradation. First, several components of the mitotic machinery such as Plk1, Aurora kinases, Tpx2, Bub1, Cdc20 or Sgo1 among others, are eliminated during mitotic exit in an APC/C-Cdh1 dependent manner (Figure 3) (Garcia-Higuera *et al.*, 2008; Li *et al.*, 2008). Many of these proteins have important roles in chromosomal segregation and cytokinesis, and its degradation may be critical to maintain chromosomal integrity (Carmena and Earnshaw, 2003; Lindon and Pines, 2004; Wasch and Engelbert, 2005; Carter *et al.*, 2006; Malumbres and Barbacid, 2009). Indeed, in Cdh1-deficient cells these mitotic substrates accumulate and cells re-enter into a new cell cycle with increased levels of these mitotic regulators. Whether this leads to a defective cell cycle exit and cytokinesis is not clear since mitotic exit occurs normally in the presence of APC/C-Cdc20 despite the lack of degradation of these mitotic regulators (Garcia-Higuera *et al.*, 2008; Li *et al.*, 2008). Yet, since Cdh1-null cells accumulate genomic aberrations, it is possible that the excess of these proteins may result in abnormal chromosome segregation in the following mitotic cycles.

2.2. Preventing unscheduled DNA replication and genomic instability

In normal cells, the mitogen-dependent accumulation of G1 cyclins and Cdk activity results in the inactivation of the pRb pathway and the transcription of genes required for DNA synthesis (Malumbres and Barbacid, 2001). In order to properly regulate DNA replication, cells need to alternate between periods of low Cdk activity and low geminin levels, in which the pre-replicative complexes (preRCs) are assembled (licensing); and periods of high Cdk activity and high geminin levels, in which origin firing and DNA

Figure 3

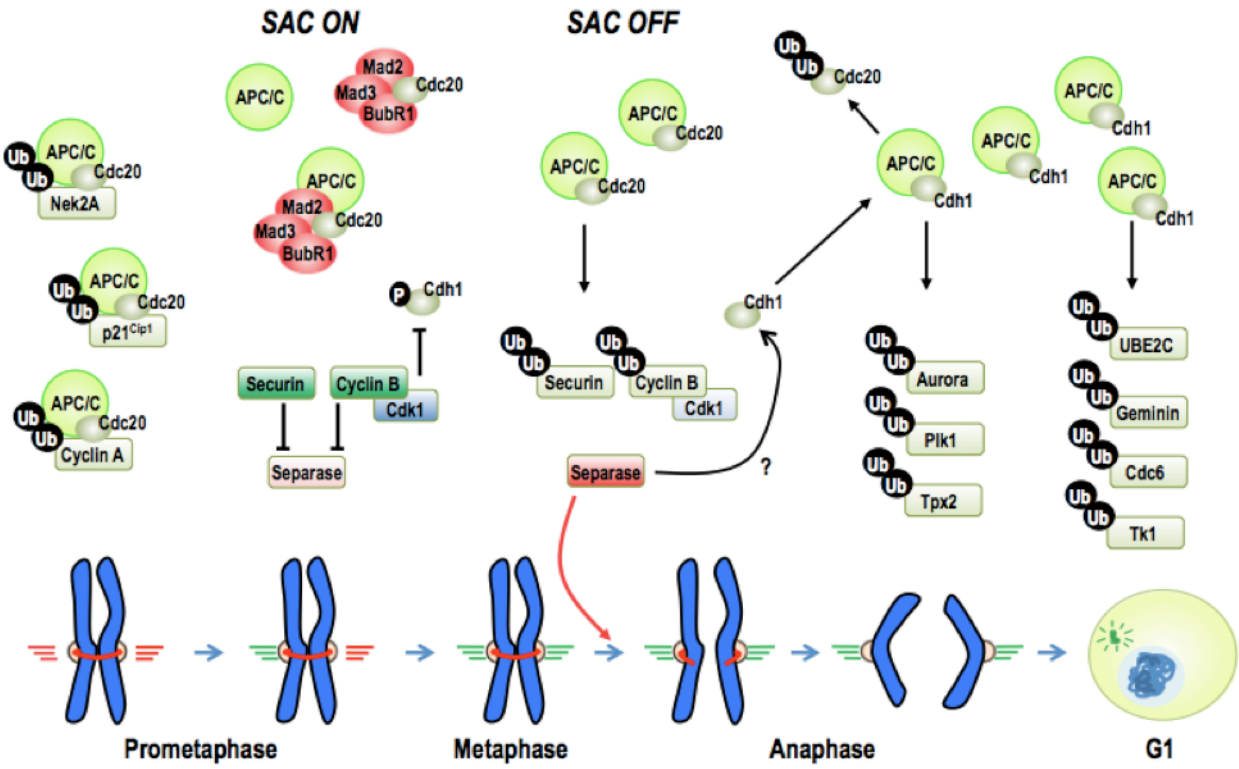

APC/C functions in mitosis. During the early stages of mitosis, APC/C-Cdc20 ubiquitinates several substrates such as Nek2A, Cyclin A and p21Cip1 promoting their degradation. Yet, in response to unattached kinetochores, the Spindle Assembly Checkpoint (SAC) is active and the APC/C is inhibited by sequestering of Cdc20 or non-fucntional APC/C-Cdc20 complexes also containing Mad2, Mad3 and BubR1. In these conditions, securin and cyclin B-Cdk1 function as inhibitors of separase. Once all chromosomes are bi-orientated on metaphase plate the SAC is extinguished resulting in APC/C-Cdc20 activation. APC/C-Cdc20 targets cyclin B1 and securin for degradation allowing separase activity, which cleaves the centromere cohesin complex leading to anaphase onset. In yeast, separase activation leads to dephosphorylation of Cdh1 although this pathway is not well established in mammals (question mark). The newly formed APC/C-Cdh1 complexes participate in mitotic exit by targeting for destruction Plk1, Aurora A or Tpx2 among other substrates as well as Cdc20 itself. During G1 phase, APC/C-Cdh1 maintains low levels of Cdk activity by targeting A- and B-type cyclins, among other Cdk regulators. In addition, APC/C-Cdh1 targets several regulators of DNA replication such as Geminin or Cdc6. Following the degradation of its substrates in G1, the APC catalyzes the autoubiquitination of its own E2 ubiquitin-conjugating enzyme UBE2C/UbcH10, leading to the stabilization of cyclin A, activation of Cdks and APC/C-Cdh1 inactivation.

replication occurs (Figure 4A) (Diffley, 2004; Blow and Dutta, 2005). APC/C-Cdh1 is crucial to properly regulate the switch between these two states.

During G1, the active APC/C-Cdh1 complexes keep low Cdk activity by two different mechanisms. On one hand, APC/C-Cdh1 directly targets mitotic cyclins (A/B types) for degradation and maintains this function during G1 (Brandeis and Hunt, 1996; Irniger and Nasmyth, 1997; Wasch and Cross, 2002). On the other hand, APC/C-Cdh1 also eliminates the Cdk activator Cdc25A as well as Skp2 and Cks1, two cofactors of the SCF E3 ubiquitin ligase. In the presence of Cdh1, SCF activity is low allowing the accumulation of Cdk inhibitors of the Cip/Kip family (p21Cip1, p27Kip1 and p57Kip2) (Bashir *et al.*, 2004; Wei *et al.*, 2004). These alterations result in Cdk inhibition, which is required for the formation of the preRC and the subsequent loading of MCM complexes onto chromatin by ORC, Cdc6 and Cdt1 (Figure 4A) (Diffley, 2004; Blow and Dutta, 2005). APC/C-Cdh1 also ubiquitinates the inhibitor of Cdt1, Geminin. The oscillation in geminin levels is necessary for the proper regulation of the loading of MCM complexes and to avoid re-duplication events (McGarry and Kirschner, 1998; Wohlschlegel *et al.*, 2000).

The accumulation of mitogenic signaling during G1 leads to the activation of G1 Cdks such as Cdk4 or Cdk2 (Malumbres and Barbacid, 2001). At the G1-S transition, Cdh1 is inactivated by inhibitory phosphorylation by active Cdks and binding to Emi1, a protein that inhibits the APC/C acting as a pseudosubstrate (Figure 4A) (Zachariae *et al.*, 1998; Reimann *et al.*, 2001; Rape and Kirschner, 2004; Miller *et al.*, 2006; Williamson *et al.*, 2009). In addition, APC/C-dependent ubiquitination is also prevented at this stage by degradation of its E2 enzymes UbcH10 and Ube2S (Rape and Kirschner, 2004; Williamson *et al.*, 2009). The increase in Cdk activity and geminin levels then allows the firing of DNA replication origins (Figure 4A). The temporal separation between these processes, DNA licensing and firing,

guarantees that the origins are only fired once per cycle and, therefore, re-replication is prevented.

Figure 4

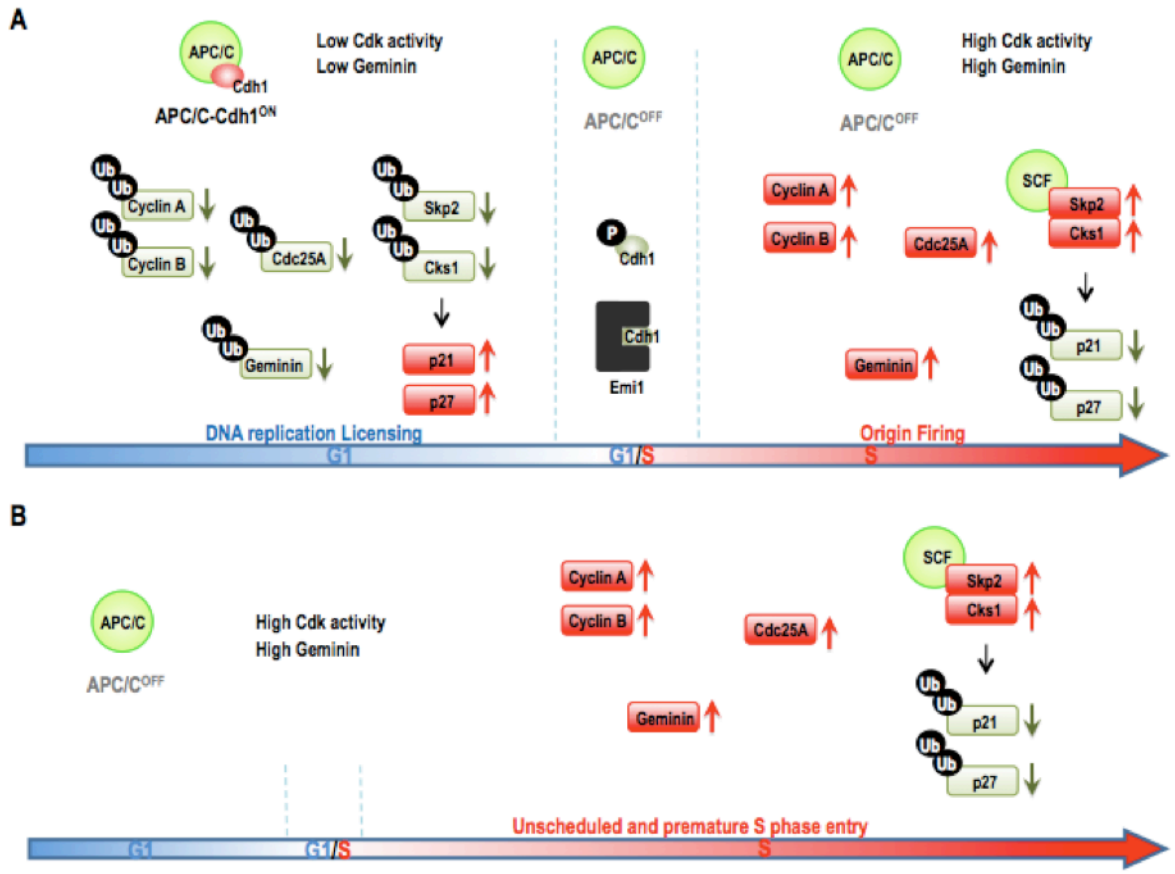

APC/C-Cdh1 function during G1 and the G1/S transition. (**A**) Normal progression throughout the initial phases of the cell cycle in the presence of Cdh1. During G1, APC/C-Cdh1 degrades geminin as well as other targets finally resulting in reduced Cdk activity. This allows the assembly of pre-replication complexes and DNA replication licensing. In response to mitogenic stimuli, the APC/C is inactivated by Cdk-dependent phosphorylation of Cdh1, binding to the pseudosubstrate Emi1, and degradation of E2 enzymes (not shown). This results in increased geminin levels and Cdk activity thus allowing the onset of DNA replication. (**B**) In the absence of Cdh1, the persistent Cdk activity and the continuous inhibition of Cdt1 by geminin prevents a correct formation of pre-replication complexes, thus leading to premature entry into S phase. This likely results in abnormal DNA replication and genome instability.

The accumulation of mitogenic signaling during G1 leads to the activation of G1 Cdks such as Cdk4 or Cdk2 (Malumbres and Barbacid, 2001). At the G1-S transition, Cdh1 is inactivated by inhibitory phosphorylation by active Cdks and binding to Emi1, a protein that inhibits the APC/C acting as a pseudosubstrate (Figure 4A) (Zachariae *et al.*, 1998; Reimann *et al.*, 2001; Rape and Kirschner, 2004; Miller *et al.*, 2006; Williamson *et al.*, 2009). In addition, APC/C-dependent ubiquitination is also prevented at this stage by degradation of its E2 enzymes UbcH10 and Ube2S (Rape and Kirschner, 2004; Williamson *et al.*, 2009). The increase in Cdk activity and geminin levels then allows the firing of DNA replication origins (Figure 4A). The temporal separation between these processes, DNA licensing and firing, guarantees that the origins are only fired once per cycle and, therefore, re-replication is prevented.

The relevance of APC/C-Cdh1 during G1 and the G1/S transition has been explored by loss-of-function studies in mammals. Loss of the APC/C core subunit Apc2 leads to unscheduled proliferation in hepatocytes, even in the absence of proliferative stimuli, suggesting a critical role for the APC/C in maintaining quiescence in these cells (Wirth *et al.*, 2004). Absence of Cdh1 results in a shorter G1 phase and early entry into S phase due to a premature increase in the levels of cyclins that lead to Cdk activation (Figure 4B) (Engelbert *et al.*, 2008; Garcia-Higuera *et al.*, 2008; Li *et al.*, 2008; Sigl *et al.*, 2009). In Cdh1-depleted cells, the shortening of G1 phase goes along with a prolonged and defective S phase (Garcia-Higuera *et al.*, 2008; Li *et al.*, 2008; Sigl *et al.*, 2009). Loss of Cdh1 function impairs the loading of MCM complexes onto chromatin and the formation of preRCs at the replication origins. In addition, the increase in geminin levels and untimely Cdk activation is likely to favor DNA synthesis (Figure 4B). The precocious initiation of DNA synthesis without the proper machinery leads to a slower S phase progression, which could result in stalled replication forks and under-replicated DNA. These replicative defects, as well as the

upregulation of mitotic kinases, can finally lead to genetic damage (Garcia-Higuera *et al.*, 2008). Thereby, this early and unscheduled entry into S phase generates some levels of genomic instability and a DNA damage response, with the activation of p53-p21Cip1 pathway (Engelbert *et al.*, 2008; Sigl *et al.*, 2009). Yet, these deficiencies in replication together with the alterations during mitotic exit are not sufficient to stop cell cycle progression, and Cdh1-deficient cells proliferate and accumulate a variety of genomic aberrations (Engelbert *et al.*, 2008; Garcia-Higuera *et al.*, 2008).

Another important role of the APC/C during these stages of the cell cycle is the destruction of two key enzymes in dTTP formation: Thymidine kinase 1 (TK1) and Thymidylate kinase (TMPK) during G1 (Ke and Chang, 2004; Ke *et al.*, 2005). The inactivation of APC/C-Cdh1 at the G1-S transition, together with the transcriptional activation of these kinase genes during G1 (Coppock and Pardee, 1987; Sherley and Kelly, 1988), allows the expansion of the dTTP pool necessary for DNA replication. Disruption of the normal degradation of TK1 and TMPK in Cdh1-deficient cells results in a severe imbalance in the dNTP pool, and an increased rate in gene mutation since fidelity of DNA synthesis is compromised (Ke *et al.*, 2005). Moreover, APC/C-Cdh1 also targets for degradation the ribonucleotide reductase R2 (Rrm2), an enzyme that catalyzes the reduction of ribonucleotides to deoxyribonucleotides, providing the precursors necessary for DNA synthesis and preventing unscheduled DNA synthesis (Chabes *et al.*, 2003). In summary, APC/C-Cdh1 plays critical roles in maintaining G1 phase and controlling the onset of DNA replication, thus protecting chromosomal integrity.

2.3. APC/C-Cdh1 function in endocycles

Whereas Cdh1 is dispensable for the normal mitotic cycle in yeast, Caenorhabditis elegans, Drosophila melanogaster and mammals (Schwab *et al.*, 1997; Visintin *et al.*, 1997; Yamaguchi *et al.*, 1997; Kitamura *et al.*, 1998; Fay *et al.*, 2002; Garcia-Higuera *et al.*, 2008; Li *et al.*, 2008; Sigl *et al.*, 2009), this cofactor is required for an alternative cell cycle that consists of repeated rounds of DNA replication without cell division (endoreduplication or endocyle). Certain cell types perform this process in order to increase cell size and ploidy. Endoreduplication also requires an oscillation between low Cdk activity periods, in which licensing is allowed leading to pre-RC assembly, and high Cdk activity periods in which origin firing takes place initiating S phase. This oscillation is allowed by APC/C-Cdh1 and different Cdk inhibitors (Figure 5) (Zielke *et al.*, 2008).

In Drosophila, endocycles are needed for cell and organism growth. Many tissues undergo endoreduplication during embryogenesis and even in the adult. Different studies in Drosophila have shown that APC/C-Cdh1 activity is required not only for the switch from mitotic cycle to endocycle, but also for maintaining the endocycle during oogenesis or in specific cells of the salivary glands (Sigrist and Lehner, 1997; Edgar and Orr-Weaver, 2001; Schaeffer *et al.*, 2004). In flies, the transition from mitotic to endoreduplication cell cycle is controlled by the activation of Notch during G2, suppressing mitosis by keeping low Cdk activity. Activation of Notch leads to down-regulation of the protein phosphatase String/Cdc25, subsequent reduced Cdk1 activity, and reduced phosphorylation of Cdh1. This results in the activation of APC/C-Cdh1 which, in turn, promotes the degradation of A/B mitotic cyclins and geminin (Schaeffer *et al.*, 2004; Shcherbata *et al.*, 2004; Narbonne-Reveau *et al.*, 2008; Zielke *et al.*, 2008). All these processes inactivate Cdk1 and allow the formation of pre-RCs. In these cells, the oscillation of Cyclin E-Cdk2 activity drives the endocycle inactivating APC/C-Cdh1 by phosphorylation and allowing a new S-phase

(Narbonne-Reveau *et al.*, 2008). In plants, overexpression of ccs52, the Cdh1 ortholog, correlates with endoreduplication and cell enlargement whereas its absence leads to reduced ploidy in alfalfa endoreduplicating cells, without affecting diploid cells (Cebolla *et al.*, 1999).

Figure 5

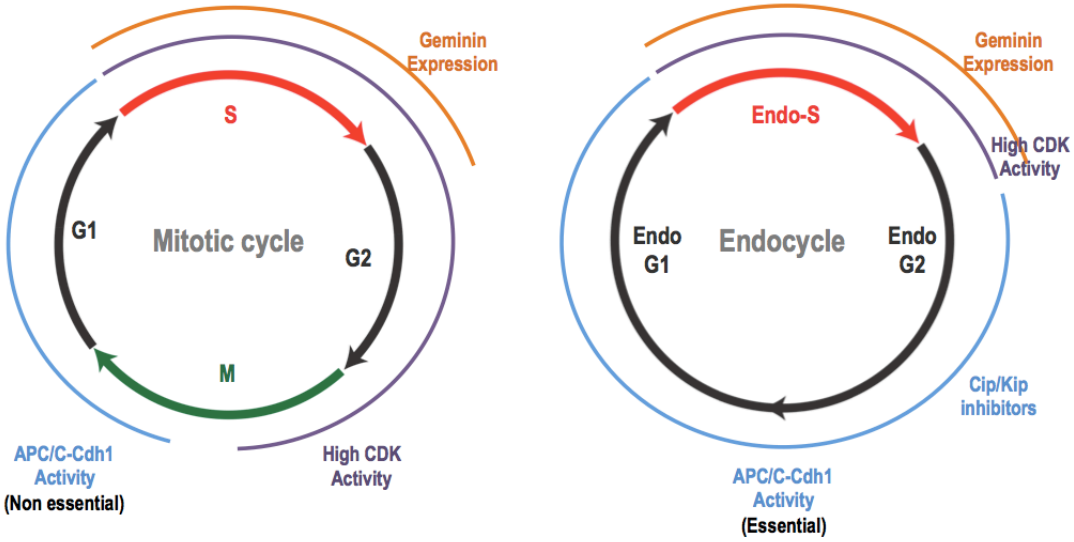

Oscillations in Cdk and APC/C-Cdh1 activity during the mitotic cycle or in endocycles. In a normal mitotic cycle, APC/C-Cdh1 is inactive from the G1/S transition to anaphase, allowing the activation of Cdk1 complexes during G2 in preparation for mitosis. During endocycles, APC/C-Cdh1 is re-activated after S phase resulting in reduced Cdk activity, thereby preventing the entry into mitosis. The presence of Cip/Kip inhibitors after S-phase also helps to prevent Cdk1 activation during the "endo G2". In this situation, the S phase alternates with G phases, and chromosome segregation is prevented resulting in increased ploidy. In both cycles, geminin prevents the formation of pre-replicative complexes once the origins have been fired during S phase.

In mammals, the availability of specific Cdk inhibitors such as p57Kip1 and p21Cip1 seems to be critical in regulating endoreduplication (Figure 5). During embryonic development, the differentiation of trophoblast stem cells into giant cells is triggered by p57Kip2-dependent inhibition of Cdk1 activity (Ullah *et al.*, 2008). In these conditions, cells undergo repeated rounds of endoreduplication maintained by fluctuations in Cyclin E-Cdk2 and APC/C-Cdh1 activities, as well as protein levels of Cdk inhibitors (Figure 5). APC/C-Cdh1

not only targets mitotic cyclins and geminin for degradation, but it also eliminates Skp2 (Bashir *et al.*, 2004; Wei *et al.*, 2004), avoiding the degradation of p57Kip2 and p27Kip1 by the SCF-Skp2 complex. Accordingly, recent studies in mammals have shown that lack of Cdh1 leads to underdeveloped trophoblast giant cells that display a reduced ploidy (Garcia-Higuera *et al.*, 2008; Li *et al.*, 2008). In fact, genetic ablation of Cdh1 results in embryonic lethality due to placental defects and this lethality can be rescued by specific ablation of Cdh1 in the embryo but not in the placenta (Garcia-Higuera *et al.*, 2008). These results suggest that vertebrate cells display strong requirements for Cdh1 to regulate Cdk fluctuations during endocycles, and to uncouple S phase from mitosis to allow the increase in ploidy required in specific tissues.

3. APC/C beyond the cell cycle

3.1. Coupling metabolic requirements with cell proliferation

Proliferating cells have a higher metabolic rate than quiescent cells. Early observations suggested that antioxidant treatment of cells induced cell cycle defects characterized by lack of accumulation of mitotic cyclins due to constant APC/C-Cdh1 activity (Havens *et al.*, 2006). The links between metabolism and the APC/C were strengthened with the identification of metabolic enzymes as direct targets of this ubiquitin ligase. APC/C-Cdh1 targets the glycolysis-promoting enzyme Pfkfb3 (6-phosphofructo-2-kinase/fructose-2,6-bisphosphatase-3) for degradation in different cell types as well as neoplastic and non-neoplastic cell lines. This enzyme catalyzes the generation of fructose-2,6-bisphosphate (F2,6P2) and the promotion of glycolysis. The Cdh1-mediated degradation of Pfkfb3 results in down-regulation of glycolysis, favoring the pentose phosphate pathway and the subsequent use of glucose to maintain the antioxidant status of the cells at the expense of

its utilization for bioenergetic purposes (Herrero-Mendez *et al.*, 2009; Almeida *et al.*, 2010; Colombo *et al.*, 2010).

Glutaminase, a critical enzyme in glutaminolysis, is also a substrate of APC/C-Cdh1 in human lymphocytes (Colombo *et al.*, 2010). This enzyme catalyzes the first reaction in the conversion of glutamine into lactate. Glutamine and glucose are essential to provide metabolic intermediaries and cover the energetic requirements of cells (DeBerardinis *et al.*, 2007). Upon APC/C-Cdh1-mediated degradation of glutaminase, the glutaminolysis is inhibited, and the formation of metabolites required for cell proliferation is prevented. Inactivation of APC/C-Cdh1 at the G1-S transition, results in increased levels of glutaminase thus supplying cells with the energy and metabolic components required for synthesis of macromolecules and eventual progression through the cell cycle. The regulation of APC/C-Cdh1 is therefore critical for linking cell proliferation with increased glycolysis and glutaminolysis (Almeida *et al.*, 2010), two processes highly active in proliferating cells.

3.2. Cell-type specific functions of the APC/C

Since the pioneer studies on the expression of APC/C subunits in mammals, it was evident that this complex is not only expressed in proliferating cells. Whereas the expression of Cdc20 is more restricted, Cdh1 is highly expressed in terminally differentiated cells such as neurons or other cell types (Figure 6) (Gieffers *et al.*, 1999).

In muscle, APC/C-Cdh1 drives cell differentiation through the destruction of two proteins, Skp2 and Myf5 (Li *et al.*, 2007b). Elimination of Skp2 leads to the accumulation of the Cdk inhibitors p21Cip1 and p27Kip1 in myoblasts, allowing the withdrawal of these cells from the cell cycle. In addition, degradation of Myf5, a bHLH transcription factor involved in

myogenesis, facilitates the myogenic fusion, a process required for myoblast differentiation (Li *et al.*, 2007b).

Figure 6

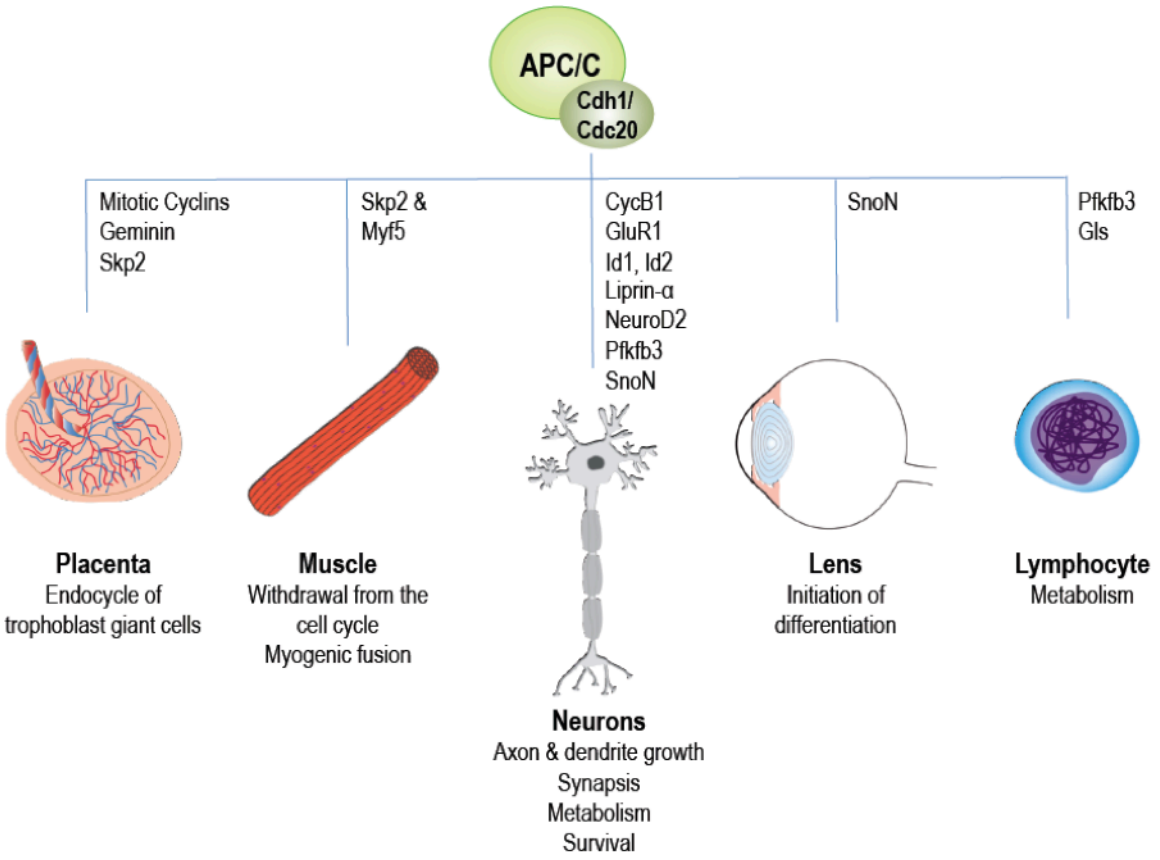

Tissue-specific functions of the APC/C. The APC/C is involved in the differentiation and function of different tissues such as placenta, muscle, and the hematopoietic or the nervous systems. Most of these functions are mediated by Cdh1, although Cdc20 may also be involved in neuron differentiation. Some of the critical APC/C substrates involved in these functions are indicated.

APC/C-Cdh1 has also been identified as a crucial regulator of lens differentiation by facilitating SnoN degradation (Wu *et al.*, 2007). Cdh1 is able to form a quaternary complex with SnoN, Smad3 and the APC/C; and SnoN is targeted for degradation in an APC/C-dependent manner in response to TGF-β signaling (Stroschein *et al.*, 2001; Wan *et al.*, 2001). SnoN is a repressor of the Cdk inhibitors p15INK4a and p21Cip1, and its APC/C-Cdh1-dependent degradation leads to the upregulation of these inhibitors which is necessary for coupling cell cycle withdrawal in response to TGF-β signaling and the initiation of lens

differentiation. Cdh1 depletion attenuates the induction of p15INK4a and p21Cip1 and significantly blocks lens differentiation (Wu *et al.*, 2007).

Although our knowledge on the involvement of APC/C-Cdh1 in the differentiation of other tissues is more limited, its critical function in the degradation of cell cycle proteins is likely to play relevant roles in linking quiescence and differentiation in many other cell types.

Perhaps more unexpectedly, several studies during the last years have demonstrated that the APC/C is particularly important in postmitotic neurons at different levels (Figure 6). Several core subunits of the APC/C are expressed in postmitotic terminally differentiated neurons and these proteins are tightly associated to Cdh1 (Gieffers *et al.*, 1999). In these cells, APC/C-Cdh1 maintains low levels of cyclin B in order to avoid an inappropriate entry into the cell cycle that could lead to apoptosis thus participating in the survival of these differentiated cells (Almeida *et al.*, 2005).

In addition, pioneer studies of Cdh1 depletion by RNA interference in primary cerebellar granule neurons *ex vivo* led to the identification of a relevant function of the APC/C in axonal growth and patterning (Konishi *et al.*, 2004). APC/C-Cdh1 directs these processes through the degradation of two nuclear proteins, SnoN and Id2 (Konishi *et al.*, 2004; Lasorella *et al.*, 2006; Stegmuller *et al.*, 2006). The TGF-β signaling pathway is basally activated in neurons resulting in APC/C-Cdh1-dependent degradation of SnoN (Stegmuller *et al.*, 2006). SnoN interacts with the transcriptional coactivator p300 and modulates the expression of Ccd1, a protein enriched at axon terminals that activates the growth promoting kinase JNK (Ikeuchi *et al.*, 2009). Inhibition of TGF-β signaling stimulates axonal growth in a Cdh1 dependent manner, suggesting the presence of an intrinsic TGF-β-APC/C pathway to modulate the transcriptional activity of SnoN and its effect in axonal growth

(Stegmuller *et al.*, 2008). Id2 is another crucial substrate of neuronal APC/C-Cdh1. This bHLH transcription factor induces a cluster of genes with potent axonal inhibitory functions, such as the gene encoding for the Nogo receptor, a key transducer of myelin inhibition. The APC/C-Cdh1-dependent degradation of Id2 in neurons results in the accumulation of Nogo and the subsequent inhibition of axonal growth (Lasorella *et al.*, 2006). In Cdh1-depleted neurons, the stabilization of SnoN and Id2 leads to an increase in axonal growth that goes along with a disrupted axonal patterning without affecting dendrite morphology.

Cdc20 has also been proposed to play specific roles in these terminally differentiated cells. APC/C-Cdc20 regulates presynaptic axonal differentiation by triggering the degradation of NeuroD2, a transcription factor that suppresses presynaptic differentiation through its target gene Cplx2 encoding Complexin II (Yang *et al.*, 2009). Cdc20 knockdown in cerebellar slices reduces synapsin cluster density, an effect mediated by the stabilization of NeuroD2 and the induction of Cplx2. APC/C-Cdc20 may also regulate dendrite morphogenesis in cerebellar neurons through a centrosomal-dependent activity (Kim *et al.*, 2009). In these cells, APC/C-Cdc20 targets the transcription factor Id1 for degradation. This function is stimulated by histone deacetylase 6 (Hdac6), a centrosome-associated protein. Destruction of Id1 is necessary for the regulation of dendrite size, and downregulation of Cdc20 in cerebellar granule neurons leads to an impairment in dendrite growth and branching (Kim *et al.*, 2009).

The APC/C has also been reported to act at the synapse both at the pre- and postsynaptic level in Drosophila and C. elegans, respectively (Juo and Kaplan, 2004; van Roessel *et al.*, 2004). In Drosophila, the APC/C controls synaptic size exerting its function by targeting liprin-α (van Roessel *et al.*, 2004). In C. elegans, APC/C regulates the postsynaptic side, controlling the numbers of glutamate receptors (Juo and Kaplan, 2004). Consistently, a recent study in mammals suggests a critical role for APC/C in regulating the synaptic

strength (Fu *et al.*, 2011). This work shows that APC/C-Cdh1 targets for degradation the GluR1 subunit of functional AMPA receptors (AMPARs) after elevated synaptic activity. This role is mediated by Ephrin-A4 (EphA4), which in response to elevated synaptic activity interacts with APC/C-Cdh1 complexes leading to the degradation of GluR1 and the downregulation of surface AMPARs at synapses (Fu *et al.*, 2011). These results suggest a critical role for APC/C-Cdh1 in regulating neuronal excitability and synaptic strength during homeostatic plasticity. All together, these roles of APC/C-Cdh1 are likely to have relevance *in vivo* since several mouse models of APC/C or Cdh1 deficiency display multiple defects in learning and memory (Garcia-Higuera *et al.*, 2008; Li *et al.*, 2008; Kuczera *et al.*, 2011).

4. Relevance of the APC/C in cancer

The requirements for the APC/C during mitotic exit have been recently used to propose new therapeutic strategies against proliferative diseases such as cancer (Manchado *et al.*, 2012). Downregulation of APC/C-Cdc20 results in metaphase arrest and subsequent cell death, suggesting a therapeutic use for the inhibition of mitotic exit, by targeting the APC/C in cancer cells (Huang *et al.*, 2009; Manchado *et al.*, 2010b). One possible complication of these strategies resides in the possible undesired effect of inhibiting APC/C-Cdh1, since lack of Cdh1 activity may result in the accumulation of proliferative molecules such as cyclins or oncogenes such as Pttg1/Securin or Aurora kinases that could drive increased cellular proliferation.

Whereas Cdc20 is essential for the metaphase-to-anaphase transition (Manchado *et al.*, 2010b), Cdh1 is dispensable for cell cycle progression from yeast to mammals (Garcia-Higuera *et al.*, 2008). Yet, lack of mammalian Cdh1 results in pleiotropic defects that include early entry into S-phase, defective chromosome segregation and accumulation to

polyploid cells, as well as chromosomal and genomic instability (Garcia-Higuera *et al.*, 2008; Li *et al.*, 2008; Sigl *et al.*, 2009). Indeed, Cdh1-null cells display multiple genomic defects such as binucleated or multinucleated cells, metaphase plates with mis-aligned chromosomes in diploid or polyploid cells and multipolar spindles. Other alterations such as chromosome breaks, small chromosomal fragments, non-disjunction figures, and complex translocations affecting several chromosomes are also common although the origin of these abnormalities is not clear (Garcia-Higuera *et al.*, 2008).

Whereas Cdc20 is able to target only a reduced number of proteins for degradation, the activity of Cdh1 is much more promiscuous. Known Cdh1 substrates include proteins involved in mitosis and cytokinesis (A- and B-type cyclins, Aurora A and B, Tpx2, Plk1, etc.), DNA replication (geminin, thymidine kinase 1 and thymidylate kinase), neuron biology, metabolism, etc.. Interestingly, many of these substrates have important roles in malignant transformation and their modulation by Cdh1 may have relevant implications in cancer. Partial ablation of Cdh1 results in increased tumor susceptibility *in vivo* (Garcia-Higuera *et al.*, 2008). Multiple APC/C-Cdh1 substrates are upregulated in human tumors and Cdh1 activity, which is inhibited by Cdk-dependent phosphorylation, may be impaired in these cases due to the widespread upregulation of Cdks in human cancer (Malumbres and Barbacid, 2001; Lehman *et al.*, 2007). In some cases, Cdh1 protein levels are overexpressed in tumors and this is thought to be a consequence of its defective function, as Cdh1 targets itself for degradation (Listovsky *et al.*, 2004; Lehman *et al.*, 2007).

Despite the relevance of Cdh1 as a major regulator of the cell cycle and a critical modulator of cellular transformation, it is not currently clear which are the Cdh1 substrates that mediate genomic instability or how the defects found in Cdh1-deficient tumor cells can be manipulated for therapeutic intervention in cancer.

Aim of the work

In this work we have taken advantage of mouse models and cells deficient for Cdh1 to accomplish the following goals:

1. Unveil the role of Cdh1 in mammalian tissues *in vivo*

2. Unearth new APC/C-Cdh1 substrates and characterize the impact of their upregulation by Cdh1

3. Evaluate the consequences of inhibiting APC/C-Cdh1 in cancer

Material and Methods

1. Generation and Characterization of Mutant Mice

All animals were maintained in a mixed 129/Sv (25%) x CD1 (25%) x C57BL/6J (50%) background. Mice were housed in the pathogen-free animal facility of the Centro Nacional de Investigaciones Oncológicas (Madrid) following the animal care standards of the institution. These animals were observed on a daily basis and sick mice were killed humanely in accordance with the Guidelines for Humane End Points for Animals used in biomedical research. All animal protocols were approved by the ISCIII committee for animal care and research. Fzr1(lox) mice (Garcia-Higuera *et al.*, 2008) were used to conditionally deplete Cdh1 upon Cre expression, using Tg.Sox2-Cre mice, that express Cre in embryonic but not in extra-embryonic tissues (Hayashi *et al.*, 2002) or Tg.Nestin-Cre mice that express this recombinase in the developing nervous system (The Jackson Laboratory: Strain Name: B6.Cg-Tg(Nes-cre)1Kln/J; Stock Number: 003771) (Tronche *et al.*, 1999). The LSL-YFP allele, and p53- and Cyclin B1-deficient mice were reported previously (Jacks *et al.*, 1994; Brandeis *et al.*, 1998; Srinivas *et al.*, 2001).

1.1. Genotyping of the mutant mice

The genotyping of the mutant mice was done by PCR. The PCR was performed using DNA from the tail of the mice.

The standard PCR protocol was: 5 minutes at 95ºC for denaturalizing the DNA; then 35 cicles with the following steps: Denaturalizing, 1 minute at 95ºC; annealing, 30 seconds at 58ºC; and elongation, 1 minute at 72ºC. The protocol finished with a final elongation step of 10 minutes at 72ºC.

1.2. Object recognition test

Animals underwent the object recognition test following a protocol described previously (Bevins and Besheer, 2006) with minor modifications (Garcia-Higuera *et al.*, 2008).

Briefly, mice were placed in an experimental cage that consists of an open plastic box (73-cm long × 55-cm wide × 32-cm high) with opaque walls. The two similar objects (objects X and Y) were plastic parallelepipeds and the dissimilar object (object Z) was a plastic bottle. The objects were placed along the long axis of the experimental cage, each 7 cm from each cage end. Mice were first exposed to the cage and to objects X and Y. After a familiarization period, each mouse was released in the experimental cage with objects X and Z. After each exposure, the objects and the cage were wiped with 70% ethanol to eliminate odour cues. The size and weight of the objects used did not allow their movement or displacement by the animals. Animals were considered to show recognition activity when the head of the animal was less than 2 cm close to the object. The total time of recognition activity was scored manually using a stopwatch and recorded.

1.3. Histology and immunohistochemistry (IHC)

For histological observation, dissected organs or embryos were fixed in 10%-buffered formalin (Sigma) and embedded in paraffin wax. Sections of 3- or 5-µm thickness were stained with haematoxylin and eosin (H&E). Antigen retrieval with citrate was done in the sections, before additional immunohistochemical examination of the embryos, tissues and pathologies analyzed were performed using specific antibodies (Table 2). Some of the slides were digitalized by a MIRAX digital slide scanner (Zeiss).

Table 2

Antigen	Source Ig	Source	Clone	Catalogue#	Use*
Actin	Mouse	Sigma-Aldrich	AC-40	A4700	WB
AurkA	Mouse	Becton Dickinson (BD)	4/IAK1	610938	IHC
AurkA	Mouse	Abcam		ab13824	WB
AurkB	Rabbit	Abcam		ab2254	IHC/WB
β-Catenin	Mouse	Sigma-Aldrich		C 7207	WB
βIII-tubulin	Mouse	Sigma-Aldrich	SDL.3D10	T 8660	IF
Bromo-deoxyuridine (BrdU)	Mouse	GE Healthcare	(BU-1)	RPN202	IHC
Caspase 3 Active (C3A)	Rabbit	RYD Systems		AF835	IHC
Cdc6	Mouse	Millipore	DCS-180	05-550	WB
Cdc20/p55CDC	Rabbit	Santa Cruz Biotech.		Sc-8358	WB
Cdc27	Mouse	AbCam		Ab10538	WB
Cdh1	Mouse	Neomarkers	CH01	MS-1116-P	WB
Cyclin B1	Mouse	Millipore	(V152)	MAB3684	IHC/WB
γ-Tubuliln	Mouse	Sigma-Aldrich	GTU-88	T6557	IF
Gapdh	Mouse	Sigma-Aldrich		G9545	WB
Geminin	Rabbit	Santa Cruz Biotech.	(FL-209)	sc-13015	IHC, WB
GFP	Mouse	Roche		11814460001	WB
Ki67	Rabbit	Master Diagnostica	SP6	0003110QD	IHC
Kif11/Eg5	Rabbit	Cytoskeleton		AKIN03	WB/IF
Kpna2	Rabbit	Novus Biologicals			WB
Nestin	Mouse	Developmental Studies Hybridoma Bank (DSHB)	(RAT-401)		IF
p21	Rabbit	Santa Cruz Biotech.		sc-397	WB
p27	Mouse	BD Transduction Labs.		610242	WB
p53	Rabbit	Leica	(CM5p)	NCL-p53-CM5p	IHC
PCNA	Mouse	Merck	PC10	NA03	IHC
Phospho-Histone H2A.X (Ser139)	Mouse	Millipore	(JBW301)	05-636	IHC, IF
Phospho-Histone H3 (Ser10)	Rabbit	Millipore		06-570	IHC, IF
Phospho-RPA32	Rabbit	Bethyl		A300-245A	WB
Rock2	Rabbit	Santa Cruz Biotech.	H-85	sc-5561	WB
S100	Rabbit	Dako		Z0311	IHC
Securin	Mouse	AbCam		Ab3305	WB
Skp1 p19	Rabbit	Santa Cruz Biotech.	H-163	sc-7163	WB
Sox2	Rabbit	Millipore		AB5603	IHC, WB
Sox9	Rabbit	Millipore		AB5535	IHC, IF
Tbr1	Rabbit	Abcam		ab31940	IF
Tbr2	Rabbit	Abcam		ab23345	IF

Top2α	Rabbit	TopoGEN		2011-1	WB/IF
Tpx2	Rabbit	Lifespan Biosciences		LS-B146	IHC, WB
Tpx2	Rabbit	Hyman's Lab (MPI-CBG)			IF
Tpx2	Mouse	AbCam		Ab32795	WB
Vinculin	Mouse	Sigma-Aldrich	hVIN1	V9131	WB

Primary antibodies used in this work.

1.4. Molecular imaging

1.4.1. Computerized axial tomography (CT Scan).

CT scan was performed on anesthetized mice (1-3% of Isoflurane [Isoba Vet]) using the eXplore Vista microPET-CT (GE Healthcare) with the following parameters: 200 µA, 35 kV, 160 µ, 16 shots y 360 projections. MMWKS (GE Healthcare) and MicroView software were used to analyze the images.

1.4.2. Nuclear magnetic resonance (NMR).

NMR was performed using a 4.7-tesla Biospec 47/40 (Bruker) and analysis with the equipment software. Images of transverse relaxation time (T2) were taken.

2. Cell culture

2.1. Neural progenitor culture

Progenitor cells from diverse tissues are typically cultured *in vitro* under nonadherent conditions as spheres. In order to study neural progenitors we have cultured them in floating conditions forming neurospheres (Pastrana *et al.*, 2011).

This system allows to assess the capacity of primary neurosphere-forming cells to be propagated as secondary cultures after neurospheres are mechanically dissociated and sub-cultured (self-renewal). Moreover, when plated on an adherent substrate under specific conditions, they are also able to differentiate into both neurons and glial cells. Neurosphere cultures are widely used as both functional properties of progenitor cells, self-renewal and differentiation, can be evaluated at the single-cell level and provide as well a quantitative readout of the number of stem cells *in vivo*.

2.1.1. Isolation and culture of neural progenitors

Mouse cerebral cortices from different embryonic stages (E12.5-E17.5) were dissected and gently dissociated manually, as described previously (Ferron *et al.*, 2004). Single dissociated cortical cells were cultured in uncoated 6-well plates for 7 days in serum-free medium containing DMEM with high glucose, sodium pyruvate, glutamine, N2, B27 (all from Gibco), 2mM N-acetyl-cysteine (Sigma), and 20 ng/mL each FGF2 (Invitrogen) and EGF (Gibco) and maintained at 35°C in 6% CO2. For subcloning, neurospheres were collected and enzymatically dissociated using papain (Worthington) for 30 min at 37°C with gentle agitation.

2.1.2. Self-renewal assay

In order to evalute the capacity of progenitor cells to proliferate and be propagated as secondary neurosphere cultures, single dissociated cells were cultured at a density of 20000 cells/ml for 5-7 days in serum-free medium containing DMEM with high glucose, sodium pyruvate, glutamine, N2, B27 (all from Gibco), 2mM N-acetyl-cysteine (Sigma), and 20 ng/mL each FGF2 (Invitrogen) and EGF (Gibco) and maintained at 35°C in 6% CO2. The number of neurospheres formed was counted and the neurosphere volume was calculated.

2.1.3. Differentiation assay and immunofluorescence

Single dissociated cells were plated on matrigel-coated coverslips (BD BIOSCIENCES) and cultured for 24h in medium as above, without EGF and reducing FGF2 concentration to 10 ng/mL FGF2 (Invitrogen). Cells were fixed with 4% paraformaldehyde (Polysciences) during 10 min at RT, and incubated with PBS-Triton X-100 0.5% for permeabilization. Neurospheres were then blocked with 3% BSA and incubated with primary antibodies (Table 3) for 1-2 h at RT. The matching fluorochrome-conjugated secondary antibodies (Alexa 488, 594 or 647) used were from Molecular Probes (Invitrogen). For EdU staining, 10µM 5-ethynyl-2´-deoxyuridine (EdU) was added to neurospheres after 3-4 days of growth *in vitro*. 1h later they were attached to matrigel-coated coverslips (BD BIOSCIENCES), fixed with 4% paraformaldehyde (Polysciences) during 15-20 min at RT, and incubated with PBS-Triton X-100 0.5% for permeabilization. Neurospheres were then incubated with EdU Click-iT cocktail (Invitrogen) blocked with 3% BSA and incubated with primary antibodies (Table 2) for 1-2 h at RT. The matching secondary antibodies (Alexa 488, 594 or 647) used were from Molecular Probes (Invitrogen). Images were obtained using a laser scanning confocal microscope TCS-SP5 (AOBS) Leica. Settings were kept unchanged across matched samples acquisition, and when necessary, contrast and brightness levels were adjusted always to whole images and applied likewise to controls.

2.1.4. Biochemical analyses of neural progenitors

For Western blotting, neurospheres were harvested after 7-9 days *in vitro*, lysed in RIPA buffer and 50 µg of total protein was separated by SDS-PAGE, transferred to nitrocellulose membranes (BioRad) and probed with different antibodies (Table 2). The secondary antibodies were HRP-conjugated antibodies (DAKO) and the WBs were developed using the ECL system (PerkinElmer).

2.2. Cortical neurons culture

Mouse cerebral cortices from E14.5 embryos were dissected and dissociated with Trypsin (Sigma), as described previously (Ferron et al, 2004). Single dissociated cortical cells were cultured in poly-D-lysine (Sigma) coated 24-well plates for 7 days in serum-free medium containing Neurobasal medium supplemented with B27, glutamine and Penicillin/Streptomycin (all from Gibco). 10 µM Cytosine β-D-arabinofuranoside (AraC; Sigma) was added 4 days after the dissection to avoid the growth of astrocytes in the culture.

2.3. Flow cytometry

Viability assays by FACS were performed by adding 0.2ug/ml DAPI (Sigma) to the samples prior to run then on the LSR Fortessa (BD, San Jose). We acquired at least 20,000 single events for what we use pulse processing of the scatter signal. All data was analysed using FlowJo v9.6.4 (Treestar, Oregon).

2.4. MEFs isolation

MEFs were isolated from E13.5-E14.5 mutant and control embryos and cultured using routine procedures (Malumbres *et al.*, 2004). The whole embryo was minced and dispersed in 0.1% trypsin (5 min at 37 °C). Cells were grown for two population doublings and then frozen. On reaching confluence, MEFs were subcultured at a ratio of 1:4. All cultures were maintained in Dulbecco's modified Eagle's medium (DMEM; Gibco) supplemented with 1% penicillin/streptomycin and 10% fetal bovine serum (FBS).

2.5. Viral infections

For RNA interference, Fzr1+/+ and Fzr1–/– MEFs at 60-70% confluency were infected with retroviruses with Kif11/Eg5 or Top2α shRNAs (Scott W. Lowe's laboratory; MSKCC) in the presence of polybrene (4 µg/mL). For videomicroscopy, Fzr1+/+ and Fzr1–/– MEFs at 60-70% confluency were infected with retroviruses containing H2B-RFP in the presence of polybrene (4 µg/mL). In order to increase the infection efficiency, two consecutive rounds of infection were performed.

2.6. Transfection / Nucleofection

Human cell lines and MEFs were transfected in subconfluency with Lipofectamine 2000 (Invitrogen) and NEON transfection system (Invitrogen), respectively, in accordance with the manufacturer's instructions.

2.7. Drugs

The following drugs were used in cultured cells at the indicated concentrations: nocodazole (Sigma; 100 ng/ml); taxol (Sigma; 600 nM); Thymidine (Sigma); roscovitine (Sigma; 0.2–10 µM; see figure legends); monastrol (Sigma; 100 µM); etoposide (Sigma; 25-100 µM); proTAME (Boston Biochem., Inc.; 10-20 µM); cycloheximide (Sigma; 100 µg/mL); and actinomycin D (Sigma; 1 µM).

3. Biochemical procedures and Microscopy

3.1. Degradation and ubiquitination assays

Degradation and ubiquitination assays were performed in Dr. Yamano's laboratory (UK) under collaboration. Top2α and Eg5 genes were subcloned into pHY22 (Yamano *et al.*,

1996). Xenopus cytostatic factor-arrested egg extracts (CSF extracts) were prepared as described previously (Murray *et al.*, 1989). A cell-free APC/C-Cdh1-dependent destruction assay was reconstituted by adding 280 nM purified Xenopus His-Cdh1 protein to interphase egg extracts (Trickey *et al.*, 2013). To produce 35S-labeled substrates, mRNAs of wild type or mutant versions of Top2α and Eg5 were first synthesized using mMESSAGE mMACHINE kit (Ambion), and then translated using Rabbit Reticulocyte Lysate System (Promega). Ubiquitylation assays were essentially performed as described (Trickey *et al.*, 2013). Reactions were performed at 23 °C in 20 µl of buffer (20 mM Tris-HCl, pH 7.5, 100 mM KCl, 2.5 mM MgCl2, 2 mM ATP, 0.3mM DTT) containing 0.075 mg/ml Xenopus APC/C, 0.05 mg/ml E1, 0.025 mg/ml UbcX, 0.75 mg/ml ubiquitin, 1 µM ubiquitin-aldehyde, 150 µM MG132, 280 nM purified His-Cdh1 protein, and 1 µL of 35S-labeled substrates. The reactions were stopped at the indicated time points with SDS sample buffer and resolved by SDS-PAGE followed by autoradiography.

3.2. Real-time reverse-transcription PCR (qRT-PCR)

For qRT-PCR studies, total RNA was isolated by using the Qiagen RNeasy kit, according to the manufacturer's instructions. cDNA was synthetized with a Superscript III reverse transcriptase (Invitrogen) and PCR amplification was performed using SYBR Green PCR Master mix (Applied Biosystems) with specific primers

3.3. Immunoblot (WB)

For Western blotting (WB), cultured cells were harvested and lysed in RIPA or Laemmli buffer. Embryonic brains were lysed in 6M urea, 2 M thiourea, 1% N-octyl glucoside, 10 mM DTT, 100mM Hepes pH 8.0 plus protease inhibitors, phosphatase inhibitors cocktail I and 2 (Sigma-Aldrich) and 0.1% Benzonase nuclease (Novagen). 50 µg of total protein was separated by SDS-PAGE, transferred to nitrocellulose membranes (BioRad) and probed with

different antibodies (Table 2). The secondary antibodies were HRP-conjugated antibodies (DAKO) and the WBs were developed using the ECL system (PerkinElmer).

3.4. Cells and tissue immunofluorescence (IF)

For immunofluorescence, cultured cells were grown in coverslips, fixed with 4% paraformaldehyde for 10 min at RT and incubated with 0.15-0.5% Triton X-100 for 5-10 min at RT for permeabilization. Cells were then blocked with 3% BSA or 10% FBS and incubated during 1h at RT or 24h at 4ºC with the indicated primary antibodies (Table 2) and/or with 4,6 diaminophenylindole (DAPI; Prolong Gold antifade, Invitrogen) to visualize nuclei. Secondary antibodies (Alexa 488, 594 or 647) from Molecular Probes (Invitrogen) were used and images were captured using a laser scanning confocal microscope TCS-SP5 (AOBS) Leica or a Leica DMI 6000B microscope. Tissues were fixed in 10%-buffered formalin (Sigma) and embedded in paraffin wax or frozen in tissue-Tek OCT compound (Sakura). Antigen retrieval with citrate was performed in sections from paraffin embedded samples. Tissue sections were permeabilized with 0.2%-0.5% Triton X-100, blocked with 10% normal goat serum or 10% FBS and incubated with primary antibodies (Table 2) for 1-2 h at RT or 24h at 4ºC. Secondary antibodies (Alexa 488, 594 or 647) from Molecular Probes (Invitrogen) were used and images were obtained using a laser scanning confocal microscope TCS-SP5 (AOBS) Leica.

3.5. Wholemount staining

In order to examine the complete cytoarchitecture and cellular relationships present at the lateral ventricle wall, wholemount preparations were performed as previously described (Mirzadeh *et al.*, 2008). Briefly, the brain was extracted and cut in the midline. The overlying cerebral cortex, medial ventricular wall, and hippocampus were dissected to reveal the lateral ventricular wall. Wholemounts were fixed in 4% paraformaldehyde with

0.1% Triton-X 100 at 4°C overnight. Then, they were extensively washed in phosphate buffered saline (PBS) with 0.1% Triton-X 100 (PBS+), blocked in 10% FBS in PBS+ at room temperature, and incubated at 4°C for 48h with primary antibodies (Table 2) in PBS+ containing 10% FBS. After rinsing in PBS+, whole mounts were incubated for 2h at RT with secondary antibodies (Alexa 488, 594 or 647) from Molecular Probes (Invitrogen). Whole mounts were trimmed to 200–300 µm sections and mounted on Superfrost slides with adhesive spacers and Fluoromount-G mounting medium (Southern Biotech). Images were obtained using a laser scanning confocal microscope TCS-SP5 (AOBS) Leica. Settings were kept unchanged across matched samples acquisition, and when necessary, contrast and brightness levels were adjusted always to whole images and applied likewise to controls.

3.6. High-throughput microscopy (HTM)

For HTM, MEFs and human cell lines were grown on µCLEAR bottom 96-well plates (Greiner Bio-One). After 24h with Etoposide and/or ICRF, 1 µM TO-PRO®-3 Iodide (642⁄661; Invitrogen T3605) and 5 µg/ml Hoechst 33342 (Invitrogen H3570) were added, and then incubated 30 min at 37ºC. Neural progenitors were treated for 8h with Roscovitine or nucleosides and EdU was added during the last 30min. Then, they were attached to µCLEAR bottom 96-well plates (Greiner Bio-One) after disaggregation with Accutase (Gibco). Cells were permeabilized with 0.2%-0.5% Triton X-100, blocked with 3% BSA or 10% FBS and incubated with primary antibodies (Table 3) for 1-2 h at RT at 4ºC. Secondary antibodies (Alexa 488, 594 or 647) from Molecular Probes (Invitrogen) were used. Images were automatically acquired from each well by an Opera High-Content Screening System (Perkin Elmer). A 20x magnification lens was used and pictures were taken at non-saturating conditions. Images were segmented using the Hoechst 33342 or DAPI stainings to generate masks matching cell nuclei from which the mean TO-PRO®-3, γH2AX and EdU signals were calculated. Data were represented with the use of the Prism software (GraphPad Software).

3.7. Videomicroscopy

For videomicroscopy, H2B-RFP expressing cells were plated on eight-well glass-bottom dishes (Ibidi) and recorded with a DeltaVision RT imaging system (Applied Precision, LLC; IX70/71; Olympus) equipped with a Pl APO 20X/ 1.42 NA objective lens, maintained at 37 °C in a humidified CO2 chamber. Images were acquired every 10 min. Images were processed and analyzed using ImageJ or Imaris imaging software.

4. Proteomic analysis

4.1. Stable isotope labeling by amino acids in cell culture (SILAC)

For SILAC (Ong *et al.*, 2002) analysis, equal number of asynchronous Fzr1(+/+) (light labelled) and Fzr1(–/–) (heavy labelled) mouse MEFs were mixed. Subcellular protein extraction was performed using the ProteoExtract Subcellular Proteome Extraction Kit (Calbiochem) as indicated by the manufacturer. All samples were fractionated on the basis of their isolectric point (Ernoult *et al.*, 2008) using the 3100 OFFGEL Fractionator system (Agilent Technologies). Additionally, in the SILAC assay, fifty µg of proteins were separated by SDS-PAGE, sliced into 24 pieces and digested with trypsin as described (Shevchenko *et al.*, 2006). Desalted peptides were separated by reversed-phase chromatography (Reprosil-Pur C18 3 µm, 200x 0.075 mm, Dr. Maisch GmbH), using a nanoLCUltra1D+ system (Eksigent), directly coupled in line with a LTQ-Orbitrap Velos (Thermo Fisher Scientific) via nanoelectrospray source (Thermo Fisher Scientific) (Olsen *et al.*, 2005). Mass spectra were acquired in a data-dependent manner, with an automatic switch between MS and MS/MS scans using a top 15 method. Raw files were analyzed by MaxQuant (version 1.1.1.25) (Cox and Mann, 2008) interrogating the IPI-mouse V3.77 database. Oxidation of methionines, acetylation of protein n-terminus, SILAC-K8 and SILAC-R10 were set as variable

modifications, whereas carbamidomethylation of cysteines was set as fixed. Minimal peptide length was set to 6 amino acids and a maximum of two missed-cleavages were allowed. For protein assessment, at least two unique peptides with a FDR <= 1% were required. For quantification purposes, only proteins identified with two or more unique peptides and with two or more SILAC pairs were considered. The thresholds used to determine proteins being up-regulated were calculated by manual inspection of the data. To this end, ratios were plotted against intensities and a cut-off was chosen based on the distribution of the vast majority of proteins showing no change.

4.2. Isobaric tags for relative and absolute quantitation (iTRAQ)

For iTRAQ (Ross *et al.*, 2004) assays in cultured cells, primary MEFs were synchronized in G0 by confluence and low serum (0.1% FBS) for 36 h. For iTRAQ studies in brains, E15.5 embryo brains from Fzr1(lox/lox) and Fzr1(Δ/Δ) mice (Garcia-Higuera *et al.*, 2008) were lysed. Protein samples were digested using the filter aided sample preparation (FASP) method (Wisniewski *et al.*, 2009). Each tryptic digest was labelled with one isobaric amine-reactive tag iTRAQ according to the manufacturer's instructions (Applied Biosystems, Framingham, MA) and mixed in equal amounts. All samples were fractionated on the basis of their isolectric point (Ernoult *et al.*, 2008) using the 3100 OFFGEL Fractionator system (Agilent Technologies). Desalted peptides were separated by reversed-phase chromatography (Reprosil-Pur C18 3 µm, 200x 0.075 mm, Dr. Maisch GmbH), using a nanoLCUltra1D+ system (Eksigent), directly coupled in line with a LTQ-Orbitrap Velos (Thermo Fisher Scientific) via nanoelectrospray source (Thermo Fisher Scientific) (Olsen *et al.*, 2005). Mass spectra were acquired in a data-dependent manner, with an automatic switch between MS and MS/MS scans using a top 15 method. Raw files were processed by Proteome Discoverer 1.3 (Thermo Scientific). Data were searched by interrogating the Uniprot_Mouse database, comprising both the canonical and manually reviewed isoform

sequences (release 2012_09, 50544 entries) using MASCOT (v 2.2) (Perkins *et al.*, 1999) as the search engine. Lysine and peptide N-termini labelling with iTRAQ-4plex reagent as well as carbamidomethylation of cysteine were considered as fixed modifications, while oxidation of methionine was chosen as variable modification for database searching. Both peptide and protein identification were filtered at 1% false discovery rate (FDR) using the target-decoy approach (Elias and Gygi, 2007). The thresholds used to determine proteins being up-regulated were calculated by manual inspection of the data. To this end, ratios were plotted against intensities and a cut-off was chosen based on the distribution of the vast majority of proteins showing no change for each analyses. The narrower distributions of the iTRAQ-labelled experiments are due to the compression of ratios associated with this technique.

5. Statistical analysis

Statistical analysis was carried out using Prism 5 (Graphpad Software Inc.). All statistical tests of comparative data were done using two-sided, unpaired Student's t tests. Data with $P < 0.05$ were considered statistically significant (*, $P < 0.05$; **, $P < 0.01$; ***, $P < 0.001$).

Results

1. Physiological relevance of Cdh1 in the nervous system

In this first part we show that elimination of Cdh1 in the developing nervous system by a Cre recombinase expressed under the nestin regulatory sequences resulted in defects in the neural progenitor compartment, hydrocephalus (accumulation of cerebrospinal fluid in the cavities of the brain), and death of these mutant mice. This particular requirement for Cdh1 during neurogenesis is related to the ability of Cdh1 of preventing replicative stress in progenitors of the developing brain. In the absence of Cdh1, Sox2- and Sox9-positive neural progenitors display aberrant phosphorylation of H2AX, a marker of replicative stress, and undergo apoptosis. This cell death is prevented after genetic ablation of p53 suggesting that the ubiquitin ligase APC/C-Cdh1 prevents p53-dependent apoptosis as a consequence of replicative stress in the developing cortex.

1.1. Generation of mouse knockout for Cdh1 in the nervous system

The essential roles of Cdh1 in the murine nervous system have not been studied because Cdh1 is required for endoreduplication of trophoblast giant cells in the placenta and homozygous Fzr1 mutation results in lethality at embryonic day (E)9.5-10.5 (Garcia-Higuera *et al.*, 2008; Li *et al.*, 2008). This lethality can be rescued by using Sox2-Cre transgenics that specifically express the Cre recombinase in the proper embryo but not in the extraembryonic tissues (Garcia-Higuera *et al.*, 2008). However, these mice die shortly after birth with multiple defects (See below). We have therefore induced the conditional ablation of the Cdh1-encoding gene in specific tissues during embryonic development or in the adulthood. Surprisingly, we observed no major defects after specific constitutive ablation in the mammary gland or the skin or after induced ubiquitous ablation of Cdh1 in adult mice (data not shown).

Cdh1 is highly expressed in the brain (Gieffers *et al.*, 1999) and we and others previously observed several defects in behavior, neuromuscular coordination and learning, together with abnormal proliferation of progenitor cells in the adult brains of mice with just one functional allele of the Cdh1-endoding gene, known as Fzr1 in mammals (Garcia-Higuera *et*

al., 2008; Li *et al.*, 2008). We therefore used Nestin-Cre transgenic mice (Tronche *et al.*, 1999) to eliminate Cdh1 function in the developing nervous system.

1.2. Specific ablation of Cdh1 in the developing nervous system results in reduced cortical neurogenesis

Fzr1(Δ/Δ); Nestin-Cre mice were viable but about 50% of them died during the first two months of life, whereas Fzr1(lox/lox) (not shown) or Fzr1(+/Δ); Nestin-Cre mice remained viable during that period (Fig. 7a). Adult Fzr1(Δ/Δ); Nestin-Cre mice scored poorly in the object recognition assay (Fig. 7b), suggesting defects in learning which were even stronger than the ones observed in Fzr1(+/–) heterozygous mice (Garcia-Higuera *et al.*, 2008). Since both Nestin and Cdh1 are expressed in the mouse retina, we cannot rule out a possible defect in the object-recognition assay due to the specific ablation of Cdh1 in the eye.

Figure 7

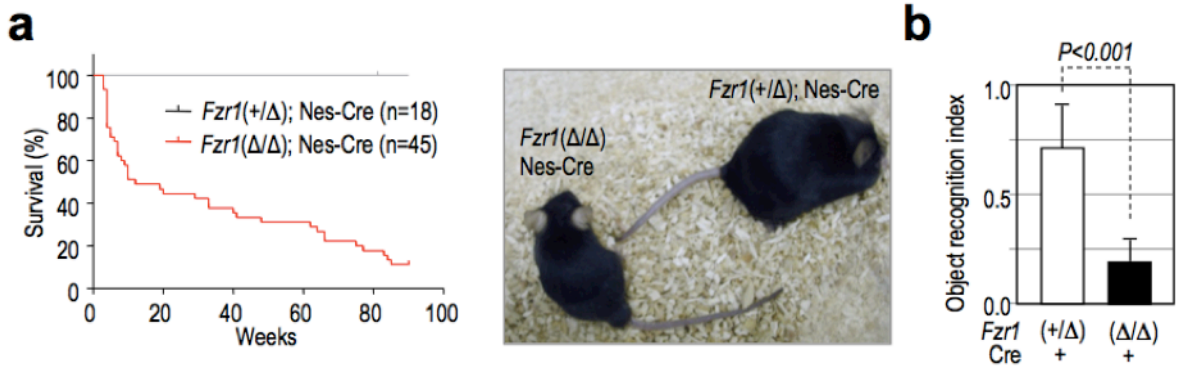

Cdh1 depletion in the developing nervous system. (**a**) Survival curve of Fzr1(Δ/Δ); Nestin-Cre and control mice. A representative picture of 50 week-old littermates is also shown. (**b**) Results from the object recognition assay in mutant [Fzr1(Δ/Δ); Nestin-Cre; n=7] and control [Fzr1(+/Δ); Nestin-Cre; n=9] adult (13-25-week-old) mice.

Morphological analysis of the skull by computerized axial tomography (CT scan; Fig. 8a) revealed that these mice display an aggressive hydrocephalus, showing a progressive increase in the size of Fzr1(Δ/Δ); Nestin-Cre heads at different stages during postnatal development. This defect was accompanied by the accumulation of liquid in the brain ventricles as detected by nuclear magnetic resonance imaging (NMR; Fig. 8b).

Figure 8

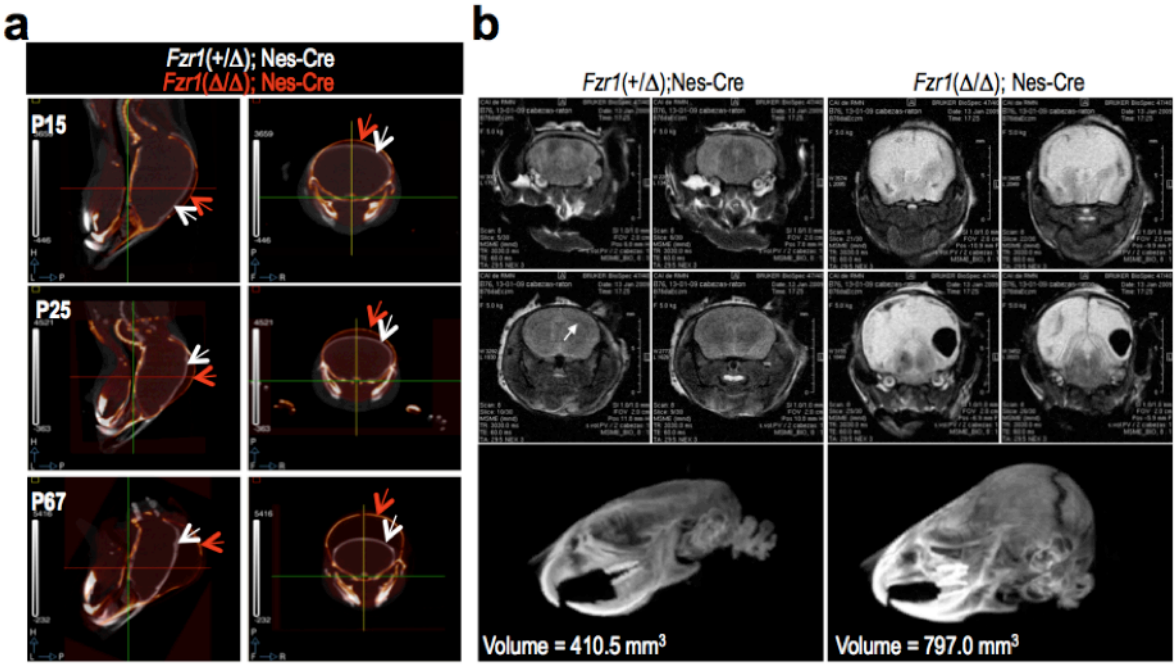

Cdh1 depletion in the developing nervous system causes hydrocephalus. (**a**) Analysis of the progression of hydrocephalus in Fzr1(Δ/Δ); Nestin-Cre mice at P15, P25 and P67 by computerized axial tomography (CT scan). Figures show an overlap of the cranial shape from mutant (red) or control (white) mice in sagittal (left panels) or coronal (right panels) sections. (**b**) Coronal T2-weighted magnetic resonance images of 9-week-old Fzr1(Δ/Δ); Nestin-Cre and control brains (top panels). Whereas control ventricles are barely visible (arrow), Fzr1(Δ/Δ); Nestin-Cre brains display a marked enlargement of the ventricles with a noticeable presence of liquid all over the brain (shown by the whitish aspect of the cortex)

In agreement with the *in vivo* imaging data, brains of Fzr1(Δ/Δ); Nestin-Cre mice displayed enlarged ventricles, accompanied by thinned cortex and agenesis of the corpus callosum (Fig. 9 and Fig. 10a).

Figure 8

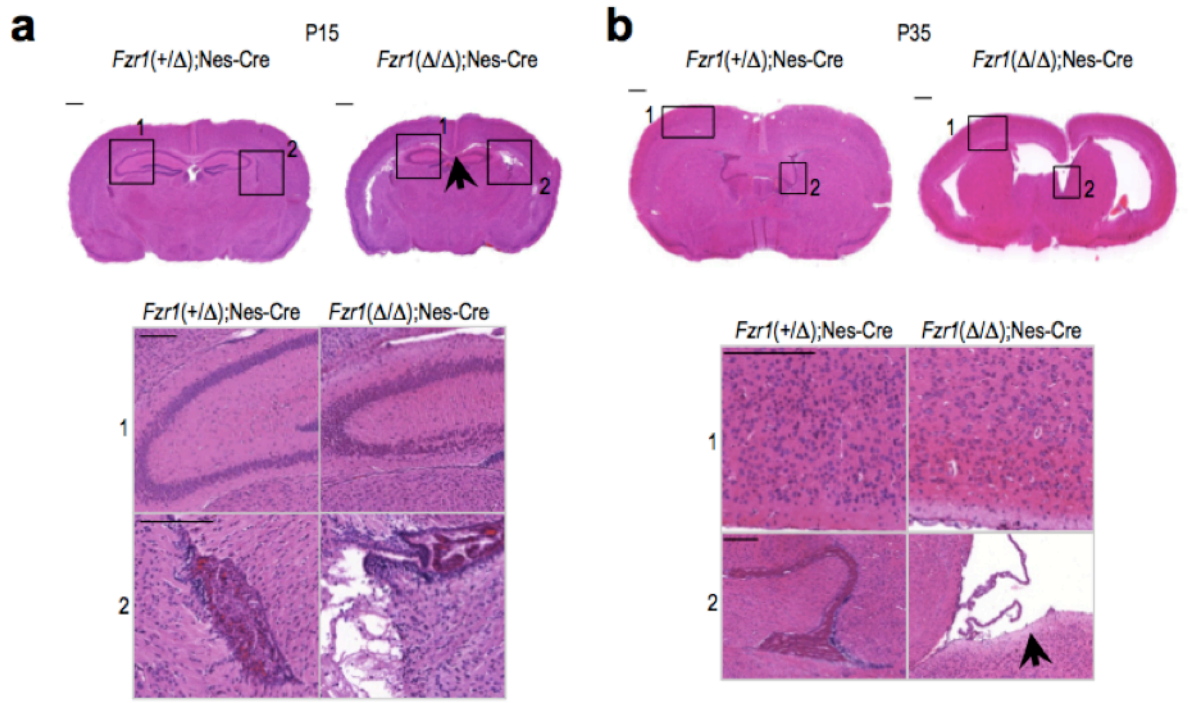

Alterations in Fzr1(Δ/Δ);Nestin-Cre brains. (**a**) H&E staining of P15 mice showing dysgenesis of the corpus callosum (arrow), and the presence of oedema in the wall of the lateral ventricle. (**b**) H&E staining of P35 mice with an aggressive hydrocephalus present a vacuolized cortex and damage in the ependymal layer (arrow). Scale bars, 200 µm.

Closer inspection of coronal brain sections from postnatal day (P)10 Cdh1-deficient mice revealed a significant reduction (about 20%) in the thickness of the cortex and the apparent absence of the corpus callosum, as seen in conventional H&E stainings as well as in immunohistochemical stainings for myelin basic protein (MBP), a marker of axon myelin sheath (Fig. 10a,b). The robust expression of Cdh1 in postmitotic neurons (Gieffers *et al.*, 1999) and its reported function in the control of axon growth and patterning in the developing mammalian brain (Konishi *et al.*, 2004) suggested the possibility that corpus callosum agenesis and cortical reduced thickness were the result of a failure of differentiating neurons to extend their axons. However, other major forebrain axon tracts such as the anterior and hippocampal commissures appeared normal, suggesting that the

Figure 10

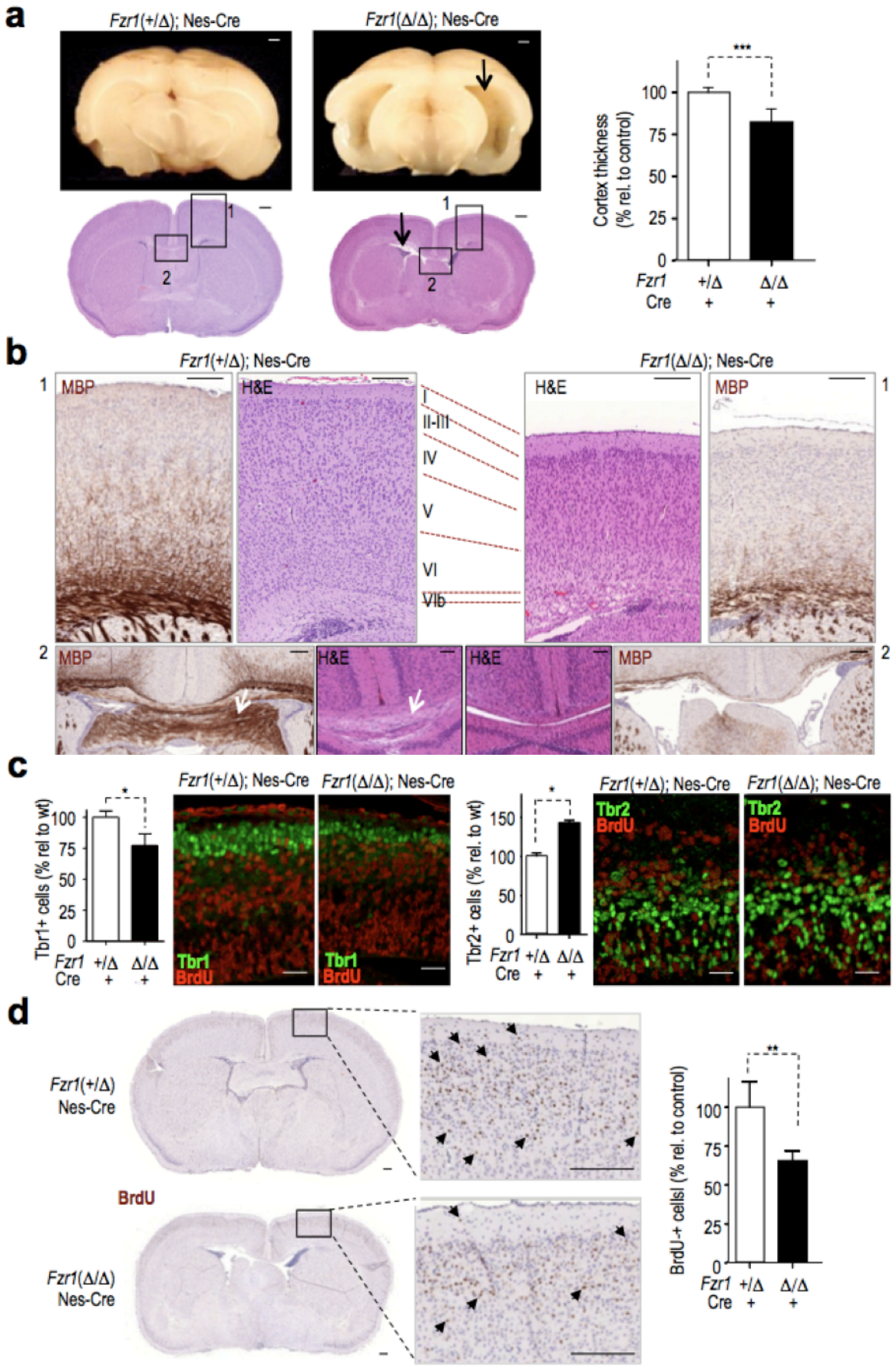
a
Fzr1(+/Δ); Nes-Cre
Fzr1(Δ/Δ); Nes-Cre
Cortex thickness (% rel. to control)
***
100
75
50
25
0
Fzr1 +/Δ Δ/Δ
Cre + +
b
Fzr1(+/Δ); Nes-Cre
Fzr1(Δ/Δ); Nes-Cre
MBP
H&E
I
II-III
IV
V
VI
VIb
c
Fzr1(+/Δ); Nes-Cre
Fzr1(Δ/Δ); Nes-Cre
Tbr1+ cells (% rel to wt)
Tbr1
BrdU
Tbr2+ cells (% rel. to wt)
Tbr2
BrdU
d
Fzr1(+/Δ) Nes-Cre
Fzr1(Δ/Δ) Nes-Cre
BrdU
BrdU+ cells (% rel. to control)
**

Figure 10 Legend

Cdh1 ablation results in defective neurogenesis. (**a**) Macroscopic (P21) and microscopic (P10) brain sections of Fzr1(Δ/Δ); Nestin-Cre and control mice. Cdh1-deficient brains display enlarged ventricles (arrows) and reduced thickness in the cortex. Cortex thickness is quantified in P10 Cdh1-null and control newborns (n=6 per genotype). (**b**) Detail micrographs of areas 1 and 2 from panel (**a**) indicating the different layers of the cortex. Cdh1-deficient brains display low levels of Myelin basic protein (MBP) in the cortex (area 1), and corpus callosum dysgenesis (white arrows, area 2). (**c**) Tbr1, Tbr2 and BrdU immunofluorescence in E14.5 cortices. Histograms show the quantification of Tbr1 and Tbr2 positive cells. (**d**) Reduced generation of neurons in Cdh1-deficient brains. Detection of BrdU-retaining positive cells in P10 sections after injection of BrdU in E15.5 embryos. (**a-d**) are coronal sections. (*, p<0.05; **, p<0.01; ***, p<0.001). Scale bars, 500 µm (**a**), 250 µm (**b**), 25 µm (**c**) and 250 µm (**d**).

defect in callosal development did not result from global defects in axon growth or midline development. Moreover, the defects in the postnatal cortex correlated with a decrease in the thickness of the cortical plate at E14.5, revealed by antibodies against Tbr1, a marker for postmitotic neurons, along with an increase in the area occupied by Tbr2-positive intermediate progenitor cells. Quantitation indeed showed that the number of Tbr2+ progenitor cells was increased whereas the number of Tbr1+ neurons was decreased in mutant cortices relative to wild types (Fig. 10c), suggesting that Cdh1 is required for the timely production of cortical neurons. Cdh1 is actually highly expressed in embryonic brains with strong representation in the subventricular area (Fig. 11). We also scored reduced numbers of BrdU-retaining cells, corresponding to postmitotic neurons, in the cortex of P10 Fzr1(Δ/Δ); Nes-Cre mice born from females injected with BrdU at gestational day E15.5, a developmental time-point in which only layer 2/3 cortico-cortical callosal pyramidal neurons are being generated from cortical progenitors. Cdh1-deficient brains showed a significant reduction in the number of neurons generated in that assay (Fig. 10d), indicating that neurogenesis was severely affected when Cdh1 is deleted in Nestin+ cortical progenitors.

Figure 11

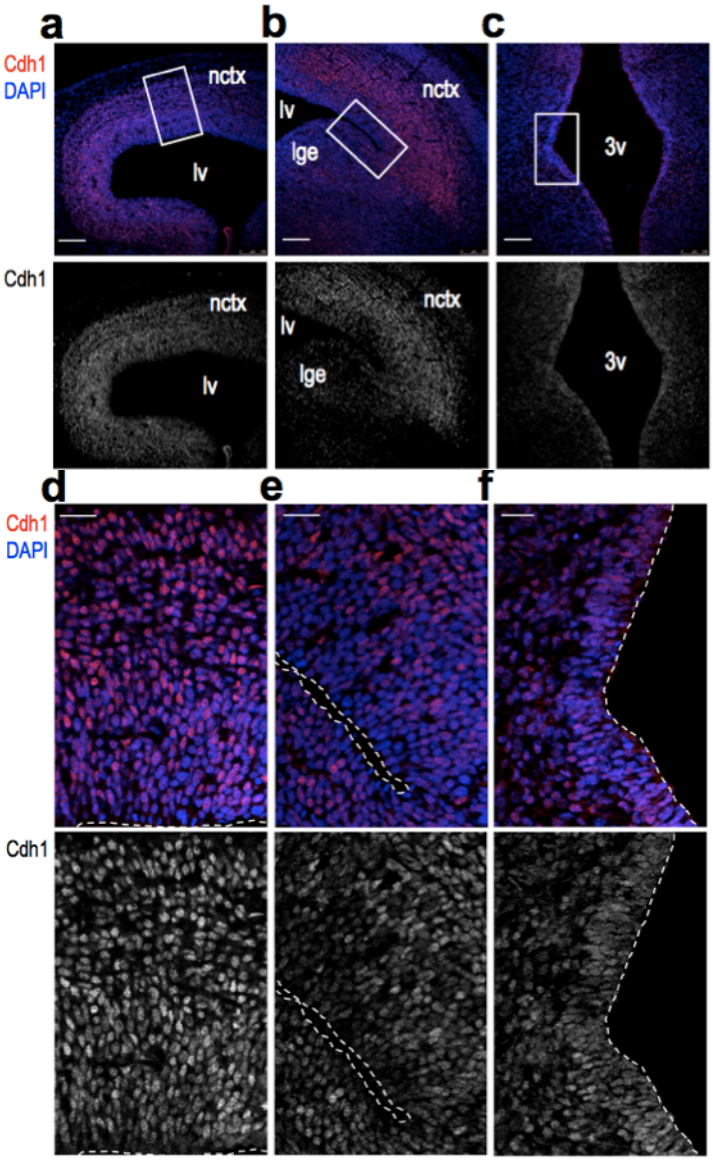

Cdh1 expression in the developing brain. Dashed white lines mark the limit of ventricles. E14.5 embryos were fixed in 4% parafolmaldehyde for 2 h, cryoprotected in 30% sucrose and frozen. Cryosections were obtained in a Leica cryostat. Staining was performed using anti-cdh1 antibodies (from J.M. Peters, IMP, Vienna; red signal) at 1:2000 dilution and appropriate secondary Alexa 488 conjugated secondary antribodies (Molecular Probes). nctx: neocortex; lge: lateral ganglionic eminence; lv: lateral ventricle; 3v: third ventricle. Scale bars in **a-c**, 100 µm; in **d-f**, 25 µm.

Generation of a conditional Cdh1 mutant from a Sox2 promoter also resulted in increased perinatal death, reduced size by P10, problems in motility and coordination, with a similar cortical phenotype, accompanied by hypoplasia and cell death in many other tissues (Fig. 12). All these data together indicated that Cdh1 might be essentially required for cortical neurogenesis during fetal development.

Figure 12

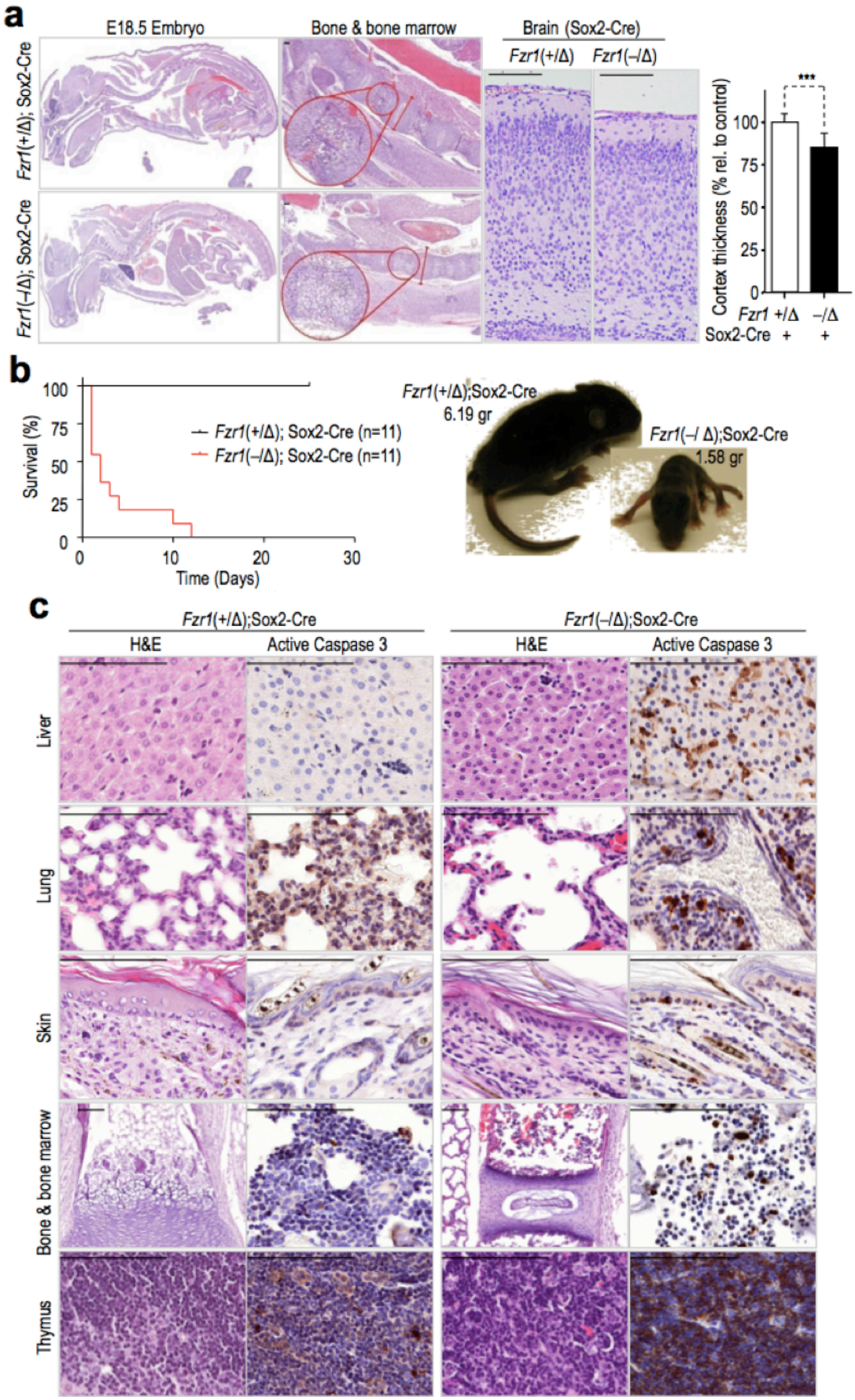
a
E18.5 Embryo
Bone & bone marrow
Brain (Sox2-Cre)
Fzr1(+/Δ)
Fzr1(–/Δ)
Fzr1(+/Δ); Sox2-Cre
Fzr1(–/Δ); Sox2-Cre
Cortex thickness (% rel. to control)
***
100
75
50
25
0
Fzr1 +/Δ
–/Δ
Sox2-Cre +
+
b
Survival (%)
Time (Days)
Fzr1(+/Δ); Sox2-Cre (n=11)
Fzr1(–/Δ); Sox2-Cre (n=11)
Fzr1(+/Δ);Sox2-Cre
6.19 gr
Fzr1(–/ Δ);Sox2-Cre
1.58 gr
c
Fzr1(+/Δ);Sox2-Cre
Fzr1(–/Δ);Sox2-Cre
H&E
Active Caspase 3
Liver
Lung
Skin
Bone & bone marrow
Thymus

Figure 12 Legend

Defective development of Fzr1(–/Δ);Sox2-Cre mice. (**a**) Representative micrographs of E18.5 (embryo and bone marrow) or P10 (brain) Fzr1(–/Δ);Sox2-Cre embryos with detailed images of the bone and the brain cortex. (**b**) Survival curve of Fzr1(–/Δ);Sox2-Cre and control mice (left), and representative pictures of these mutant mice at postnatal day (P)10 indicating the weight of these animals (right). (**c**) Microscopic analysis of the aberrations displayed by Fzr1(–/Δ);Sox2-Cre mice at P10. The majority of mutant tissues present a significant increase in active caspase-3 staining (apoptosis). H&E, hematoxylin and eosin. Scale bars, 100 µm.

1.3. Cdh1 ensures proper DNA replication in neural progenitors

To elucidate the possible cause of these defects, we analyzed cell proliferation during embryonic development in these mutant mice. By E14.5, many known Cdh1 substrates implicated in mitotic progression, including Aurora A, Aurora B, Tpx2 or Cyclin B1 were upregulated in Cdh1-deficient embryos (Fig. 13a,b). Accordingly, whereas the labeling for proliferation marker Ki67 was restricted to the ventricular germinal layer in E14.5 wild-type embryos, it was more extended in Cdh1-null brains (Fig. 13c). Moreover, E14.5 mutant embryos displayed increased incorporation of the nucleotide analog bromodeoxyuridine (BrdU), suggesting increased DNA replication *in vivo* (Fig. 13d).

We next decided to further analyze the proliferative behavior of neural progenitors by generating neurospheres in culture (See Methods) in collaboration with Isabel Fariñas lab (Valencia University). We first tested that Nestin-Cre was active in these neurospheres by introducing in these animals a Rosa26-lox-STOP-lox(LSL)-YFP allele (Fig. 14a). The activity of Cre recombinase on this allele results in the excision of the LSL cassette thus driving the expression of the yellow fluorescent protein (YFP) from the ubiquitously expressed Rosa26 locus. Cdh1 is normally expressed in these primary neurospheres and its ablation resulted in the overexpression of its known substrates such as Tpx2, Cyclin B1, Geminin or Cdc6 (Fig. 14a) as well as reduction in cell cycle inhibitors such as p21Cip1 or p27Kip1, a possible

Figure 13

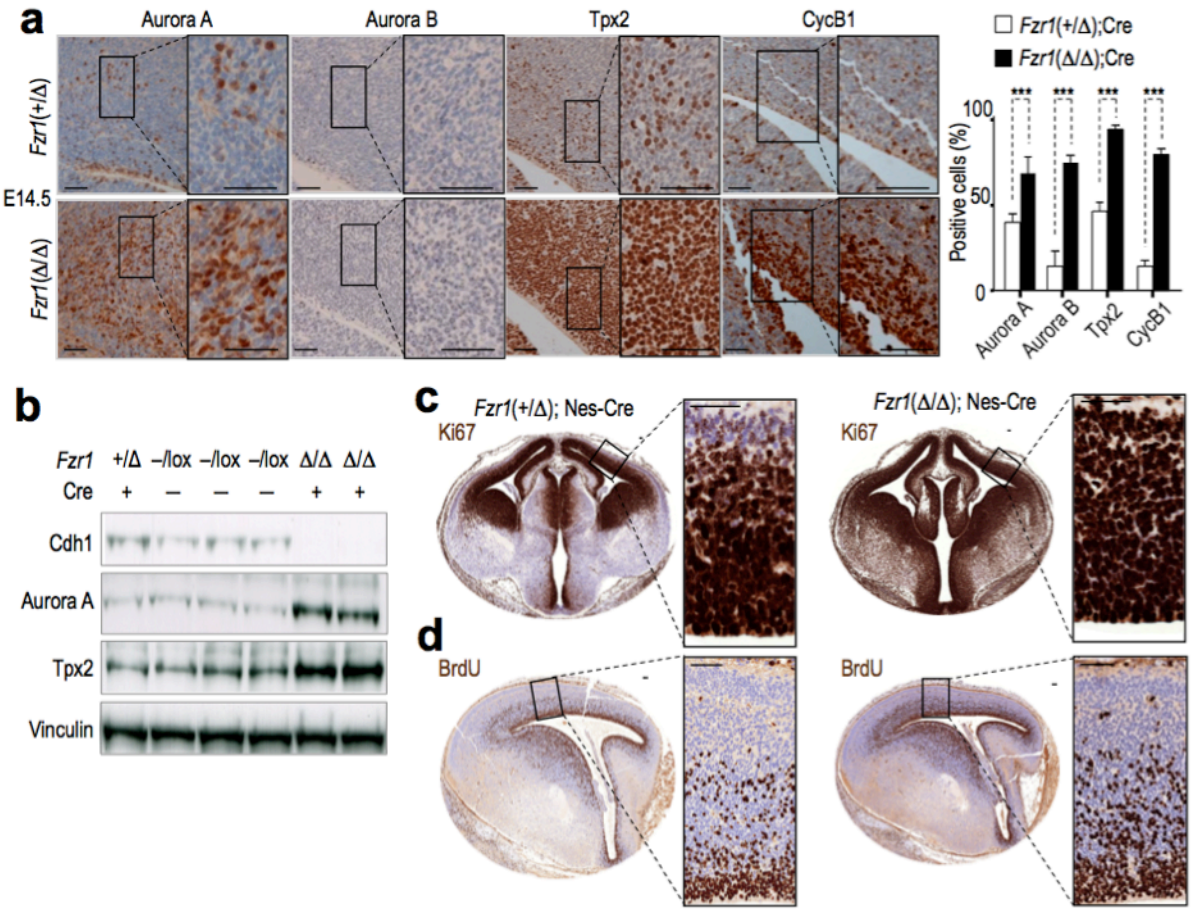

Upregulation of Cdh1 substrates and increased proliferation in Fzr1(Δ/Δ); Nestin-Cre neural progenitors *in vivo*. (**a**) Protein level of several Cdh1 substrates in histological sections of E14.5 brains detected by immunohistochemistry with specific antibodies against the indicated proteins (brown signal). The quantification of these data is shown in the histogram. (**b**) Levels of Cdh1 substrates in E15.5 brain lysates from the indicated genotypes. Vinculin was used as a loading control. (**c**) Increase in the proliferation marker Ki67 in E14.5 Fzr1(Δ/Δ);Nes-Cre brains compared to controls. (**d**) Increased BrdU incorporation in E14.5 Fzr1(Δ/Δ);Nes-Cre brains compared to controls 6 h after the injection of BrdU (100 µg BrdU/g) in the pregnant female. (**a**) and (**d**) are sagital sections; (**c**) are coronal sections. Scale bars, 50 µm.

consequence of the increased levels of the Cdh1-target Skp2, an F-box protein that targets these cell cycle inhibitors for degradation (Fig. 15). Genetic elimination of Cdh1 did not alter the number of primary neurospheres obtained from E14.5 cortices but incorporation of nucleotide analogue EdU in 3-4-day cultures of primary neurospheres was augmented in Cdh1-null neurospheres (Fig. 16a) in agreement with the increased incorporation of BrdU in

Figure 14

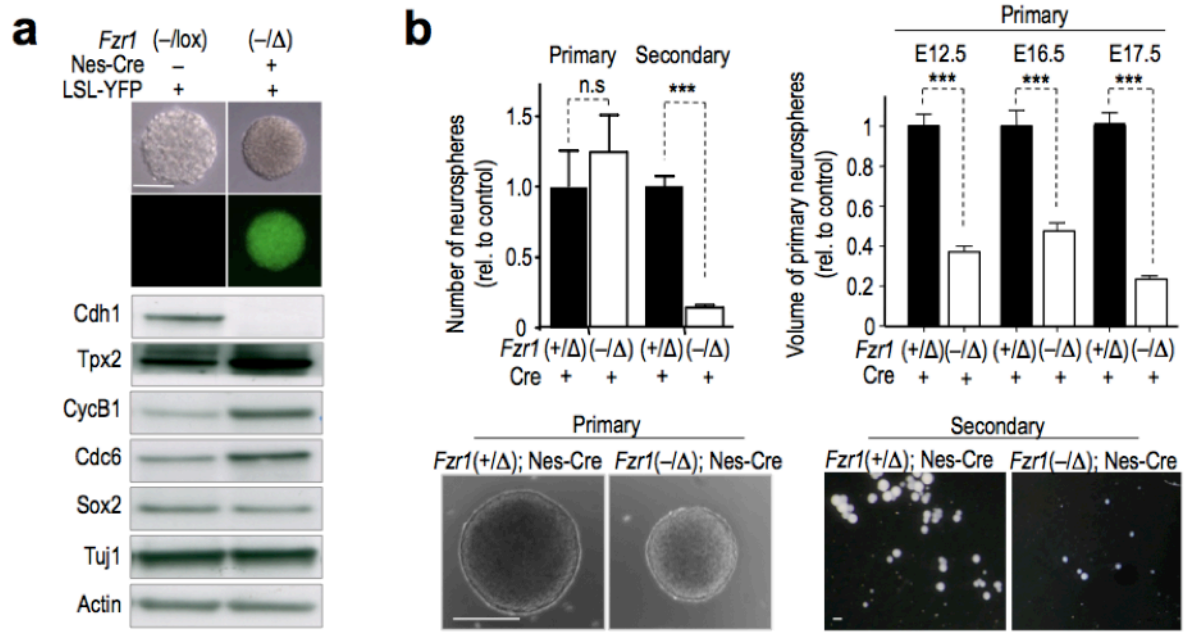

Accumualtion of Cdh1 substrates and proliferation defects in Fzr1(Δ/Δ); Nestin-Cre neurospheres *in vitro*. (**a**) Analysis of Nestin-Cre expression and activity using the Rosa26-loxP-STOP-loxP(LSL)-YFP reporter allele in cultured neurospheres. Cre activity results in the excision of the LSL cassette and expression of YFP. This activity also results in the genetic ablation of Cdh1 and the stabilization of several Cdh1 substrates such as Tpx2, Cyclin B1, geminin or Cdc6 in mutant neurospheres. Actin is used as a protein loading control whereas the presence of Sox2 and Tuj1 indicate a mixture between progenitors and neurons in these neurospheres. (**b**) Quantification of the number and size of primary or secondary neurospheres generated from E14.5 (left histograms) or E12.5-17.5 (right histograms) embryonic brains. Scale bars, 100 µm.

utero (Fig. 13d). Intriguingly, the size of these primary neurospheres was significantly reduced (20-50% of the control volume; Fig. 14b) when using E12.5-E17.5 embryos. In agreement with these observations, the number of secondary neurospheres generated after disaggregation of the E14.5 primary neurospheres was dramatically reduced (Fig. 14b). These results suggested that Cdh1 supports normal proliferation of neural progenitors mostly by regulating entry into S-phase.

Figure 15

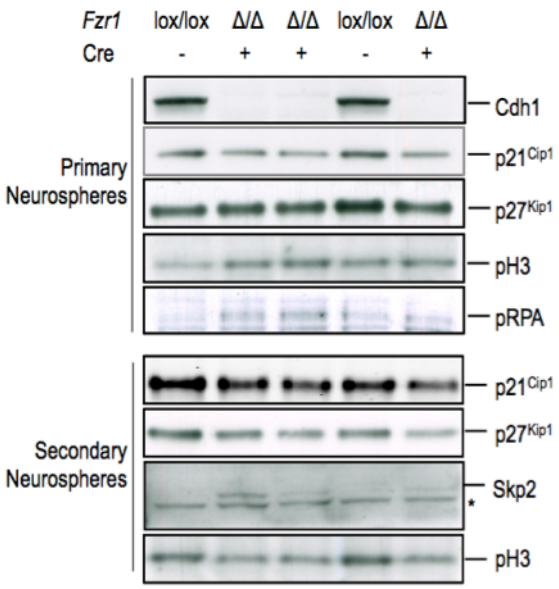

Decreased levels of Cdk inhibitors in Cdh1-null progenitors. Reduction in the levels of Cdk inhibitory proteins in Cdh1-deficient primary and secondary neurospheres. Immunoblot of Fzr1(Δ/Δ);Nestin-Cre primary and secondary neurospheres showing decreased levels of p21Cip1 and p27Kip1. Phosphorylation of histone H3 (pH3) is increased in Fzr1(Δ/Δ);Nestin-Cre primary neurospheres (probably as a consequence of increase arrest in late G2; see main text) but decreases in secondary neurospheres suggesting lack of proliferation. Primary neurospheres also display accumulation of phosphorylated (p)RPA, a marker of DNA damage. *, non-specific band.

1.4. Cdh1 modulates Cdk activity in neural progenitors preventing replicative stress

Cdh1-deficient fibroblasts are known to display a shorter G1 phase, early entry into S-phase and signs of senescence (Garcia-Higuera *et al.*, 2008; Li *et al.*, 2008). We therefore asked whether the increased entry into S-phase was causing replicative defects in these neural progenitors. Phosphorylation of H2AX (γH2AX) is normally present at low levels and in a dot-pattern during normal replication of cells but is eliminated as cells exit from S-phase and progress to mitosis. Lack of Cdh1 resulted in the accumulation of γH2AX both in primary and secondary neurospheres (Fig. 16a,b). Importantly, this signal was significantly increased in EdU-negative Cdh1-null cells, suggesting the presence of DNA damage beyond S-phase. Cdh1-null secondary neurospheres also presented increased levels of replicative stress, indicated by the presence of strong pan-nuclear γH2AX signals (in 46% of Cdh1-null versus 11% control neurospheres; Fig. 16b).

Figure 16

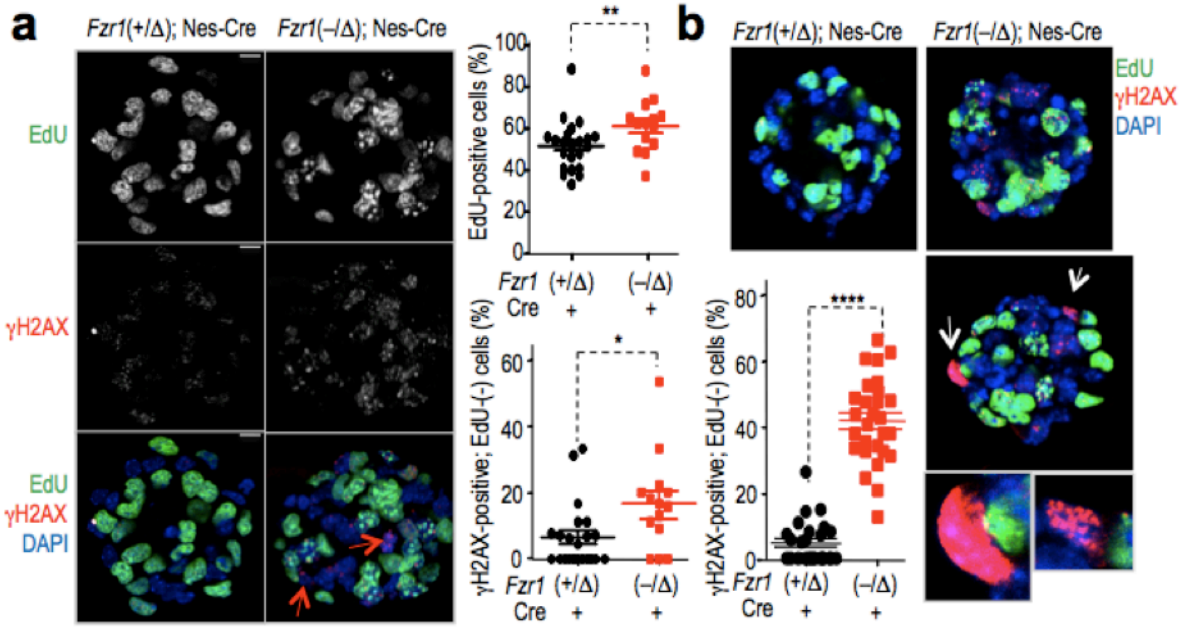

Cdh1 ablation results in replicative stress in neural progenitors *in vitro*. (**a**) EdU, and γH2AX immunofluorescence in primary neurospheres. Histograms show the quantification of EdU incorporation and γH2AX-positive/EdU-negative cells in these cultures. (**b**) EdU and γH2AX immunofluorescence in secondary neurospheres and quantification of γH2AX positive/EdU negative cells. Cdh1-deficient secondary neurospheres also display strong pan-nuclear γH2AX staining (white arrows). Scale bars, 25µm. Histograms show the quantification of positive cells for the different markers. **, p<0.01; ***, p<0.001.

The aberrant γH2AX signal was present in both Sox9-(not shown) and Sox2-positive cells of the ventricular layer (Fig. 17a) whereas this signal was not observed in control embryos indicating that lack of Cdh1 induced replicative stress in these neural progenitors *in vivo*. Importantly, replicative stress was accompanied by the induction of p53 and apoptosis (Fig. 17b). The cellular response to replicative stress in the absence of Cdh1 increased in a progressive manner during development (E12.5-E16.5; Fig. 17b). Genetic ablation of Cdh1 driven by the Sox2 promoter similarly resulted in replicative stress, induction of p53 and apoptosis (Fig. 18).

Figure 17

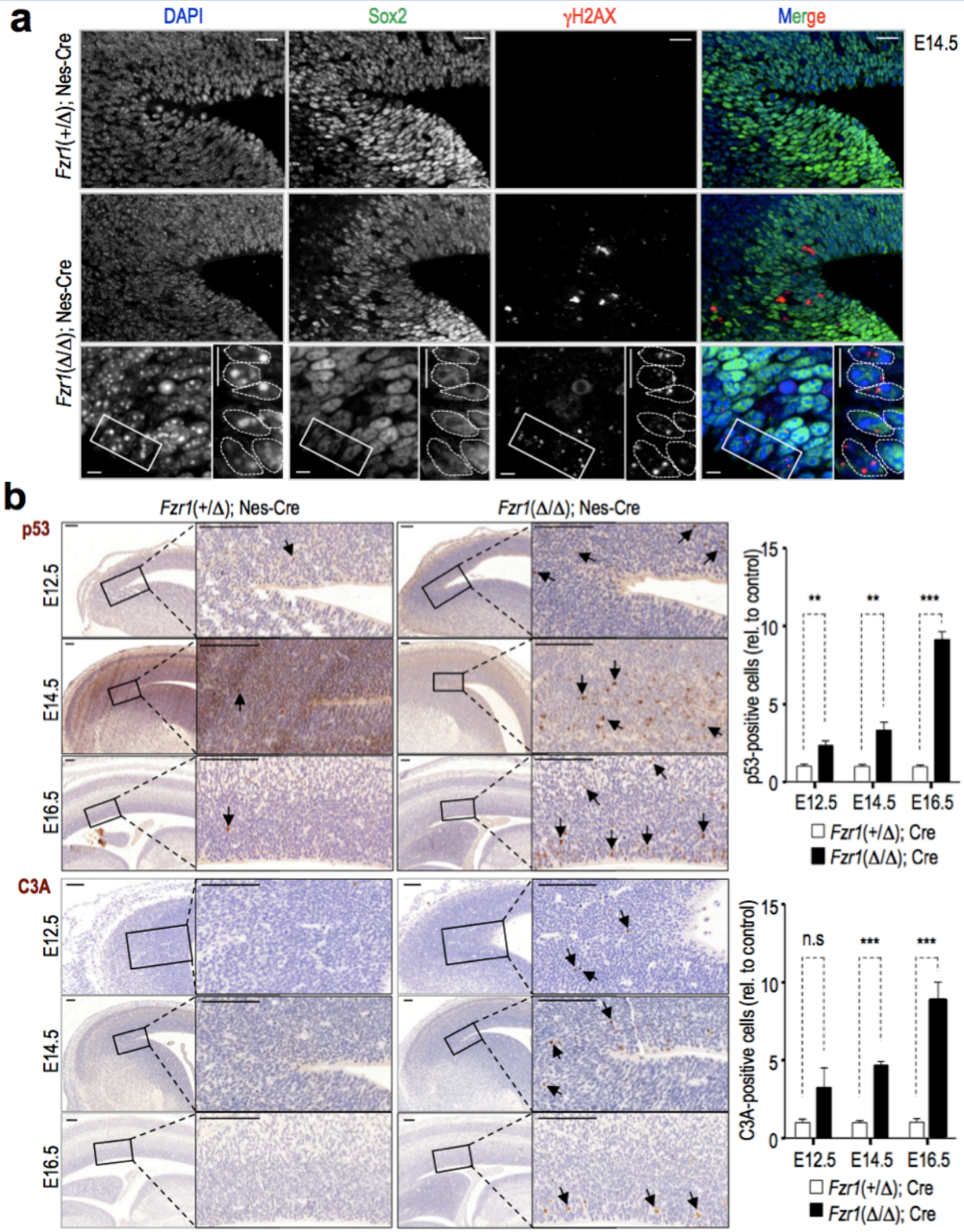

Cdh1 depletion results in replicative stress and a DNA damage-like response in neural progenitors *in vivo*. (**a**) Accumulation of phosphorylated H2AX (γH2AX; red) in neural progenitors (Sox2 staining, green) in the ventricular area of the brain from E14.5 Cdh1-null embryos. DAPI, DNA. Scale bars, 25 µm (top panels) or 10 µm (bottom panels). (**b**) Progressive increase in p53 and active caspase-3 (C3A) signal (brown) during embryonic development (E12.5-E16.5). ns, not significant ($p>0.05$), **, $p<0.01$; ***, $p<0.001$. Scale bars, 100µm.

Figure 18

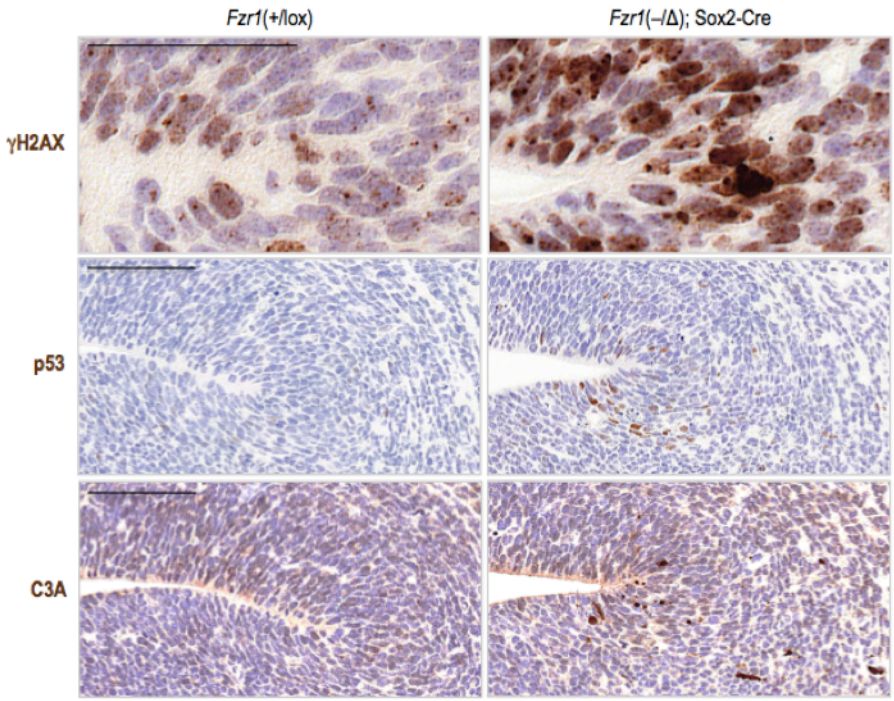

Accumulation of phosphorylated H2AX (γH2AX), p53 and apoptosis (active caspase 3, C3A) in the ventricular area of Fzr1(–/Δ); Sox2-Cre mice. Coronal sections. Scale bars, 100 µm.

Cdh1 targets for degradation multiple proteins involved in many different pathways. However, we reasoned that one of the major consequences of lack of Cdh1 is hyperactivation of Cdks due to the increased levels of cyclins during G1. We therefore explored the effect of partially inhibiting Cdks in Cdh1-null cells using the small-molecule inhibitor roscovitine. Partial inhibition of Cdks using low dose of inhibitor prevented the replicative stress observed in Cdh1-deficient cells after disaggregation of secondary neurospheres (Fig 19a). Importantly, this leads to increase proliferation (as scored by EdU incorporation; Fig. 19a), suggesting that both the replicative stress and the defective proliferation is at least partially induced by increased Cdk activation in the absence of Cdh1. Similar results were found in cells obtained from primary neurospheres (Fig. 20) although the effect of roscovitine was not as dramatic in agreement with the increased presence of replicative stress in secondary neurospheres (Fig. 16a,b). In addition, whereas high concentration of roscovitine inhibited proliferation (a well-known effect) at high dose, low dose of this inhibitor did not induce proliferation in wild-type cells and actually slightly

Figure 19

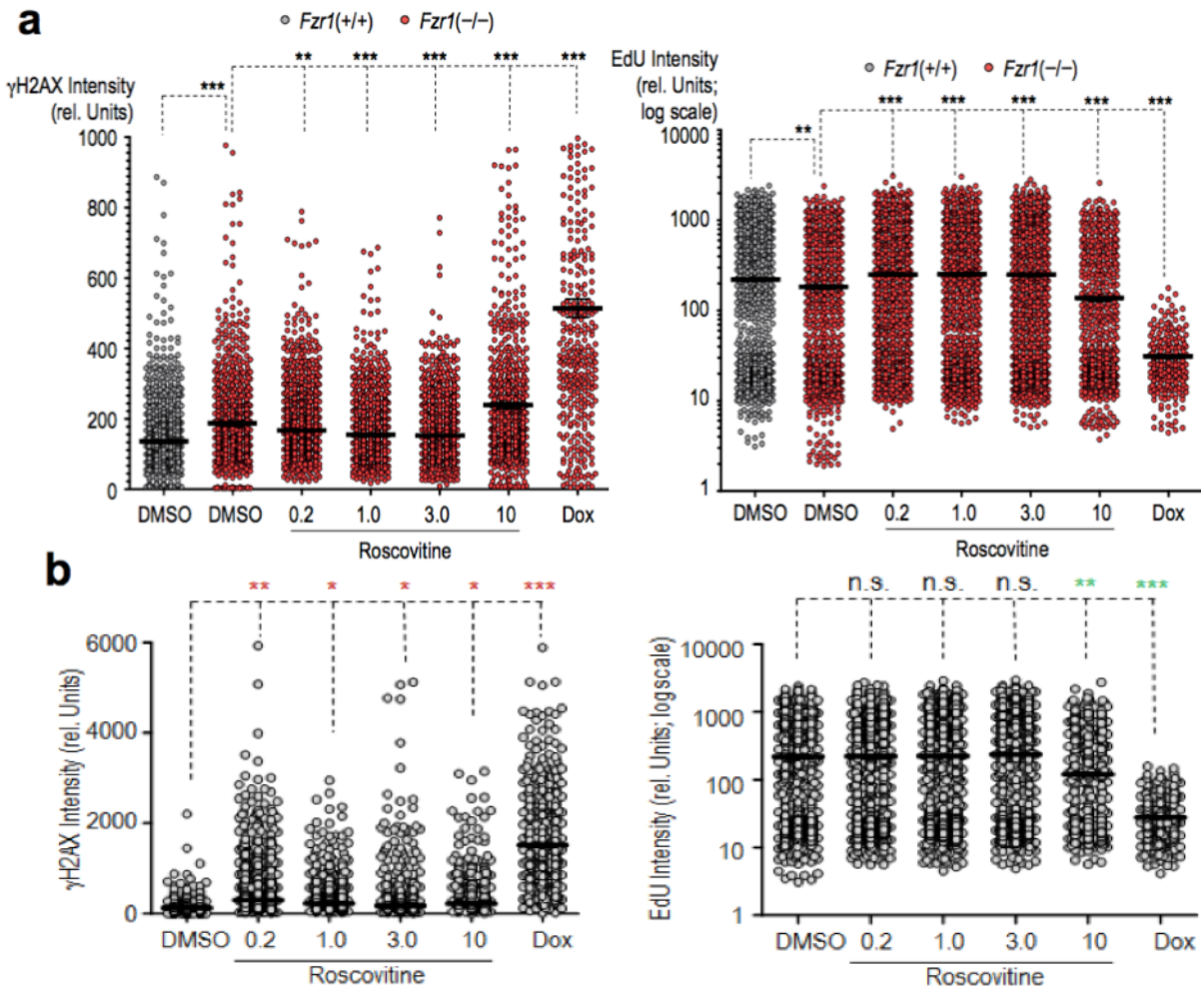

Replicative stress in Cdh1-deficient neural progenitors from secondary neurospheres is prevented by partial inhibition of Cdk activity. (**a**) Quantification of γH2AX or EdU intensity in control (grey) or Cdh1-deficient (red) neural progenitors from secondary neurospheres treated for 8h with the indicated dose of Roscovitine (µM) or Doxorubicin (0.5 µg/mL) using high-throughput microscopy (HTM). In the last 30 min of the treatment they were in the presence of EdU (10 µM). (**b**) Effect of similar treatments in wild-type controls. Doxorubicin is used as a positive control of DNA damage accumulation (µH2AX staining) and as a negative control of proliferation (absence of EdU incorporation). *, p<0.05; **, p<0.01; ***, p<0.001.

increased γH2AX signal (Fig. 19b), indicating a specific protective effect of roscovitine in Cdh1-null cells. The addition of nucleosides to these cultures also resulted in a partial protective effect in agreement with recent observations on the relevance of nucleotide levels to prevent replicative stress (Bester *et al.*, 2011).

Figure 20

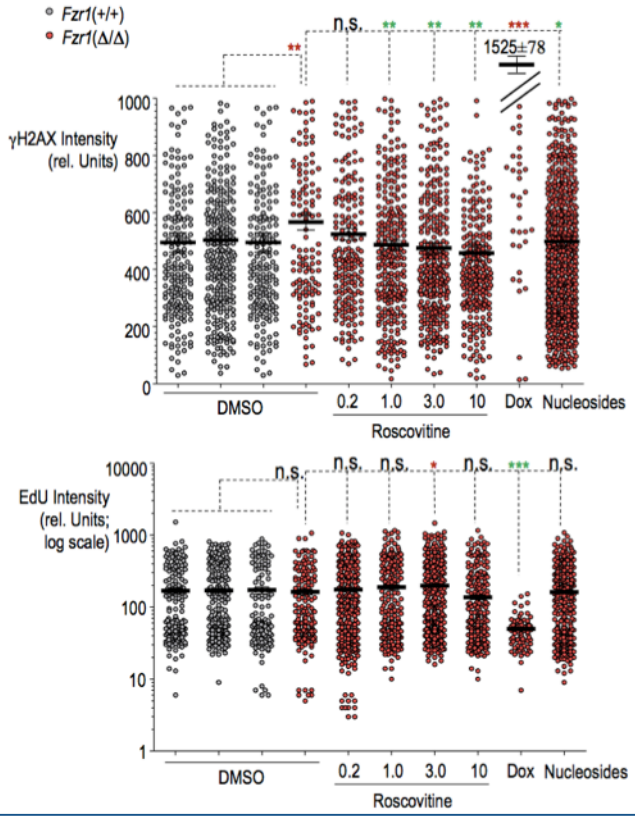

Replicative stress in Cdh1-deficient neural progenitors from primary neurospheres is prevented by partial inhibition of Cdk activity or nucleosides addition. Quantification of γH2AX or EdU intensity in control (grey) or Cdh1-deficient (red) neural progenitors from primary neurospheres treated for 8h with the indicated dose of Roscovitine (μM) or Doxorubicin (0.5 μg/mL), or the addition of nucleosides. *, p<0.05; **, p<0.01; ***, p<0.001.

1.5. Cdh1 deficiency causes a DNA damage response leading to G2 arrest

To further understand whether the increased entry into the cell cycle in the presence of replicative defects was accompanied not only by death but also by defective cell division, we analyzed the pattern of phosphorylation of histone H3 (pH3). This signal shows a spotted pattern during late G2 whereas mitotic cells are characterized by fully condensed chromosomes positive for the pH3 mark (Van Hooser *et al.*, 1998). As observed in Fig. 21a, there was a dramatic increase in the percentage of pH3-positive with spotted pattern (G2-like) in the cortex of E14.5 Cdh1-deficient embryos. These cells frequently displayed duplicated centrosomes (Fig. 21b) and approximately a 2-fold increase in nuclear volume (Fig. 21c), suggesting a DNA content of 4N and confirming that these cells arrested after S-phase, a phase in which centrosomes are duplicated.

Figure 21

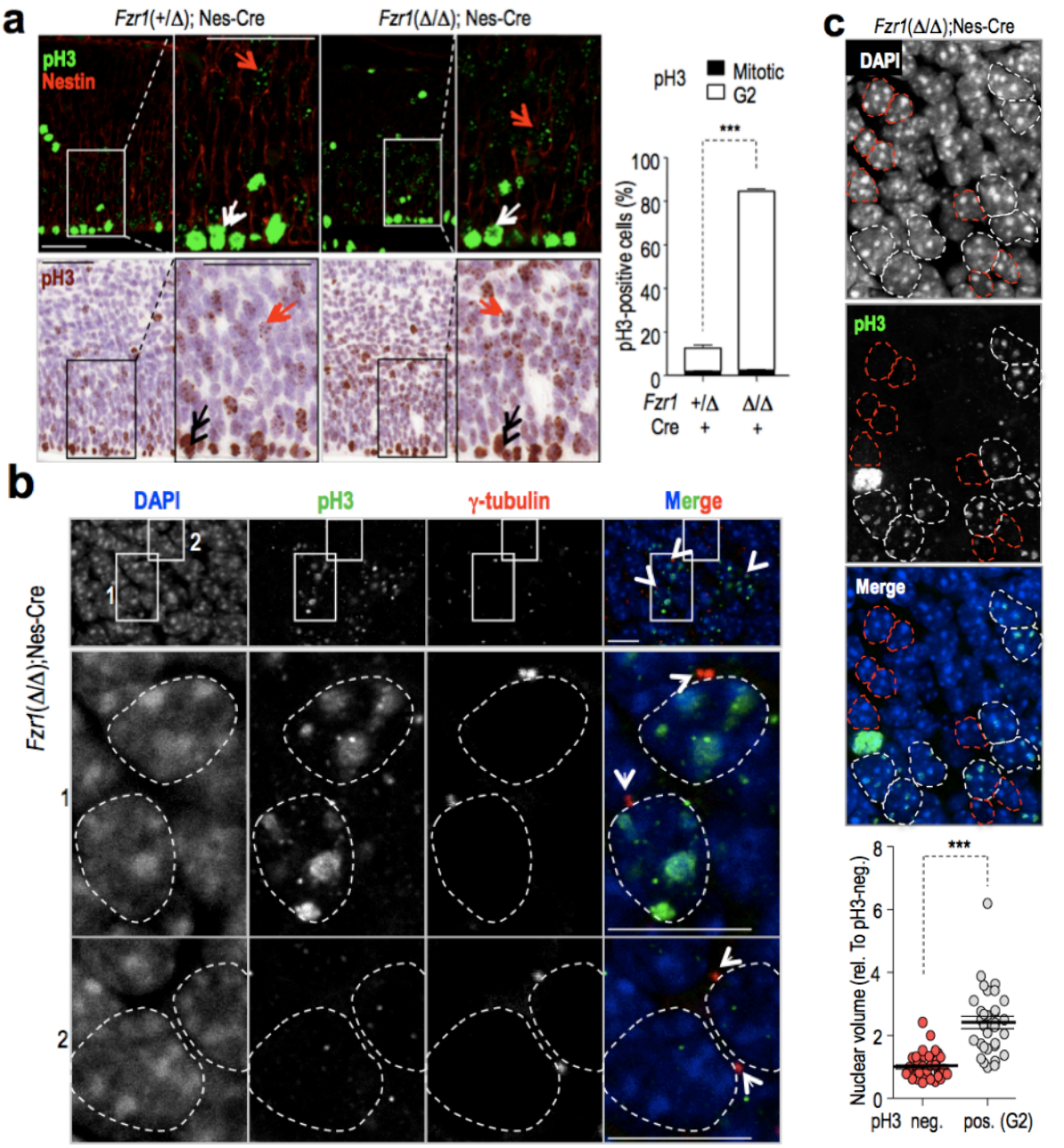

Accumulation of G2-like cells in the neuroepithelium of Cdh1-null brains. (**a**) Phosphorylation of histone H3 (pH3; red arrows) showing an increase in the number of G2-pattern pH3-positive cells in E14.5 Cdh1-deficient brains. The percentage of G2- (red arrows) or mitotic-pH3-positive (white or black arrows) cells is shown in the histogram. (n>1000 cells per genotype). (**b**) The presence of two centrosomes (γ-tubulin red staining; arrowheads) in cells with the spotted pH3 (green) pattern suggests accumulation of G2 cells in Cdh1-deficient mice (inset 1). As a control only one centrosome is observed in cells negative for pH3 (inset 2). DNA is in blue. Note that centrosomes are not evident in all cells due to the thickness (5 µm) of the section. (**c**), Quantification of the nuclear volume of pH3-negative (white lines) and pH3-positive cells (red lines) in the cortex of Fzr1(Δ/Δ);Nes-Cre embryos. The nuclear volume of at least 40 cells per genotype was calculated. Scale bars, 10 µm.

Since Cdh1 has been reported to modulate axonal growth and patterning (Konishi *et al.*, 2004) we also tested the differentiation potential of these mutant neural progenitors. Cdh1-null neural progenitors displayed normal ratios of symmetric (leading to two progenitors or two neurons) versus asymmetric (leading to one progenitor + one neuron) cell divisions *in vitro* (Fig. 22a,b), thus indicating that Cdh1 is not required for asymmetric division. Importantly, Cdh1-null cells displayed increased γH2AX signals in these assays (Fig. 22c). We also isolated and cultured postmitotic neurons from E14.5 cortices and stained them for β-III-tubulin. A significant number of the neurons generated from Cdh1-null E14.5 brains displayed abnormal morphology, with poorly developed neurites and picnotic nuclei (Fig. 22d) in agreement with cell death induced by Cdh1 loss as reported previously in postmitotic neurons (Almeida *et al.*, 2005). All together, these data suggest that, in addition to other possible defects in neurite outgrowth, lack of Cdh1 results in an abnormal proliferative response in the developing brain in which neural progenitors display an accelerated entry into S phase, replicative stress, arrest in a G2-like stage and/or cell death in the presence of p53.

1.6. The accumulation of DNA damage in Cdh1-null cells is p53-independent, but results in p53-dependent cell death

To obtain additional insights into the molecular pathways involved in the DNA damage and apoptotic response in Cdh1-null brain, we decided to study the effect of Cdh1 depletion in different genetic backgrounds. We first used cyclin B1 mutant mice since cyclin B1 is a major Cdh1 substrate and cyclin B1 overexpression is known to induce apoptotic cell death in terminally differentiated neurons (Almeida *et al.*, 2005). Since complete ablation of cyclin B1 leads to embryonic lethality (Brandeis *et al.*, 1998), we analyzed the survival of Fzr1(Δ/Δ); Nes-Cre; Ccnb1(+/–) mice harboring a single copy of the cyclin B1-encoding gene.

Figure 22

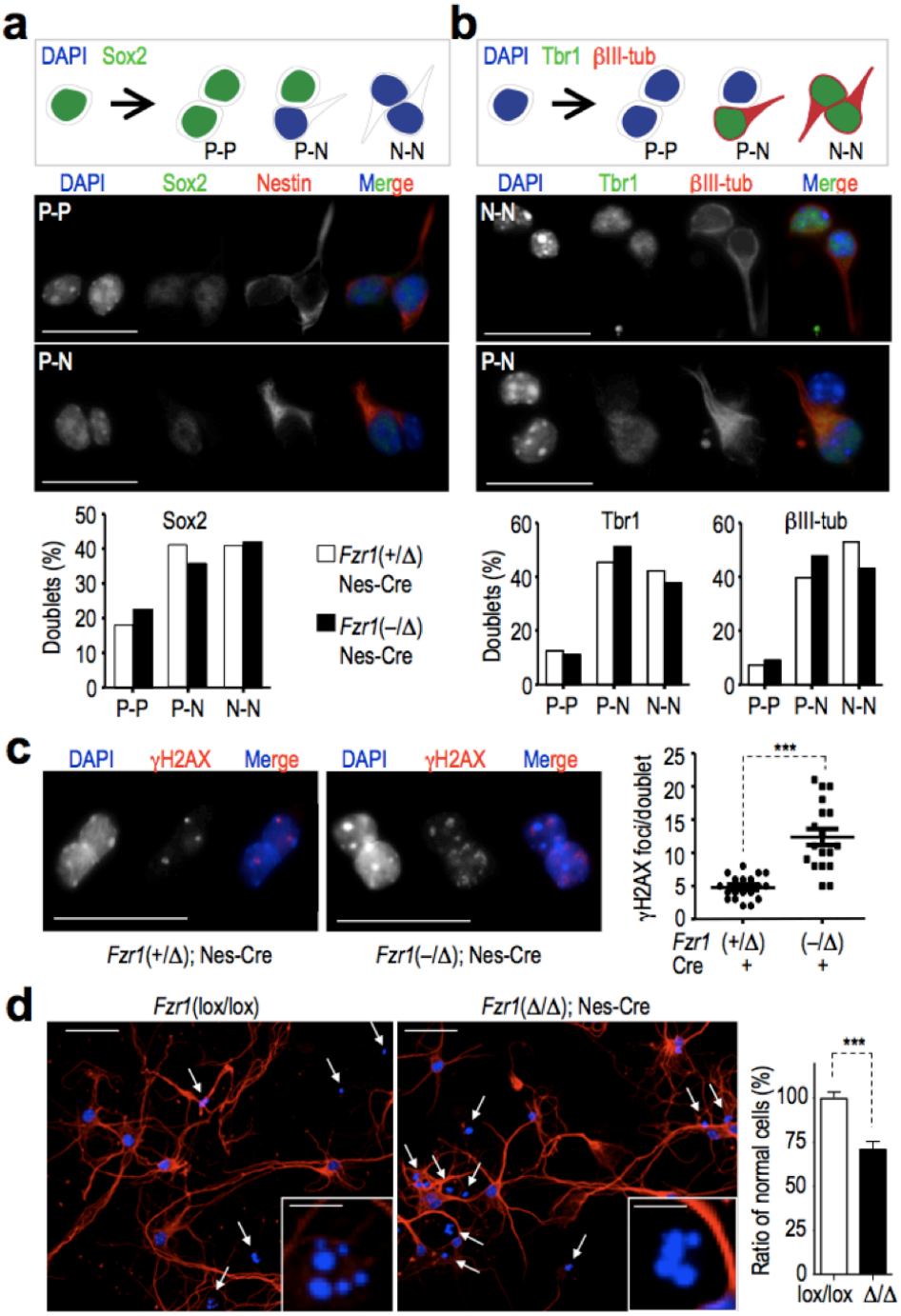

Differentiation of Cdh1-null neural progenitors. (**a**) Immunofluorescence of Sox2 and Nestin in cell doublets originated in differentiation medium. P, progenitor; N, neuron. (**b**) Similar staining for Tbr1 and βIII-tubulin. P = progenitor; N= neuron. (**c**) Quantification of DNA damage accumulated in the doublets. (**d**) Culture of primary cortical neurons from E14.5 embryos. Abnormal cells (arrows and insets) with lack of neurites and possible apoptotic nuclei are indicated by arrows and quantified in the histogram. ***, p<0.001. Data are not significantly different in (**a**) and (**b**). Scale bars are 25 µm. Scale bars, 50 µm (**a**), 25 µm (**b-d**), 10 µm (insets in **d**).

Figure 23

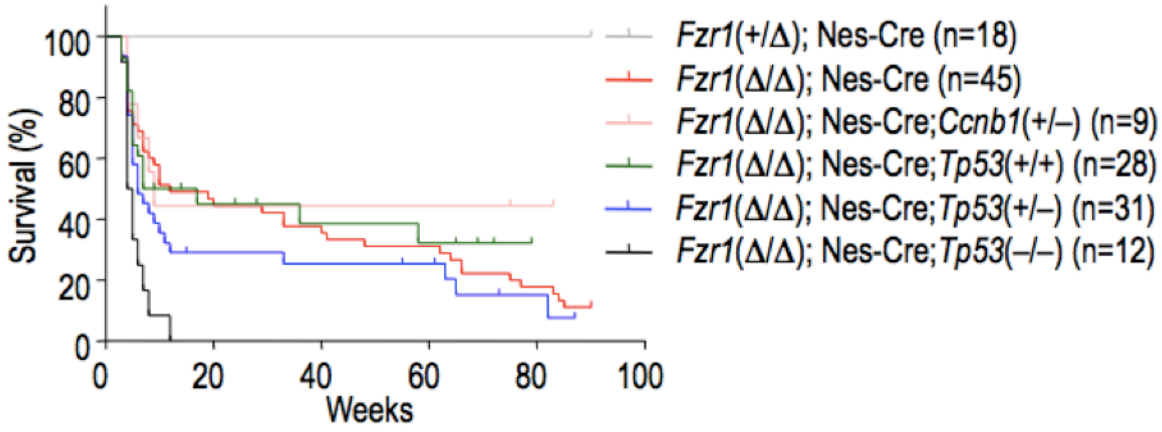

Effect of Cdh1 ablation in different genetic backgrounds. Survival curve of Fzr1(Δ/Δ); Nestin-Cre mice in a Ccnb1(+/–), Tp53(+/–) or Tp53(–/–) background. Only the complete ablation of p53 results in significant ($p<0.001$) differences when compared to Fzr1(Δ/Δ); Nestin-Cre mice.

As represented in Fig. 23, Fzr1(Δ/Δ); Nes-Cre; Ccnb1(+/–) mice display early lethality similar to Fzr1(Δ/Δ); Nes-Cre mice with normal copies of cyclin B1, accompanied by the presence of hydrocephalus (not shown). Lack of one allele of cyclin B1 partially stabilized survival of adult animals although these differences did not reach statistical significance (Fig. 23).

We next tested the effect of eliminating p53 in a Cdh1-null background. Deletion of a single allele of p53 had some effect in the survival of Cdh1-null mice, and Fzr1(Δ/Δ); Nes-Cre; Tp53(+/–) mice died with slightly accelerated kinetics when compared to Fzr1(Δ/Δ); Nes-Cre; Tp53(+/+) animals (Fig. 23). Deletion of both alleles of p53 resulted in a dramatic acceleration of lethality within the first 10 weeks of age (Fig. 23). This lethality was not due to the development of lymphomas o sarcomas typical of p53-null mice (latency ~ 6 months). Instead, Fzr1(Δ/Δ); Nes-Cre; Tp53(–/–) mice died with a more aggressive phenotype characterized by hydrocephalus and severely hypoplastic brains (Fig. 24).

Figure 24

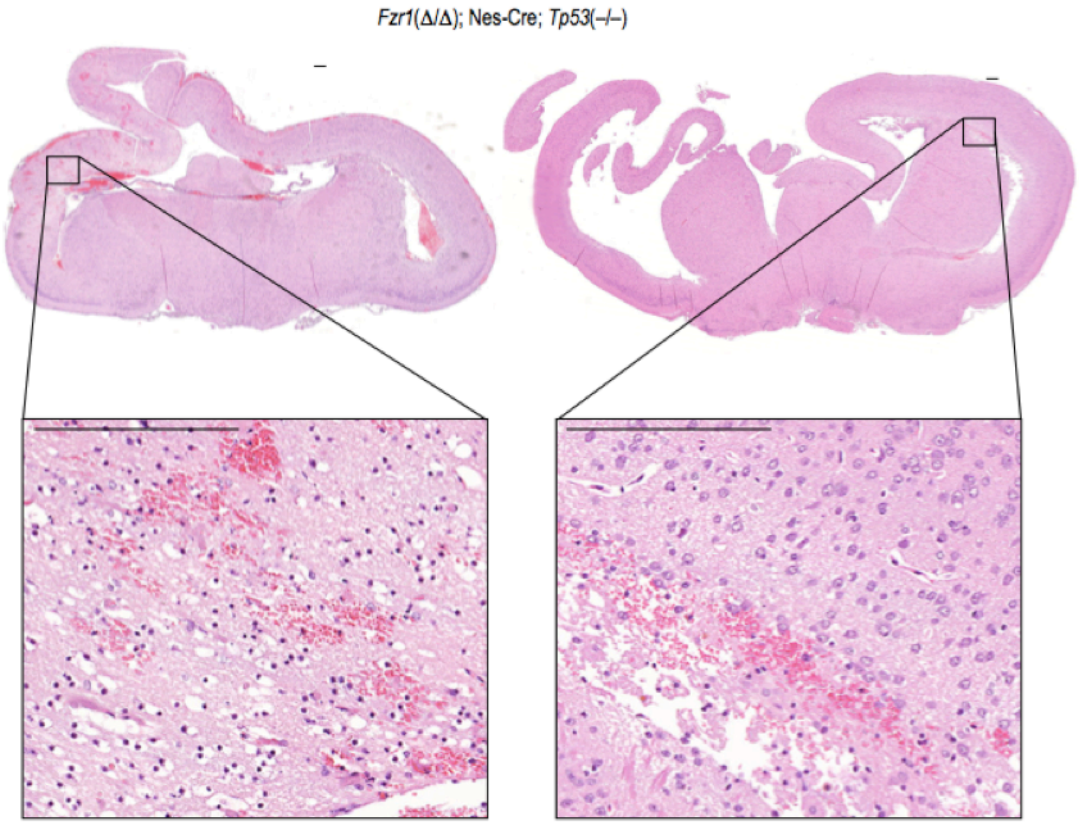

Massive hemorrhages in brains of Fzr1(Δ/Δ); Nestin-Cre; Tp53(−/−) mice. Images correspond to H&E staining of coronal sections. Scale bars, 200 µm.

Importantly, no apoptosis was observed in p53-deficient embryos (Fig. 25) suggesting that this protein is essential for cell death caused by Cdh1 loss. Instead, these double mutant brains displayed increased accumulation of cells positive for the γH2AX signal in the embryonic cortex (Fig. 25). These defects were already evident during embryogenesis (Fig. 25) but were more dramatic at postnatal stages. The presence of the γH2AX signal was dramatically increased at P10 all over the brain of Fzr1(Δ/Δ); Nes-Cre; Tp53(–/–) mice, including not only the ependymal layer but also cortical regions in which the damaged cells were rarely observed in Fzr1(Δ/Δ); Nes-Cre; Tp53(+/+) animals [4.1% in Fzr1(Δ/Δ); Nes-Cre; Tp53(–/–) brains vs. 0.4% in Fzr1(Δ/Δ); Nes-Cre; Tp53(+/+) brains; Fig. 26a,b).

Figure 25

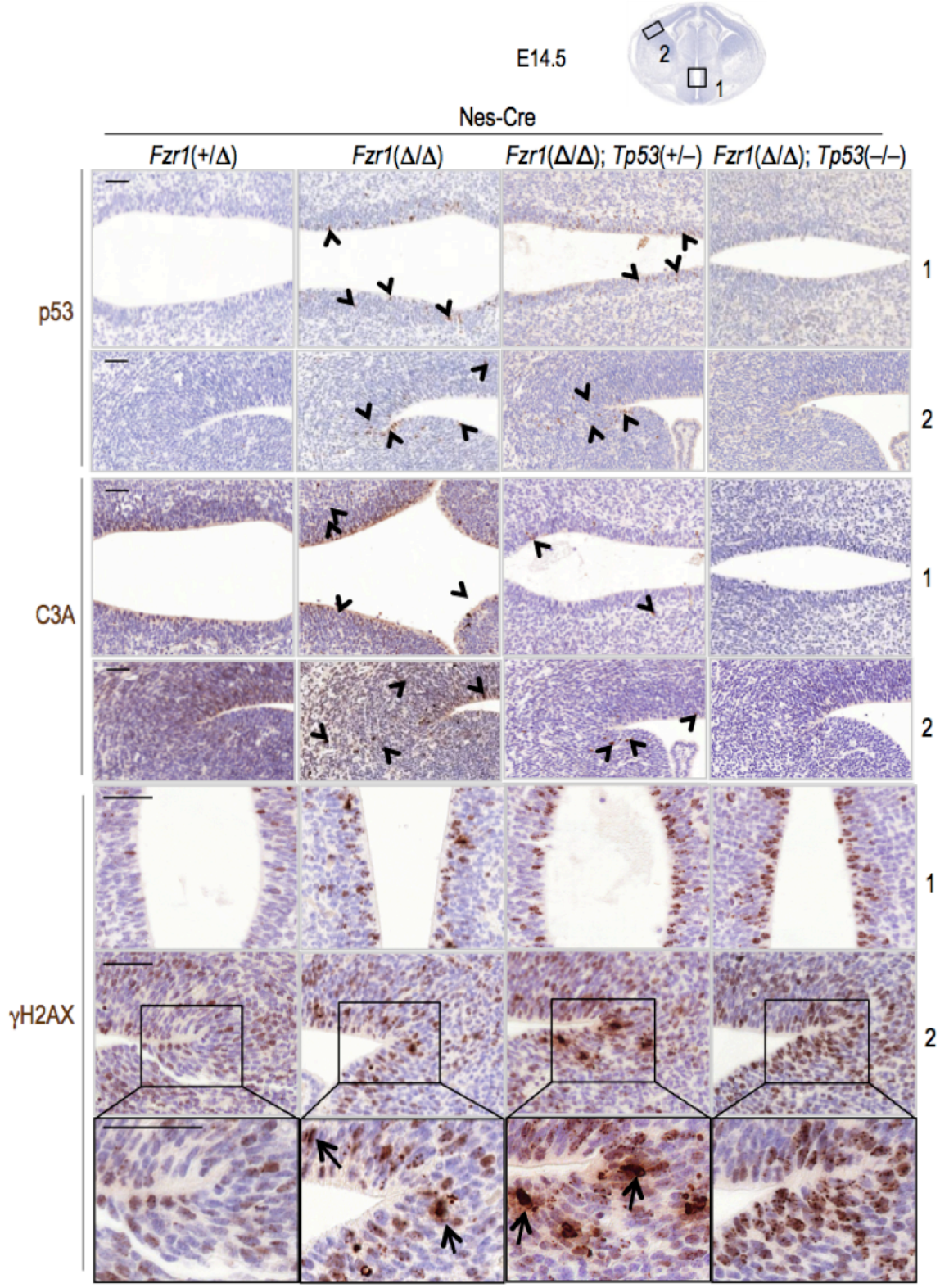

p53 concomitant depletion in Cdh1-null mice avoids the apoptotic response but not the accumulation of DNA damage. Staining of p53, active caspase-3 (C3A) and γH2AX in Fzr1(Δ/Δ); Nestin-Cre and control cortices (1) and the ependymal layer of the third ventricle (2) in E14.5 embryos. Arrowheads indicate representative positive cells for the different stainings. Scale bars, 50 µm.

Figure 26

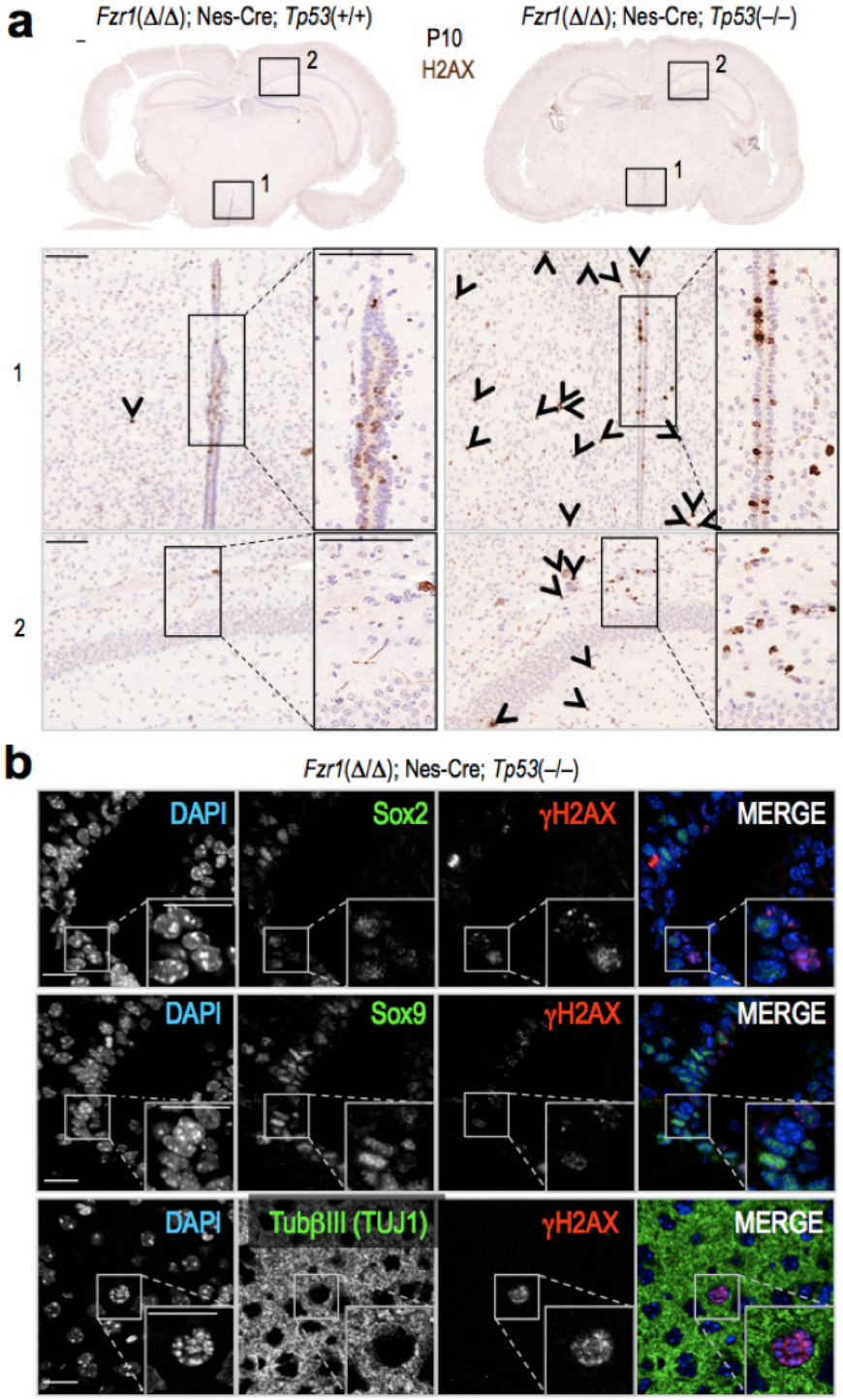

Persistence of damaged neurons after birth in double Cdh1; p53 mutant brains. (**a**) Immunohistochemical analysis of phosphorylation of H2AX (γH2AX) in P10 brain sections of Fzr1(Δ/Δ); Nestin-Cre; Tp53(+/+) and Fzr1(Δ/Δ); Nestin-Cre; Tp53(–/–) mice. The presence of DNA damage in the ventricles (1) and the cortex (2) is indicated by the γH2AX signal (arrowheads). (**b**) Immunofluorescence analysis of γH2AX, Sox2, Sox9, and Neuron-specific class III beta-tubulin (βIII-Tub) showing the presence of damage in cortical postmitotic neurons of Fzr1(Δ/Δ); Nestin-Cre;p53(–/–) mutant mice. Scale bars, 100 μm (**a**) and 20 μm (**b**).

Damaged cells included not only Sox2- and Sox9-progenitor cells in the subventricular zone of these brains but also postmitotic neurons characterized by the cytoplasmic βIII-tubulin staining (Fig. 26b).

Similarly, lack of p53 did not rescue the accumulation of Ki67 (Fig. 27) or G2-like pH3-positive cells (Fig. 28) but rather resulted in an accumulation of these damaged cells in the brains of Cdh1-null. Despite the presence of these additional damaged cells, lack of p53 did not rescue the reduced thickness of the cortex of Cdh1-deficient brains (Figs. 27, 28). Indeed, double Cdh1; p53 mutant brains presented severe malformations and massive hemorrhages (Fig. 24). All together, these results suggest that p53 is not involved in the generation of replicative stress in the absence of Cdh1, but it is critical for preventing developmental defects caused by the presence of damaged, non-functional Cdh1-null cells.

1.7. Hydrocephalus is accompanied by a cellular response to Cdh1 deficiency in ependymal cells

Hydrocephalus is an excessive accumulation of cerebrospinal fluid (CSF) in the brain resulting in an abnormal enlargement of the ventricles. This condition could be caused by impaired CSF flow, reabsortion or production. Since Fzr1(Δ/Δ); Nes-Cre mice developed hydrocephalus we first examined choroid plexus, the estructure that produces the CSF. In our model the choroid plexus showed no gross morphological aberrancies and absence of signs of replicative stress or damage (Fig. 29).

Figure 27

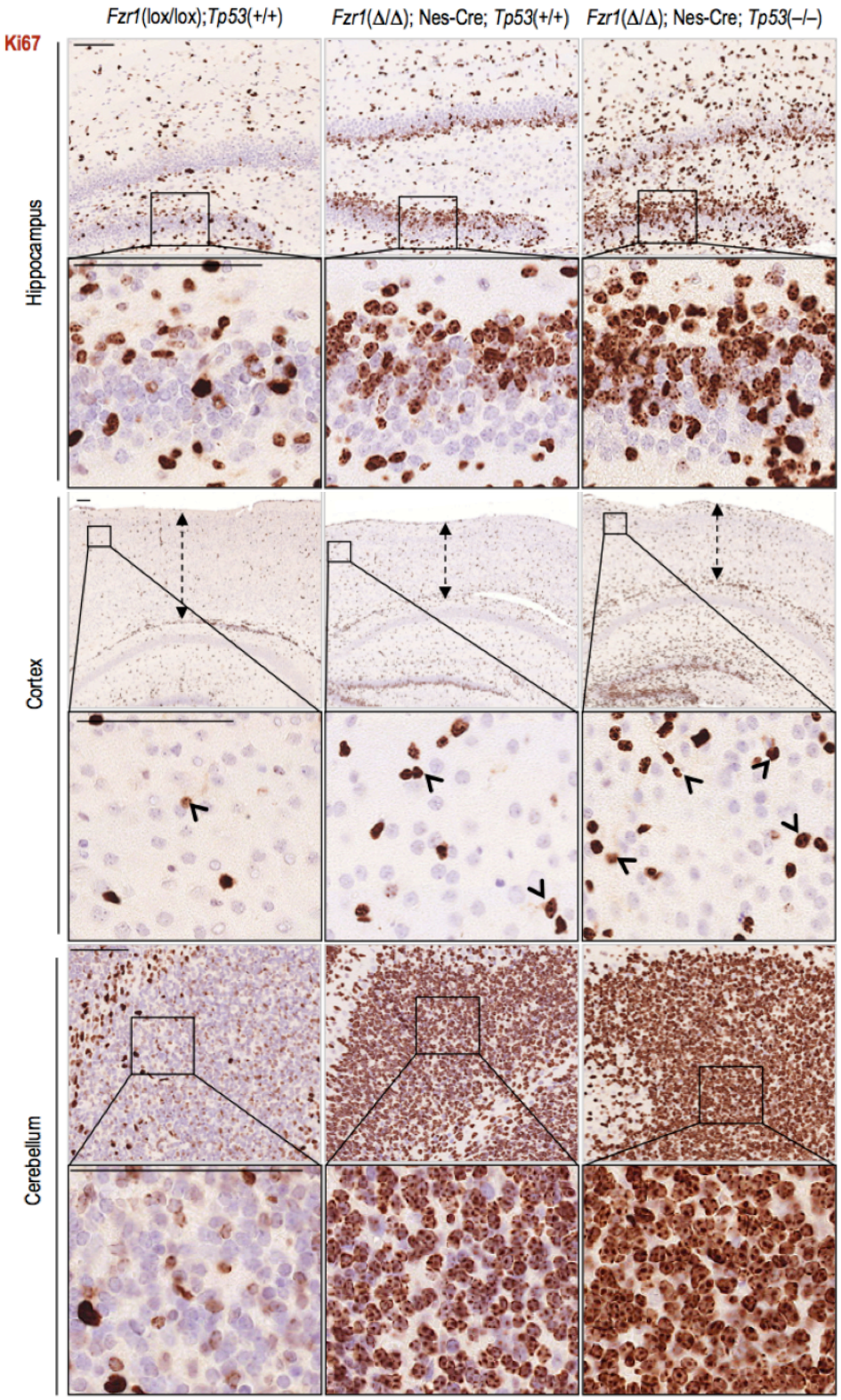

Accumulation of the proliferation marker Ki67 in the hippocampus, cortex and cerebellum of P10 Cdh1-deficient and double Cdh1; p53 mutant mice. The concomitant depletion of p53 leads to further accumulation of Ki67-positive cells (arrowheads). Cdh1-null and double Cdh1; p53-null mice display a similar reduction in the thickness of the cortex (arrows). Coronal sections. Scale bars, 100 µm.

Figure 28

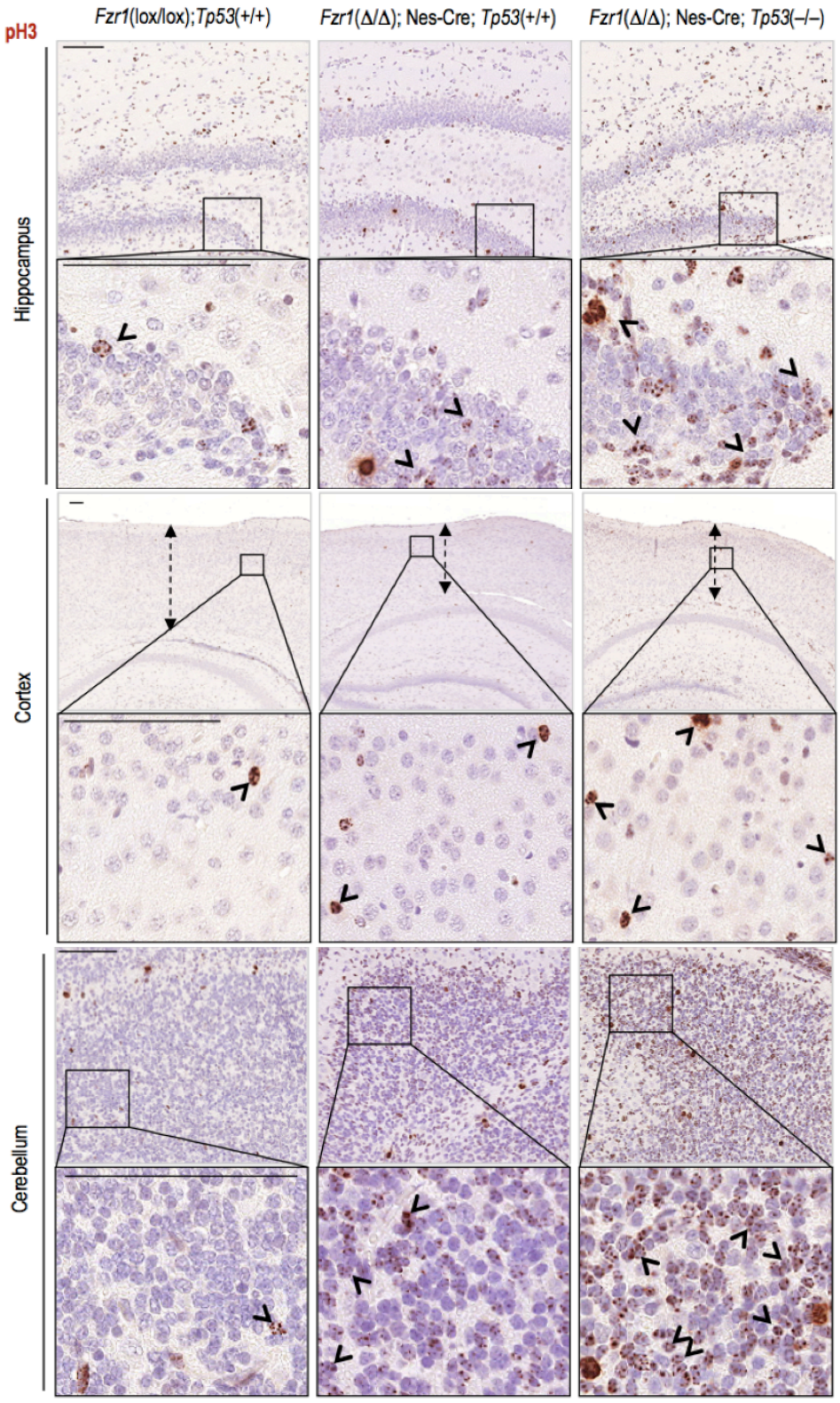

Accumulation of cells with a G2-like pattern in the phosphorylation of histone H3 (pH3) cells in the brain of P10 Cdh1-deficient and double Cdh1; p53 mutant mice. The concomitant depletion of p53 leads to further accumulation of Ki67-positive cells (arrowheads). Cdh1-null and double Cdh1; p53-null mice display a similar reduction in the thickness of the cortex (arrows). Coronal sections. Scale bars, 100 µm.

Figure 29

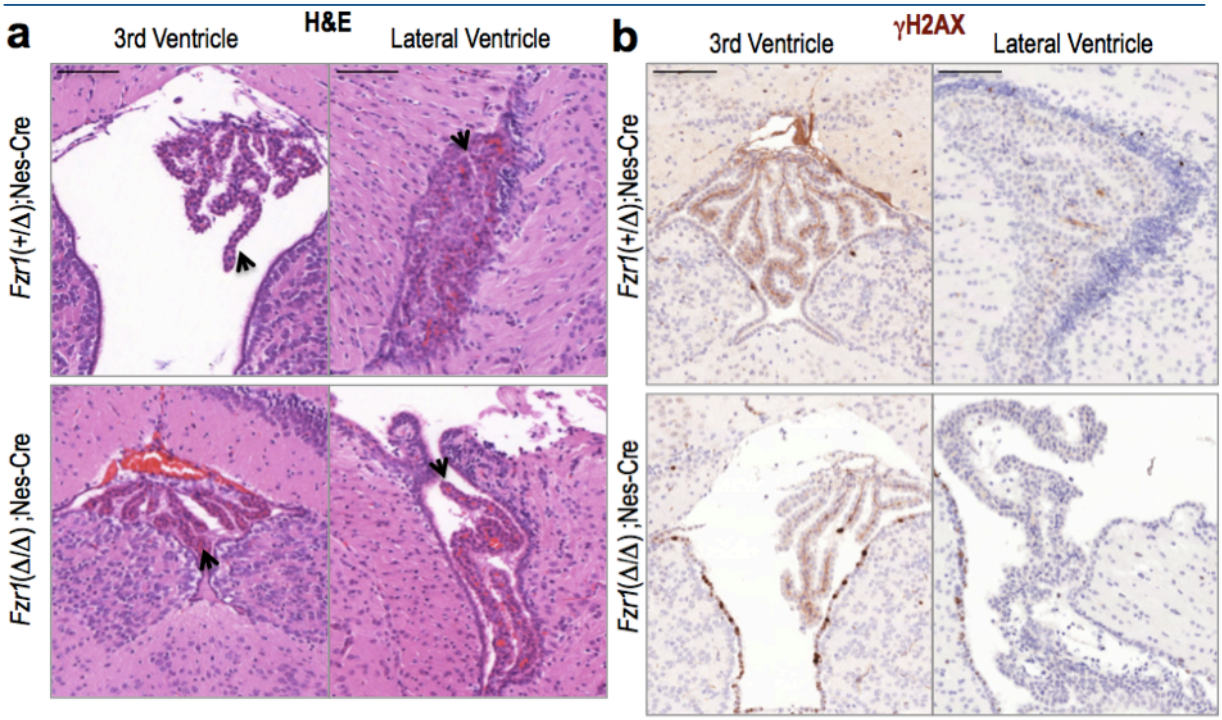

Choroid plexus in Cdh1-deficient and control embryos. Sections correspond to E14.5 embryos of the indicated genotypes. (**a**) H&E, hematoxylin and eosin. (**b**) γH2AX staining. Only positive in ependymal cells.

Next, we tested whether the DNA damage was present in the ependymal layer lining the ventricular system of the brain. Some CSF absorption occurs across this layer and the ependymal cells also circulate the CSF around the nervous system. These cells are originated from neural progenitors during late embryonic development (Spassky *et al.*, 2005), and defective integrity of this ependymal layer is known to lead to hydrocephalus (Grondona *et al.*, 1996; Jimenez *et al.*, 2001). As shown in Fig. 30, Cdh1-null ependymal cells displayed defective staining for S100β, a marker of mature ependymal cells, suggesting abnormal maturation and defective control of the cerebrospinal fluid in these mutant ventricles. Importantly, these ependymal cells displayed all the defects described above, including increased expression of Cdh1 substrates (not shown), Ki67 and PCNA signals (suggesting unscheduled cell cycle entry and increased DNA replication), γH2AX signal (replicative stress), as well as p53 induction and increased pH3 signal without mitotic

figures suggesting G2 arrest (Fig. 30a,b). These cell defects were present both during late embryonic development (not shown) as well as in postnatal stages (P10; Fig. 30) in which ependymal cells are normally quiescent (Spassky *et al.*, 2005).

Figure 30

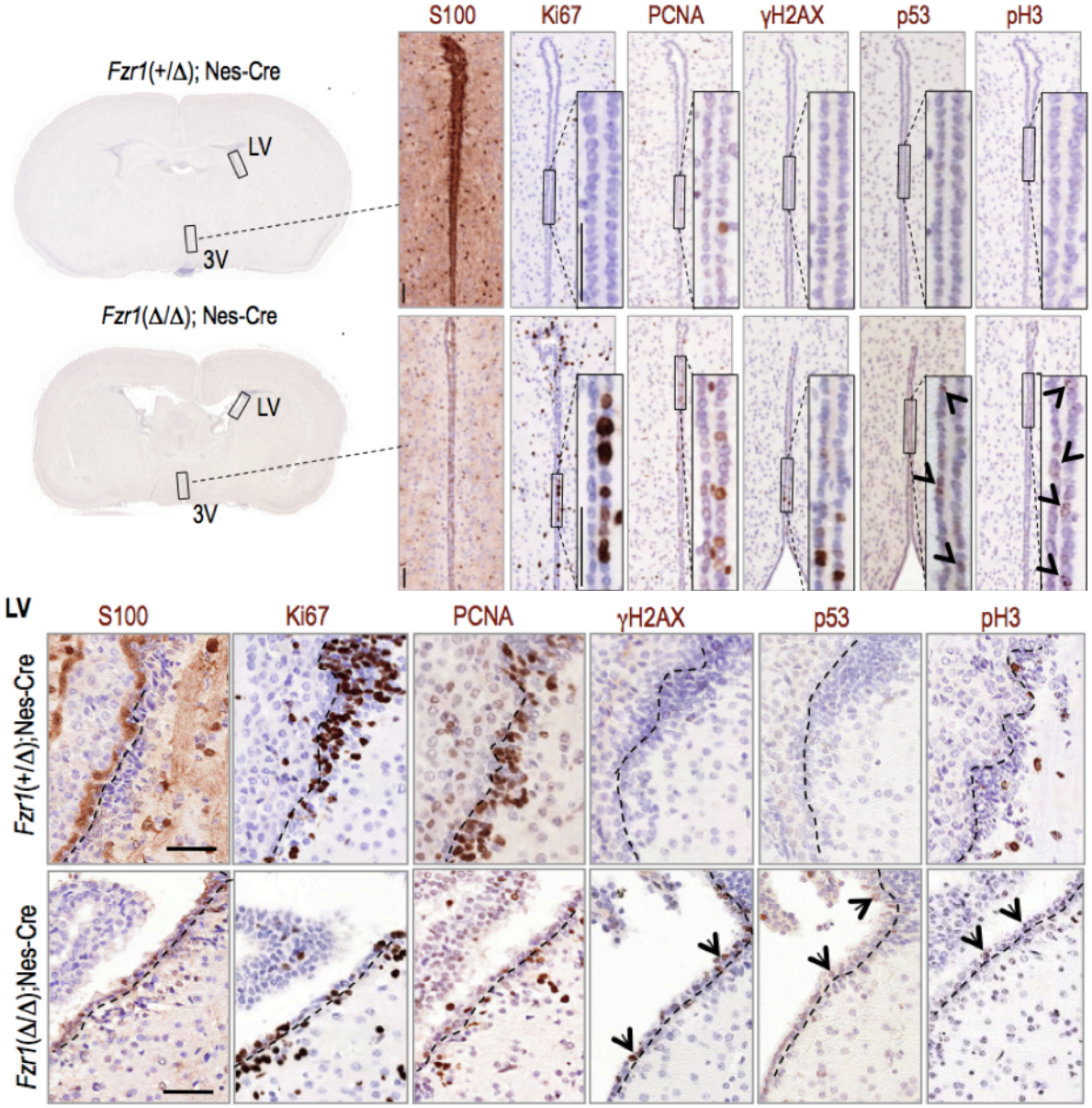

Alterations in Cdh1-deficient ependymal cells. (**a**) Proliferation markers such as Ki67 or PCNA are present in the ependymal layer of mutant but no control mice both in the third ventricle (3V, upper panels) and the lateral ventricles (LV, bottom panels). These markers are accompanied by persistent DNA damage (γH2AX signal), increased p53 levels and PH3 staining in the absence of mitotic figures suggesting G2 arrest. Some positive cells for these markers are indicated by arrows. On the other hand, Fzr1(Δ/Δ); Nestin-Cre ependymal cells display deficient S100 staining, a marker of mature ependymal cells. Scale bars, 50 µm. Scale bars, 25 µm.

In order to more thoroughly analyze the integrity of the ependymal layer lining the lateral ventricles, we performed en face whole-mount staining for the simultaneous detection of S100β, acetylated-tubulin and γ-tubulin to label both cilia and basal bodies of ependymal cells (Fig. 31). Whole-mount staining confirmed a reduced immunoreactivity for S100β protein, and decreased density of mature, multiciliated, ependymal cells. These data together indicate a compromised organization of the ependymal cell layer in Cdh1-null newborns.

Figure 31

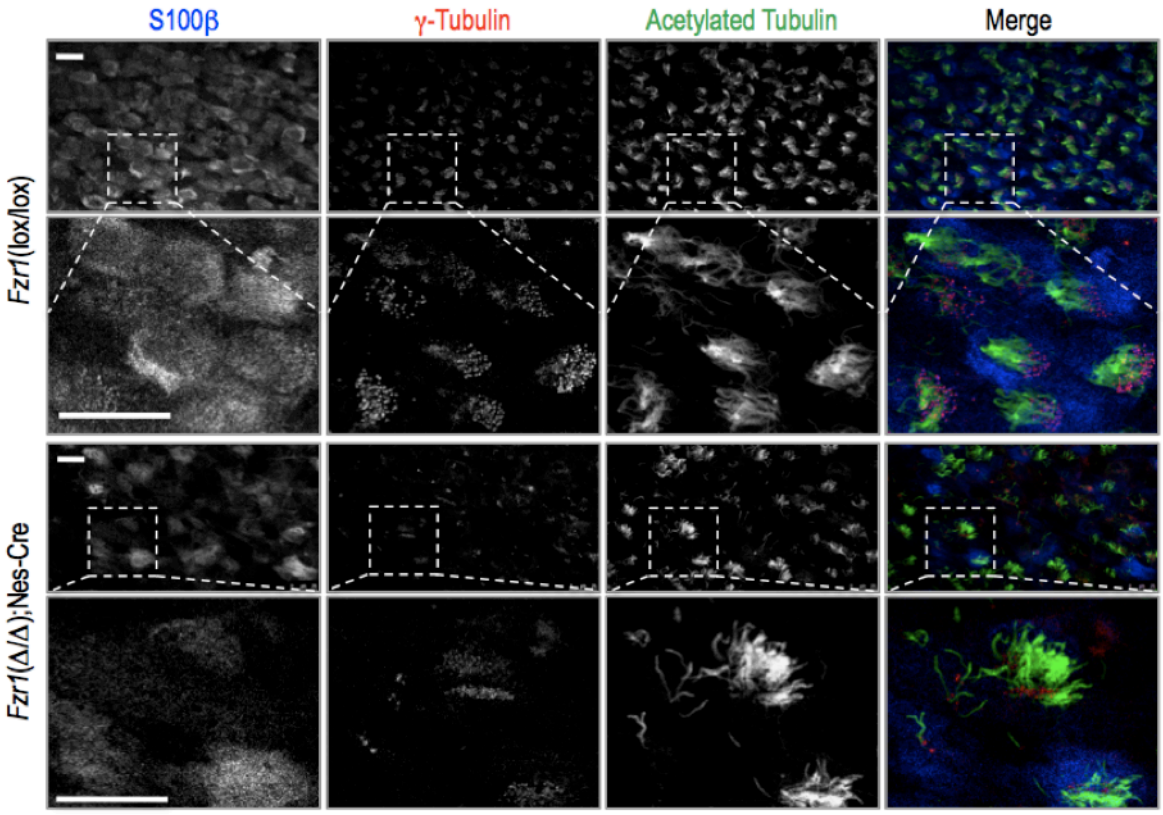

Alterations in the wall of the lateral ventricle in Cdh1-deficient mice. Co-staining for S100β, acetylated-tubulin and γ-tubulin in en face whole-mount preparations of the wall of the lateral ventricle of P10 mice confirmed decreased immunoreactivity of S100β and density of multiciliated ependymal cells. Scale bars, 25 µm.

2. A search for new APC/C-Cdh1 substrates

In this second part, in collaboration with Fernando García and Javier Muñoz (Proteomics Unit, CNIO) we have used Cdh1-null cells and mice to perform an un-biased analysis of proteins upregulated in the absence of this APC/C cofactor. Among these proteins, we have characterized the relevance of Eg5, a kinesin currently evaluated as a cancer target in early clinical trials, and topoisomerase Top2α, a target whose inhibitors are among the most effective anticancer drugs currently in clinical use. These two proteins are significantly upregulated in the absence of Cdh1, *in vitro* and *in vivo*, and are ubiquitinated in an APC/C-Cdh1-dependent manner.

2.1. Quantitative proteomics screens in Cdh1-null cells

We first analyzed the relative amount of proteins in the absence of Cdh1 by stable isotope labeling with amino acids in cell culture (SILAC; see Methods). We differentially labeled Cdh1-(encoded by the Fzr1 locus in mammals) deficient [Fzr1(Δ/Δ); (Garcia-Higuera *et al.*, 2008)] mouse embryonic fibroblasts (MEFs) and their control [Fzr1(+/Δ)] cells with heavy or light isotopes, respectively. Asynchronous cultures were harvested and proteins were quantified by mass spectrometry. Overall, we were able to obtain quantitative measurements for 2324 proteins, from which 308 showed upregulation in the absence of Cdh1 (protein log2 ratio >1; equivalent to 2-fold; Fig. 32a). Amongst them, we found known APC/C-Cdh1 substrates such as Anillin, Kif22, Ube2s or Ckap2 (Fig. 32a).

Since lack of Cdh1 may result in defects in cell cycle progression, we complemented these studies with the analysis of cells synchronized during cell cycle exit by analyzing protein profiles 36 h after removal of serum, a time in which known substrates clearly accumulate in Cdh1-null cells (Garcia-Higuera *et al.*, 2008). The corresponding protein lysates were then analyzed by using the isobaric tag for relative and absolute quantitation (iTRAQ) technique (see Methods). The relative levels of 4198 proteins were quantified and 21 proteins were upregulated (log2 ratio > 0.58; equivalent to 1.5-fold) in these Cdh1-null

Figure 32

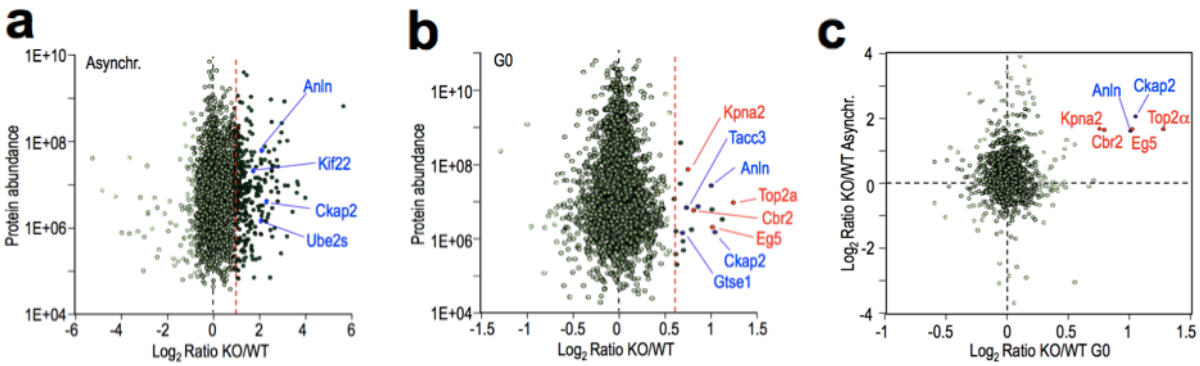

Quantitative proteomics in Cdh1-null mouse embryonic fibroblasts. (**a**) The levels of proteins were compared in immortal Fzr1(–/–) or wild-type cells using SILAC. The protein ratios between the heavy (Cdh1-null cells) and light (wild-type cells) labeled samples are plotted against their protein abundance (estimated as average area of the three unique peptides with the largest peak area per protein). Significantly upregulated known substrates are indicated in blue. (**b**) iTRAQ analysis in serum-starved MEF. The ratio between protein levels in Fzr1(–/–) and Fzr1(+/+) MEFs is shown in the X axis as a function of their abundances. Known mammalian substrates are indicated in blue, whereas additional proteins upregulated both in asynchronous and serum-starved cultures are shown in red. (**c**) Correlation between the protein accumulation in asynchronous cultures (Y axis) and serum-starved cells (X-axis). Known mammalian substrates are indicated in blue, whereas hits upregulated in both studies are shown in red.

serum-starved cultures included known mammalian substrates of the APC/C complex, such as Anillin, Tacc3, Ckap2 or Gtse1. Additional hits that were also upregulated in the previous analysis in asynchronous cultures (Fig. 32b) include Eg5, Top2α, Cbr2 or Kpna2 (Fig. 32b,c and Table 3). The differential expression of several of these proteins was validated by immunodetection in lysates from different Cdh1-null and control fibroblasts (Fig. 33a). The upregulation of two of these candidates, Eg5 and Top2α, was also validated by immunofluorescence in cultured MEFs (Fig. 33b).

Figure 33

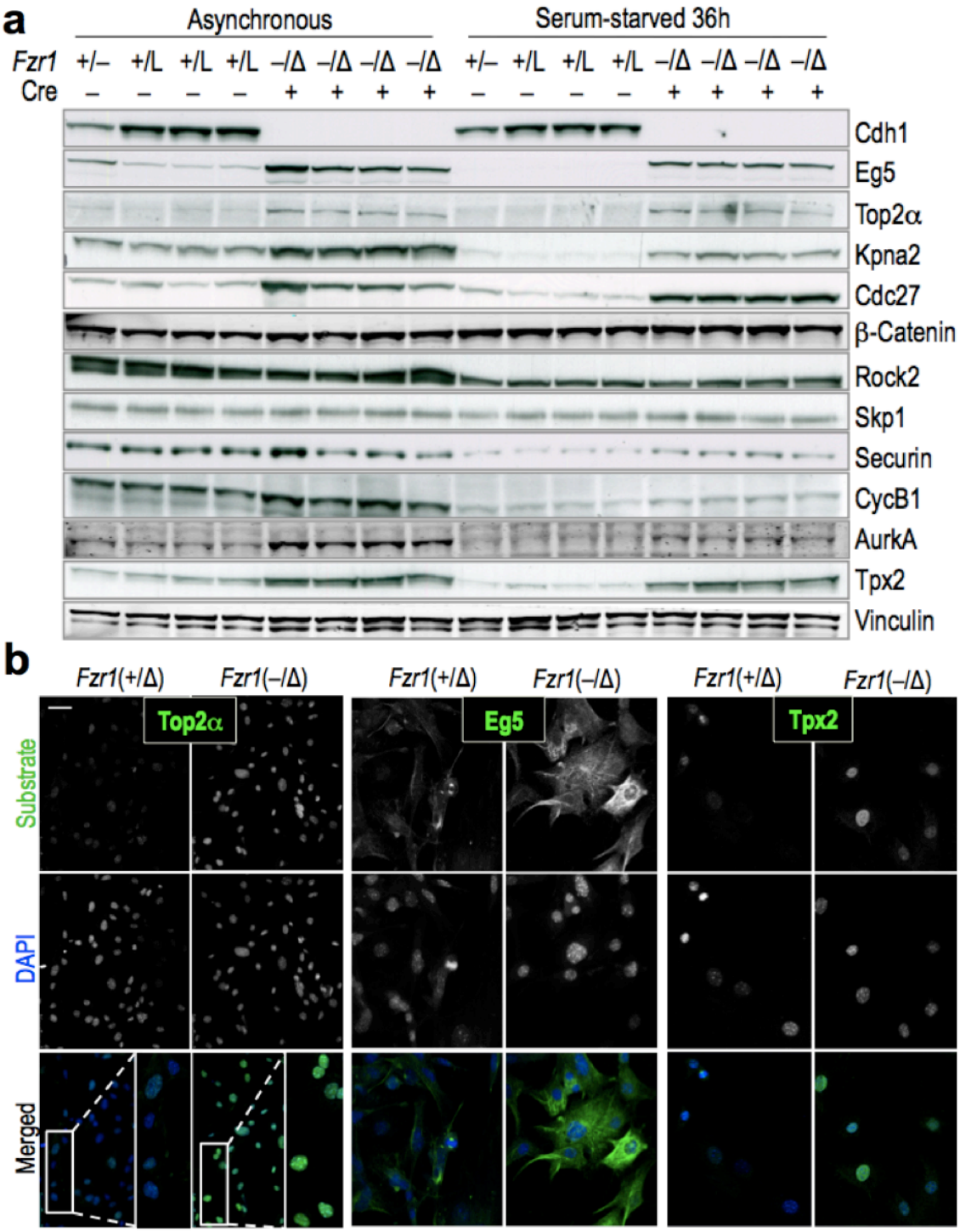

Validation of proteomic hits in mouse embryonic fibroblasts. (**a**) Protein levels of known Cdh1 substrates (Aurora A, Tpx2, Securin, Cyclin B1) and additional hits found in our previous proteomics analyses. Fzr1(+/–) are heterozygous MEFs carrying a normal allele and a germline, null allele. Fzr1(+/L) carry a lox (L) allele that normally expresses Cdh1. This allele results in a null allele [Fzr1(Δ)] after expression of the recombinase Cre. (**b**) Protein levels of Eg5 and Top2α in Cdh1-null [Fzr1(–/Δ)] and control heterozygous [Fzr1(+/Δ)] MEFs as detected by immunofluorescence. Tpx2 is used as a control. Scale bars, 50 µm.

We next tested the differential expression of proteins *in vivo* by using a genetic model of Cdh1 depletion in the brain, a tissue in which ablation of the Cdh1-encoding gene, Fzr1, results in developmental defects (Fig. XXX). Fzr1(lox/lox) conditional knockout mice were intercrossed to Sox2-Cre transgenic mice leading to Fzr1(Δ/–); Sox2-Cre mice in which the Cdh1-encoding gene has been specifically deleted in the embryo but not in placental tissues. We isolated brains from embryonic day (E)15.5 Fzr1(Δ/–); Sox2-Cre and control embryos, and samples were differentially labeled with iTRAQ reagents and analyzed by mass spectrometry. This analysis provided quantitative data for 3466 proteins, from which 31 were upregulated more than 1.5 fold (log2 ratio > 0.58) in Cdh1-null brains, including the known substrates Tacc3, Aurora B, Nusap1, Ndc80, and Ckap2 (Fig. 34a).

Figure 34

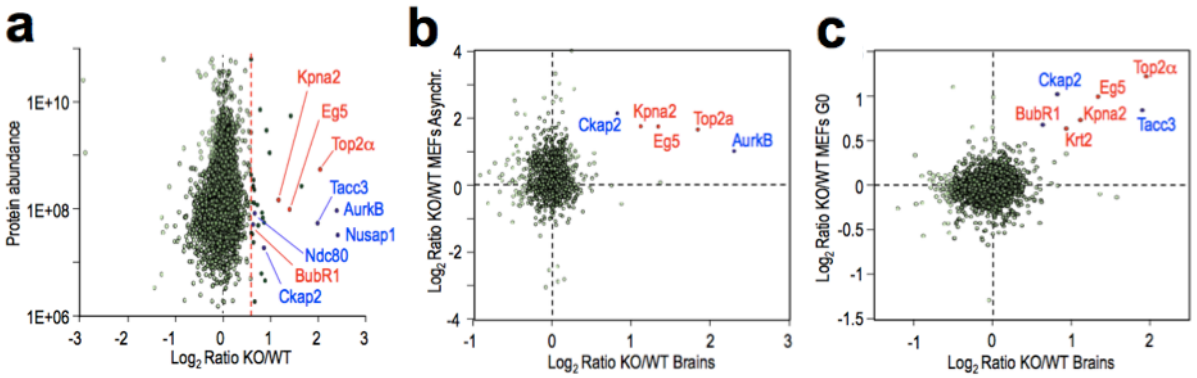

Quantitative proteomics screens in Cdh1-deficient brains. (**a**) The ratio between protein levels in Fzr1(–/Δ) and Fzr1(+/Δ) brains is shown in the X axis against the estimated protein abundance. Known mammalian substrates are indicated in blue, whereas additional proteins upregulated both in MEFs (Fig. 1) and brains assays are shown in red. (**b**) Correlation between the data from asynchronous cultures in MEFs (Y axis) and data in brains (X axis). **c**) Correlation between the data from serum-starved MEFs (Y axis) and embryonic brains (X axis). In (**b**) and (**c**) known mammalian substrates are indicated in blue, whereas hits upregulated both in MEFs and brains are shown in red.

Interestingly, three of the most differentially expressed proteins found in Cdh1-null MEFs, Eg5, Top2α and Kpna2, were also upregulated in Cdh1-null brains (Fig. 34a-c and Table X). These results were validated by immunoblot analysis using brains from different Cdh1-null and control embryos (Fig. 35a), as well as by immunofluorescence in E14.5-16.5 Cdh1-deficient and control brains (Fig. 35b,c).

Figure 35

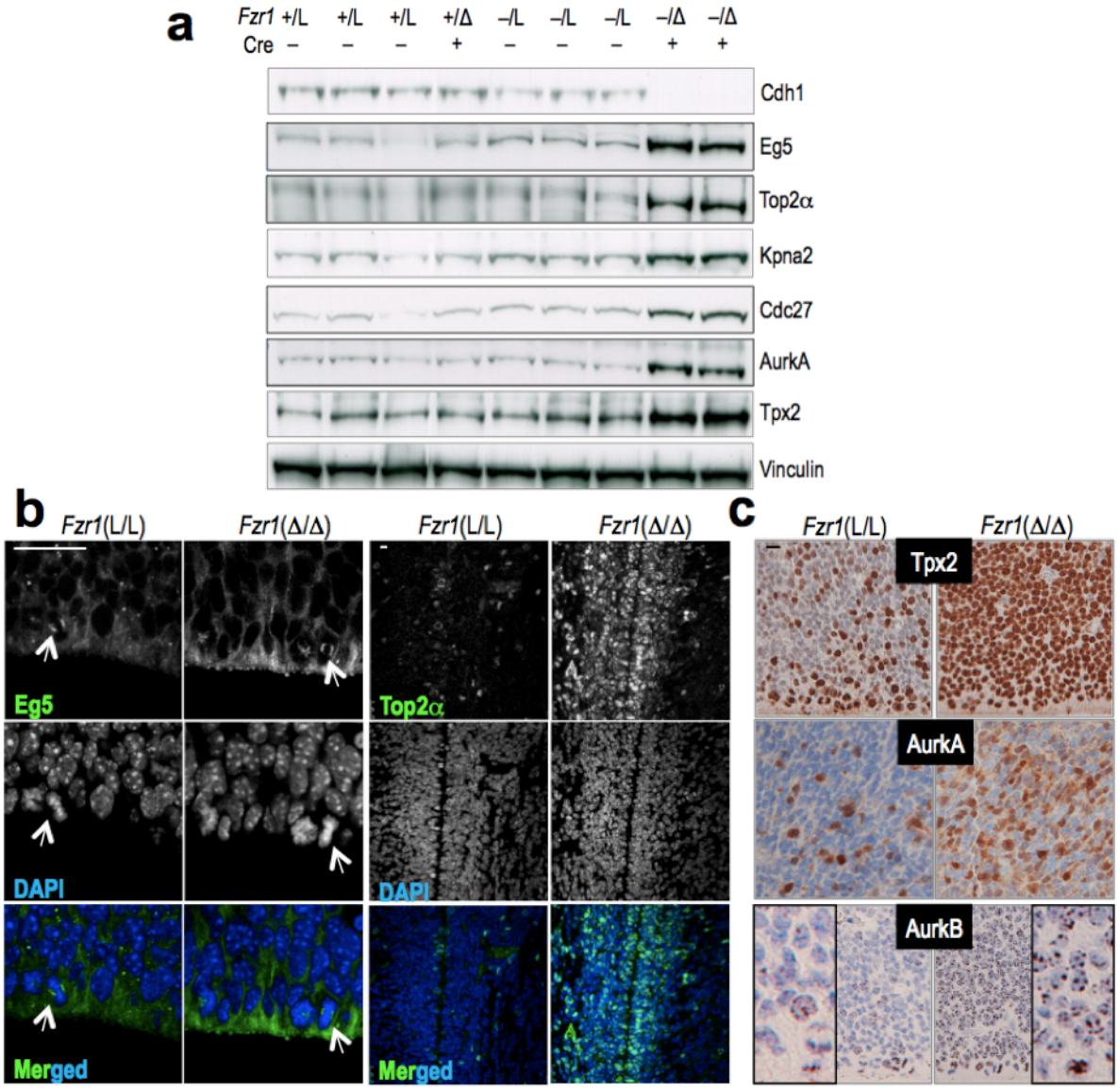

Quantitative proteomics screens in Cdh1-deficient brains. (**a**) Protein levels of known Cdh1 substrates (Aurora A, Tpx2) and molecules found in the proteomics screens in Cdh1-null [Fzr1(–/Δ)], heterozygous [Fzr1(+/Δ) and Fzr1(–/L)] and normal [Fzr1(+/L)] E15.5 brains. (**b**) Immunofluorescence of Eg5 and Top2α in Cdh1-null [Fzr1(Δ/Δ)] and control [Fzr1(L/L)] brains. (**c**) Immunohistochemistry analysis of known Cdh1 targets (Tpx2, Aurora A and Aurora B) in Cdh1-null [Fzr1(Δ/Δ)] and control [Fzr1(L/L)] brains. Scale bars, 25 μm.

Table 3

Symbol	Uniprot	Description	Log_2 KO/WT Async. MEFs	Log_2 KO/WT G0 MEFs	Log_2 KO/WT Brains	KEN [b]	D-box [c]	RXXL [d]	Ref.
Top2α	Q01320	DNA topoisomerase 2-alpha	1.584	1.222	2.01	1	2	5	
Kif11	Q6P9P6	Kinesin-like protein KIF11	1.72	0.996	1.374	1	-	3	
Ckap2	Q3V1H1	Cytoskeleton-associated protein 2	2.116	1.024	0.845	1	-	2	(Hong et al. 2007; Seki and Fang 2007)
Kpna2	P52293	Importin subunit alpha-2	1.729	0.737	1.145	-	-	2	
Tacc3	Q9JJ11	Transforming acidic coiled-coil-containing protein 3	n.d.	0.845	1.959	2	-	2	(Jeng et al. 2009)
Anln	Q8K298	Actin-binding protein anillin	1.668	0.983	n.d.	-	3	11	(Zhao and Fang 2005)
Cbr2	P08074	Carbonyl reductase [NADPH] 2	1.696	0.774	n.d.	-	-	1	
Krt2	Q3TTY5	Keratin, type II cytoskeletal 2 epidermal	n.d.	0.66	0.977	-	2	3	
BubR1	Q9Z1S0	Mitotic checkpoint serine/threonine-protein kinase BUB1 beta	n.d.	0.683	0.655	2	3	7	

Proteins significantly upregulated in at least two of the three proteomics screens in Cdh1-deficient cells.[a] a Known candidates are shaded in blue. n.d., not detected. b Indicates the number of KEN boxes (K-E-N). c Indicates the number of D-boxes (R-X-X-L-X-[LIVM]) as defined in The Eukaryotic Linear Motif resource (http://elm.eu.org/). d Indicates the number of relaxed D-boxes (R-X-X-L). The presence of these three domains (KEN, D-box and RXXL) was analyzed using ScanProsite (http://prosite.expasy.org/scanprosite/).

2.2. Cdh1 controls the protein levels of Eg5 and Top2α in mouse and human cells

We next tested the effect of Cdh1 overexpression or downregulation in human cells. Human 293T cells were transfected with vectors expressing Cdc20, Cdh1 or a hyperactive Cdh1 mutant ($Cdh1^{ALA}$) carrying nine mutations that make this protein insensitive to its inhibition by Cdk-dependent phosphorylation (Kramer *et al.*, 2000). As shown in Fig. 36a, expression of either Cdh1 or $Cdh1^{ALA}$ resulted in downregulation of Eg5, Top2α, as well as known Cdh1 substrates. These differences were not due to changes in cell cycle profile as overexpression of these APC/C cofactors did not change DNA content in these cultures (Fig.

37). In these assays, Cdc20 induced downregulation of its substrate securin, but not the other molecules. On the other hand, knock down of Cdh1 in human cells resulted in increased levels of Eg5 and Top2α, similar to the increase observed in known Cdh1 substrates such as Tpx2 and Aurora A (Fig. 36b).

Figure 36

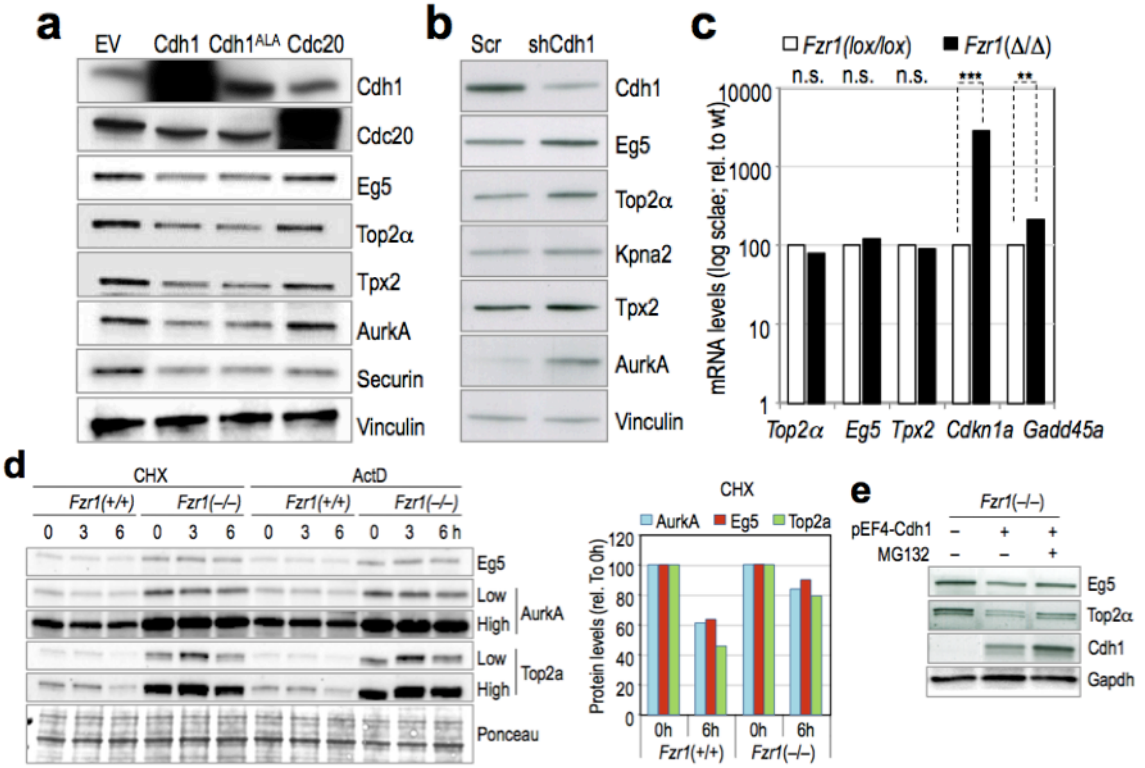

Cdh1 controls Eg5 and Top2α protein stability. (**a**) Protein levels of the indicated molecules after overexpression of Cdh1 (wild-type form or the Cdh1ALA constitutive active mutant) or Cdc20 in human 293T cells. (**b**) Protein levels of the indicated molecules 72 h after transfection of 293T cells with a short hairpin RNA against Cdh1 or against scrambled (Scr.) sequences. (**c**) Quantification (log10 scale) of mRNA levels of the indicated transcripts by real-time RT-PCR. Cdkn1a is the symbol of the locus encoding the p53-responsive cell cycle inhibitor p21Cip1. (**d**) Protein stability of the indicated molecules in the presence of cycloheximide (CHX) or Actinomycin D (ActD) in Cdh1-null and control cells. Signals after low or high exposure are indicated for Aurora A and Top2α. The quantification of protein levels at 0 and 6 after the addition of CHX is shown. e) Protein levels of the indicated molecules after expression of Cdh1 in Fzr1(–/–) MEFs in the presence or absence of the proteasome inhibitor MG132.

The upregulation of Eg5 and Top2α in Cdh1-null cells was not a consequence of increased transcription as the levels of the corresponding transcripts were not increased (Fig. 36c). These mutant cells however displayed a significant transcriptional upregulation of p21Cip1 and Gadd45a, in agreement with the DNA-damage-like response in these cells and their increased susceptibility to become senescent (Garcia-Higuera *et al.*, 2008; Li *et al.*, 2008). We also tested the effect of Cdh1 in the stability of these putative substrates. Both Eg5 and Top2α are unstable proteins after the inhibition of protein synthesis with cycloheximide or actinomycin D. Importantly, the levels of these two proteins, similarly to Aurora A, were partially stabilized in Cdh1-null cells (Fig. 36d). Finally, re-introduction of exogenous Cdh1 in Fzr1(–/–) cells, restores the levels of Eg5 and Top2α and this is dependent on the proteasome, suggesting that they are degraded in a Cdh1-dependent manner (Fig. 36e).

Figure 37

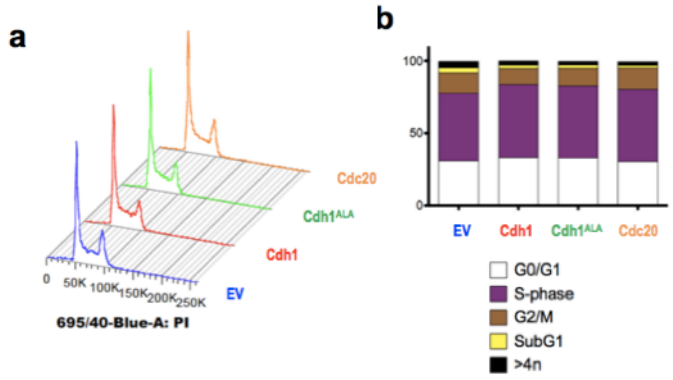

Overexpression of Cdh1 or Cdc20 does not change the cell cycle profile. (**a**) Cell cycle profile of 293T cells after the expression of the indicated proteins or the empty vector (EV). PI, propidium iodide. (**b**) Quantification of the percentage of cells in the different phases of the cell cycle in the previous assay.

We then tested the direct ubiquitination of these two proteins by APC/C-Cdh1 complexes using cell-free ubiquitination and destruction assays in Xenopus egg extracts. As shown in Fig. 38a,b, Eg5 was ubiquitinated and degraded after the addition of recombinant Cdh1 protein in these assays. Both Cdh1-dependent ubiquitination and degradation were

prevented after mutagenesis of a KEN box sequence (aa 1022-1024 in the human Eg5 sequence) and two D-box sequences (aa 944-947 and 1047-1050; Fig. 39).

Top2α was not efficiently degraded in a similar assay in Xenopus egg extracts (Fig. 38c). However, Top2α was ubiquitinated in a Cdh1-dependent manner in these Xenopus extracts following a similar kinetics to that observed for Eg5. We also generated Top2α mutant

Figure 38

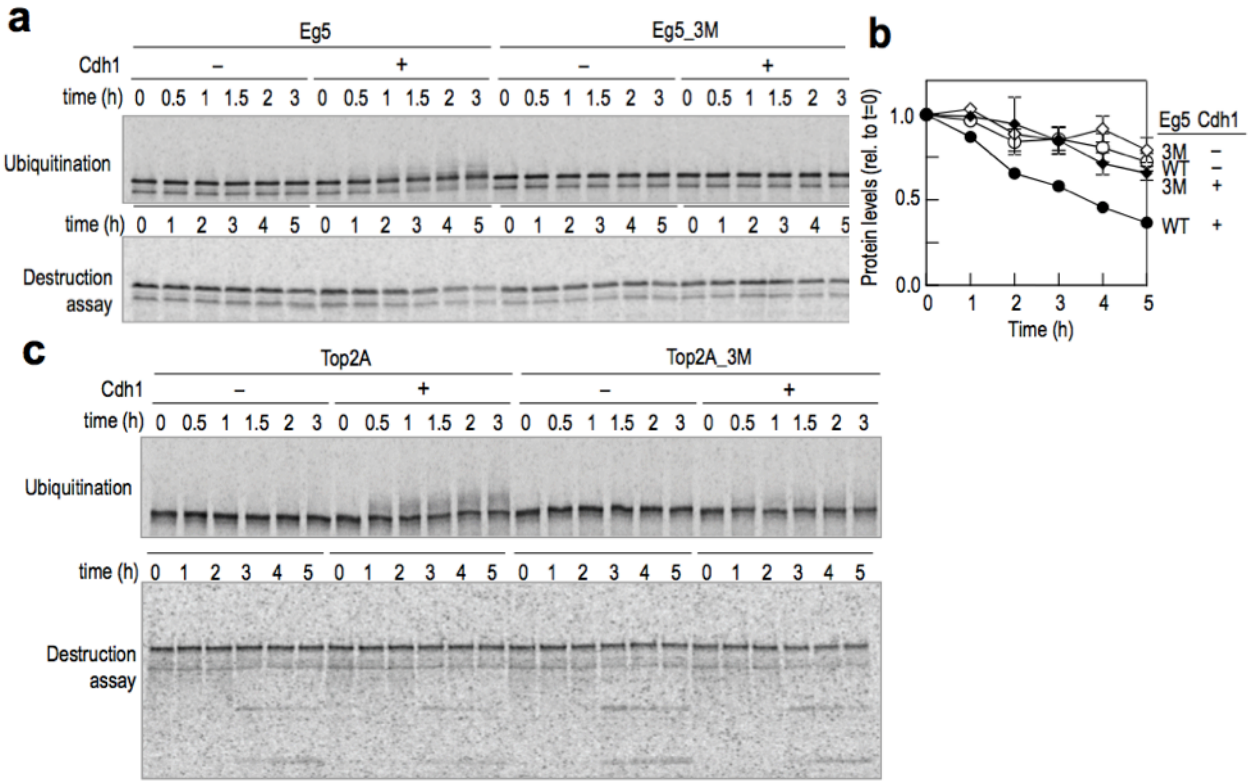

Ubiquitination and destruction assays in Xenopus egg extracts. (**a**) Cdh1-dependent ubiquitination and destruction of Eg5. 35S-labeled wild-type or triple mutant (3M; see Fig. 39) Eg5 were subjected to an in vitro ubiquitination assay using purified Xenopus APC/C in the presence or absence of Cdh1 (upper panel) or a cell-free destruction assay reconstituted in Xenopus egg interphase extracts in the presence or absence of Cdh1 (lower panel). (**b**) Quantification of Eg5 in panel (**a**). Error bars, s.e.m. from three independent experiments. (**c**) Ubiquitination and destruction assay of Top2α. 35S-labeled Top2α (wild type or 3M mutant; see Fig. 39) were subjected to an in vitro ubiquitination assay using purified Xenopus APC/C in the presence or absence of Cdh1, or a cell-free destruction assay reconstituted in Xenopus egg interphase extracts in the presence or absence of Cdh1.

proteins carrying specific mutations in a KEN box (aa 378-380) and two putative D-boxes (aa 982-985 and 1053-1056 in the human sequence; Fig. 39). As indicated in Fig. 38c, mutation of these sites significantly diminished the ability of Cdh1 to ubiquitinate this protein. These data suggest that both Eg5 and Top2α are ubiquitinated in a Cdh1-dependent manner. This ubiquitination seems to the sufficient for the proteasome-dependent degradation of Eg5, but not Top2α, at least in these Xenopus extracts.

Figure 39

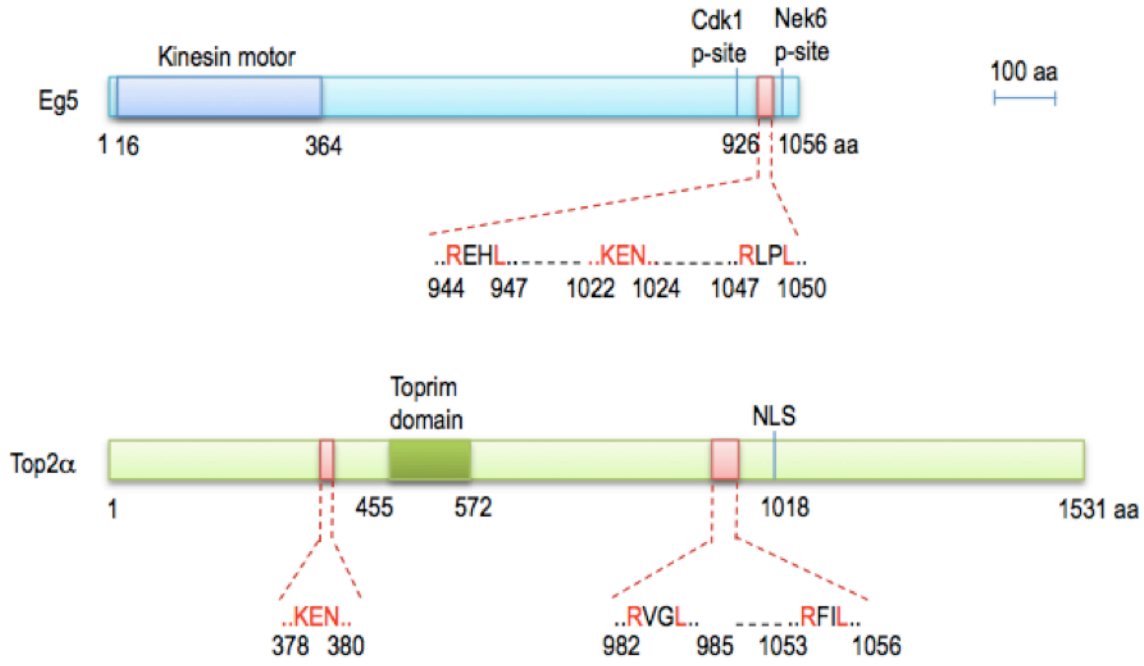

Schematic representation of the KEN and D-boxes in human Eg5 and Top2α. Residues in red were mutated to alanine to generate stable proteins (3M mutants).

3. New therapeutic implications of inhibiting APC/C-Cdh1

Finally, in the the last part we have studied how the accumulation of Eg5 and Top2α upon depleting Cdh1 or inhibiting APC/C-Cdh1 could affect the response to drugs. The upregulation of these targets in Cdh1-deficient cells results in differential responses (increased resistance or susceptibility) to specific therapeutic agents. Moreover, the combined treatment of human cancer cells with the APC/C inhibitor proTAME and the Top2 posion etoposide results in synthetic lethality due to the increase in Top2α levels. All these data highlight the clinical relevance of these findings.

3.1. Cdh1-dependent degradation of Eg5 modulates the response to Eg5 inhibitors

We then performed additional studies during cell cycle progression in mammalian cells. We synchronized MEFs in prometaphase by releasing these cells from double thymidine block in the presence of taxol. Mitotic cells were then selected by shake-off, plated in the absence of taxol and harvested at different time points for protein analysis. Endogenous Eg5 was degraded during mitotic exit with a kinetics similar to that of known APC/C-Cdh1 substrates such as Tpx2 or Aurora kinase B, and slower than APC/C-Cdc20/Cdh1 substrates such as cyclin B1 or securin (Fig. 40a,b). Importantly, the levels of all these substrates were stabilized during mitotic exit of Cdh1-null cells (Fig. 40a). Mutation of the KEN box partially stabilized Eg5 during mitotic exit in a similar experimental setting, and this effect was further enhanced upon mutation of the two putative D-boxes present in this protein (Fig. 40c). Time-lapse studies also showed that Eg5 is degraded during telophase and maintained at low levels during the following G1 phase whereas the levels of the triple mutant (3M, containing mutations in the KEN box and the two D-boxes; Fig. 39) Eg5 remained high in the cytoplasm of interphasic cells (Fig. 40d,e).

Figure 40

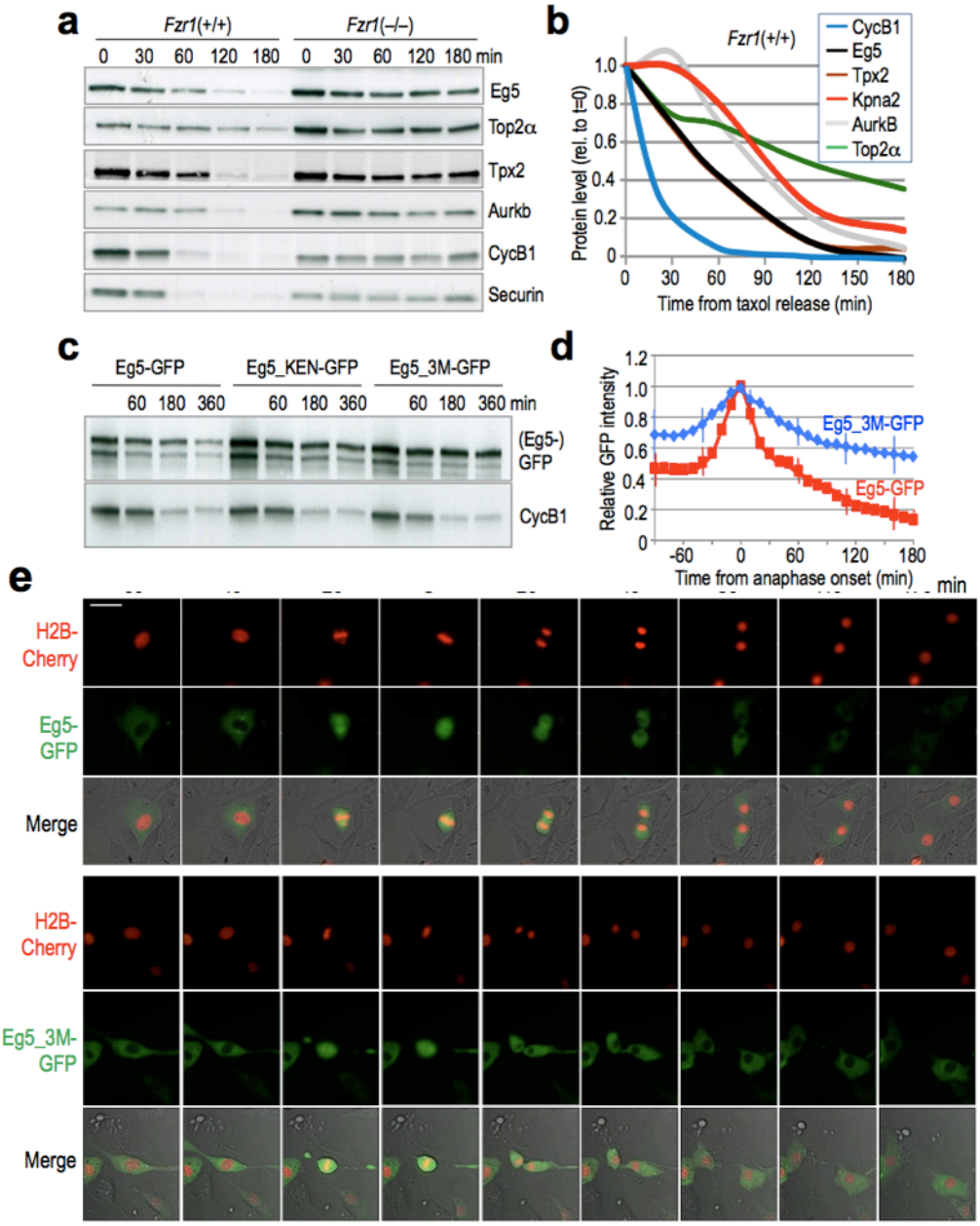

Degradation of the kinesin Eg5 during mitotic exit. (**a**) Protein levels of the indicated molecules at different time points after a release from taxol. (**b**) Comparative profiles of the levels of the indicated proteins after release from taxol from two different assays. Values are normalized to the amount of protein at t=0 (in the presence of taxol). (**c**) Protein levels of the exogenous Eg5-GFP fusion protein at different time points after a release from nocodazole. Eg5-KEN-GFP is mutated in the KEN box whereas Eg5_3M-GFP contains mutations in the KEN and two putative D-boxes (See Fig. 39). (**d**) Quantification of the degradation of Eg5-GFP fusion proteins during mitotic exit as monitored by videomicroscopy. The quantification shows the comparative levels of normal Eg5-GFP or the Eg5_3M-GFP mutant (N=16 cells). Cells were aligned in metaphase (t=0) and the intensity (± st. dev.) of the signal was arbitrarily set as 1. (**e**) Representative images of mitotic progression in the presence of Eg5-GFP or Eg5_3M-GFP (green) fusion proteins. The signal of a histone H2B-mCherry fusion protein is in red. Scale bars, 25 µm.

Pioneer screens to identify anti-mitotic drugs led to the characterization of monastrol as an Eg5 inhibitor (Mayer *et al.*, 1999). Eg5 is also upregulated in multiple tumor types (Perez de Castro *et al.*, 2007), and the requirements for this kinesin during the formation of the mitotic bipolar spindle have led to multiple preclinical and clinical studies for its validation as a cancer target (Rath and Kozielski, 2012; Doménech and Malumbres, 2013). We therefore reasoned that the overexpression of Eg5 in Cdh1-deficient cells could lead to specific defects in the response to monastrol. This Eg5 inhibitor leads to a mitotic-checkpoint-dependent mitotic arrest and lack of chromosome segregation due to the lack of a bipolar spindle. However, Cdh1-null cells displayed partial resistance to monastrol as more than 20% of these mutant cells displayed chromosome segregation in the presence of similar levels of this drug (Fig. 41a,b). Importantly, this resistance is likely to be due to the increased levels of Eg5 as concomitant downregulation of this protein using RNA interference (Fig. 42a) completely prevented chromosome segregation in the presence of monastrol (Fig. 41c,d). Parallel knock-down of Eg5 in untreated cells resulted in normal segregation in most cells and only 15% of these treated cells displayed problems during mitosis. These data suggest that Cdh1 inactivation leads to Eg5 overexpression and this overexpression results in a partial resistance of monastrol. Knock down of Eg5 restores susceptibility to monastrol in terms of chromosome segregation and also prevents the rapid exit from mitosis observed in a few (7%; N=45) Cdh1-null cells treated with monastrol (Fig. 41b,d).

Figure 41

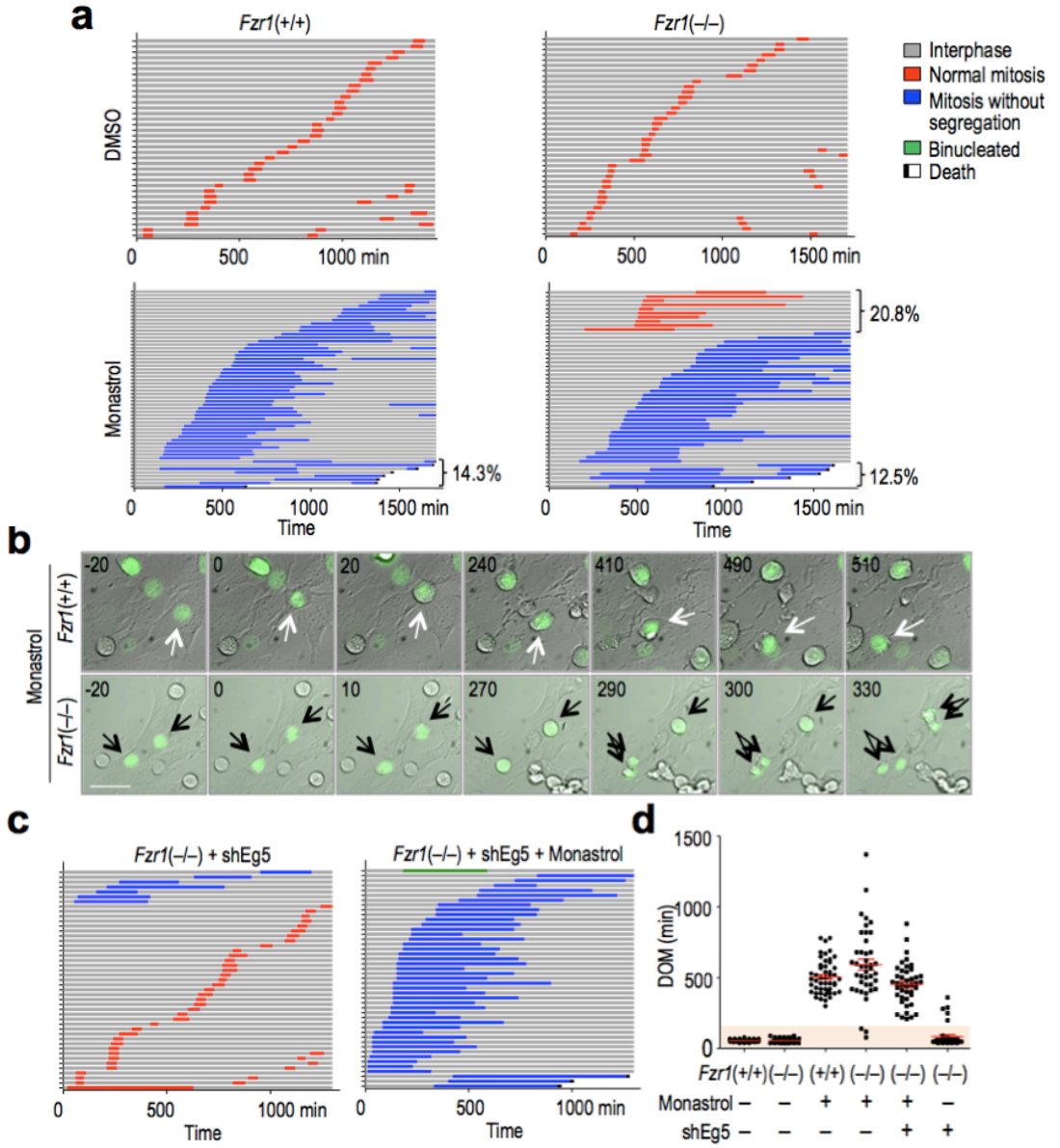

Absence of Cdh1 results in increased resistance to monastrol in an Eg5-depenent manner. (**a**) Plots showing the fate of individual Cdh1-null or control cells (rows) in the presence or absence of monastrol. The progression through interphase or abnormal or normal mitosis is represented as indicated. About 12-14% of cells die in the presence of monastrol. One fifth of Cdh1-null cells display chromosome segregation in the presence of monastrol whereas this is not observed in wild-type cells (N=45 cells per assay). (**b**) Representative images of the effect of monastrol preventing chromosome segregation (top panels) in wild-type cells. Representative examples of Cdh1-null cells undergoing chromosome segregation are shown in the bottom panels. Time 0 indicates mitotic entry (chromosome condensation and rounding of cells). Histone H2B is n green. Scale bars, 25 µm. (**c**) Effect of knock down of Eg5 in Cdh1-null cells in the presence or absence of monastrol. Colors indicate cell fate as in panel (**a**). (N=45 cells per assay). (**d**) Duration of mitosis (DOM) in the previous assays. Each dot corresponds to an individual cell (n=45 cells per condition).

Figure 42

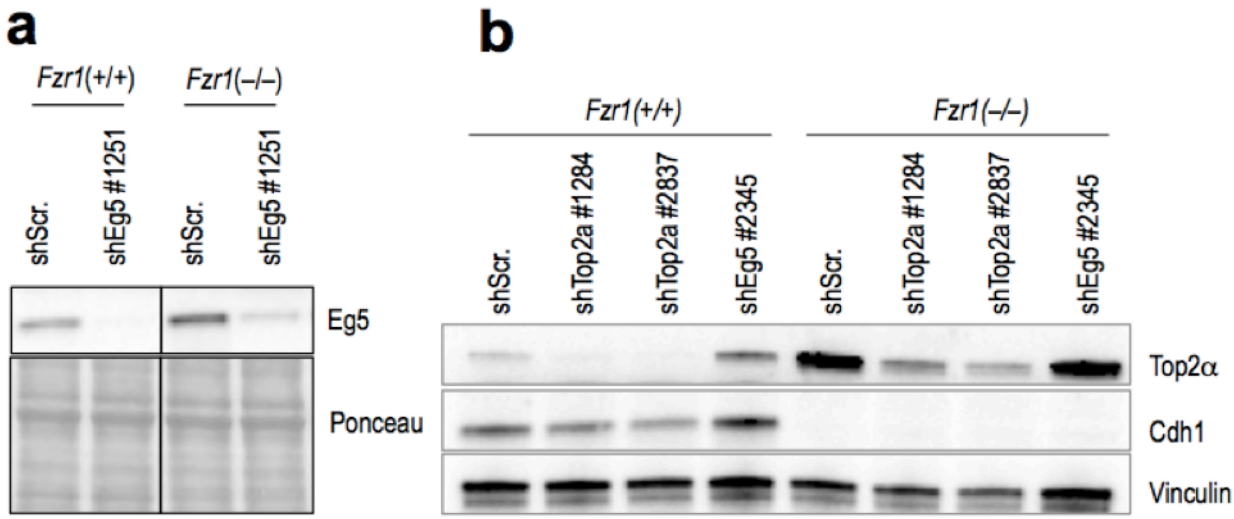

Knowk down of Eg5 or Top2α by RNA interference. (**a-b**) Downregulation of endogenous Eg5 (**a**) or Top2α (**b**) after transfection of Cdh1-null [Fzr1(–/–)] or control [Fzr1(+/+)] MEFs with short hairpin interfering RNAs against these molecules.

3.2. Genetic ablation of Cdh1 leads to increased susceptibility to topoisomerase poisons

Top2α is one of the most successful targets in cancer therapy, and drugs that target Top2α are currently used as the standard of care in several tumors (i.e. testicular cancer). Compounds that target topoisomerase II are classified into two main classes with different mechanism of action (See Discussion): topoisomerase poisons (e.g. etoposide), which target the Top2α-DNA complex after the topoisomerase has created the DNA double stranded break (DSB), and topoisomerase catalytic inhibitors (e.g. ICRF-193) which target the ATPase domain and therefore prevent the breakage made by Top2α (Nitiss, 2009). In fact, catalytic inhibitors are used to prevent some of the toxic effects of poisons, since they prevent the amount of DNA breakage in some sensitive organs such as the heart.

Top2α was ubiquitinated by APC/C-Cdh1 in Xenopus egg extracts in a KEN box and D-box-dependent manner (Fig. 38c), degraded in mammalian cells in a Cdh1-dependent

manner (Fig. 36 and 40a,b), and it is one of the most upregulated proteins in Cdh1-null cells (Figs. 32-35). Given that clinical data suggest that increased levels of Top2α correlate with the outcome of patients treated with topoisomerase inhibitors, we asked whether the increased levels of Top2α observed in Cdh1-deficient cells could modulate the sensitivity to the topoisomerase poison etoposide. Cdh1-deficient cells displayed a significant increase in the number of DSB that are generated by etoposide as monitored by the nuclear staining of the phosphorylated form of histone H2AX (γH2AX; Fig. 43a,b). In contrast, no differences were observed in the response to the catalytic inhibitor ICRF-193. These data correlated with a dramatic increase in cell death after treatment of Cdh1-null cells with etoposide, as monitored by flow cytometry (Fig. 44a) or high-throughput microscopy (Fig. 44b). For instance, about 70% of Fzr1(–/–) cells died after treatment with 25 μM etoposide whereas less than 10% of control cells were killed in these conditions. Similar differences were observed with reduced doses of this compound. The catalytic inhibitor ICRF-193, on the other hand, resulted in a low index of lethality both in Cdh1-null and control cells. Importantly, the combination of etoposide and ICRF-193 resulted in a protection versus the lethality observed after treatment with etoposide alone (Fig. 44b), in agreement with the idea that topoisomerase poisons trap topoisomerase complexes on the DNA inducing higher levels of damage that can be partially prevented by inhibiting the catalytic activity of these enzymes.

To tested whether the susceptibility of Cdh1-null cells to etoposide is a consequence of increased Top2α expression, Fzr1(–/–) and control cells were treated with etoposide or ICRF-193 in the presence of short hairpin RNA interfering molecules against Top2α transcripts or scrambled sequences. Two different shRNA sequences, #1284 and #2837, that display different efficiency in downregulating Top2α were used (Fig. 42b). Partial downregulation of Top2α with shTop2α #1284 resulted in a significant protection against

Figure 43

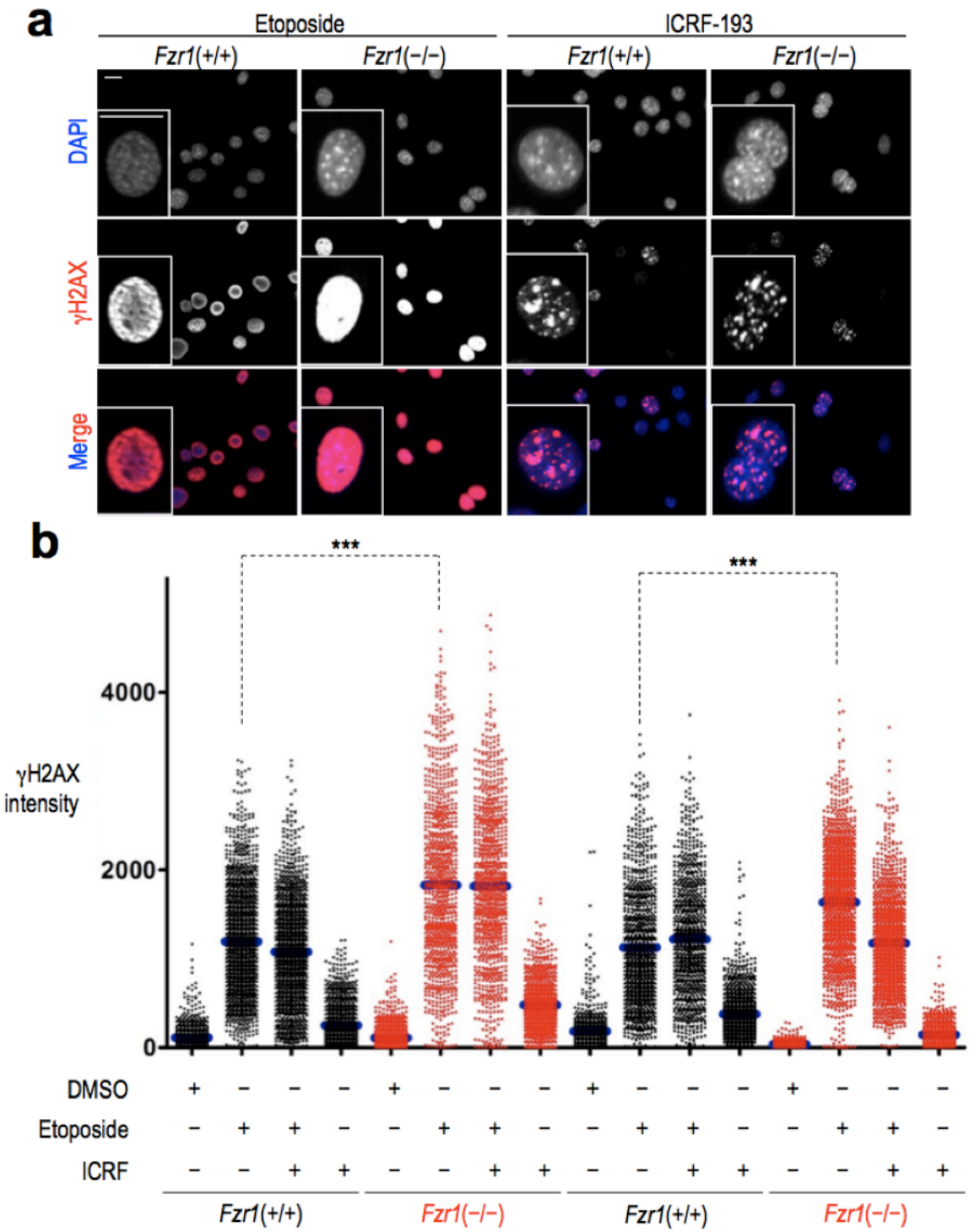

Effect of topoisomerase poisons and catalytic inhibitors in Cdh1-deficient cells. (**a**) DNA damage as monitored by phosphorylation of H2AX (γH2AX) induced by etoposide or ICRF-193 in Cdh1-null or control cells. Scale bars, 10 µm. (**b**) Quantification of phosphorylation of H2AX (γH2AX intensity per cell) after treatment of Cdh1-null or control cells with etoposide or ICRF-193. Please note that etoposide and ICRF-193 were added at the same time and, in these conditions, the addition of ICRF-193 is not efficient in preventing DNA damage induced by etoposide. *** indicates $p<0.001$.

Figure 44

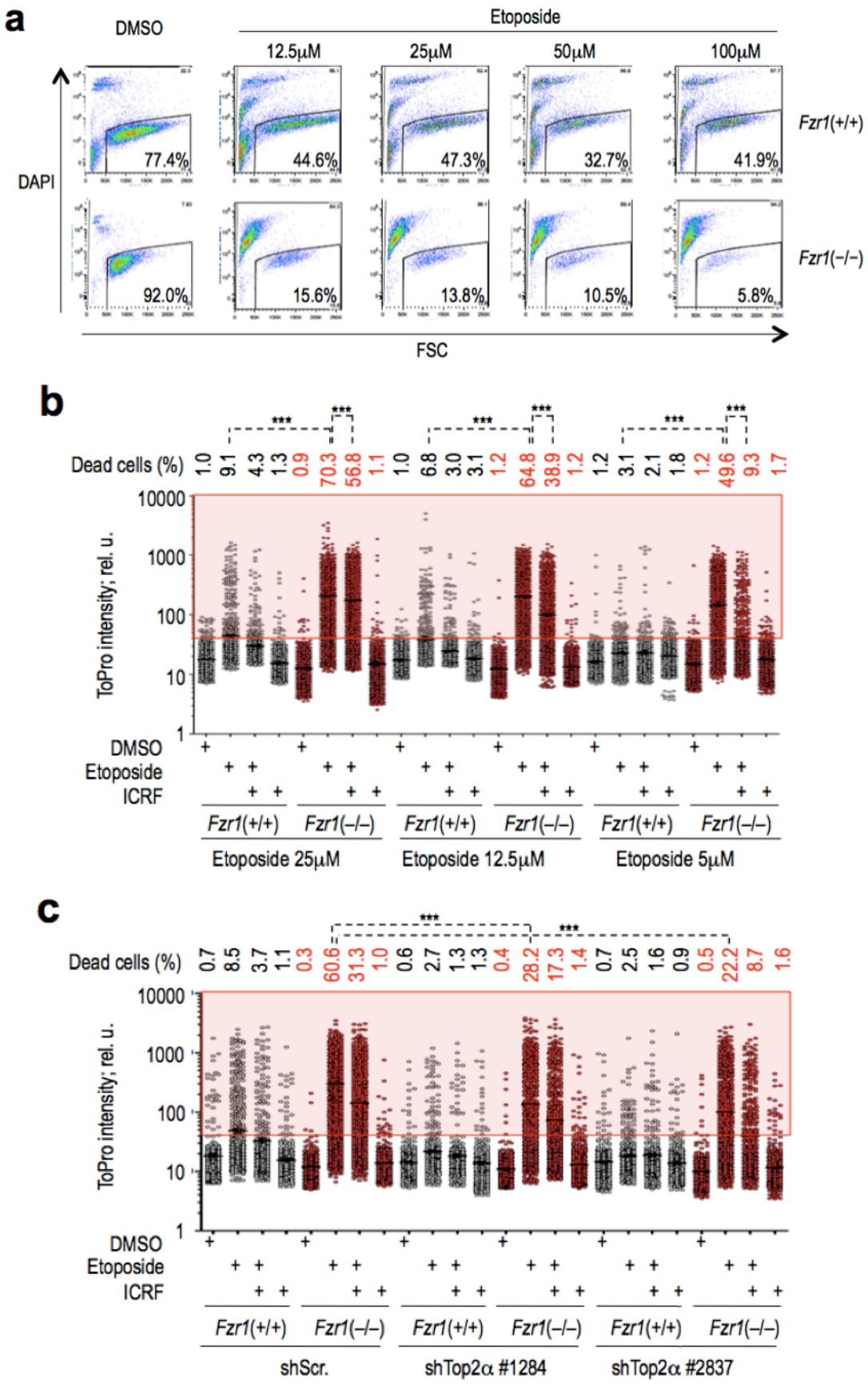
a
DMSO
Etoposide
12.5μM
25μM
50μM
100μM
DAPI
77.4%
44.6%
47.3%
32.7%
41.9%
92.0%
15.6%
13.8%
10.5%
5.8%
Fzr1(+/+)
Fzr1(−/−)
FSC
b
Dead cells (%)
1.0 9.1 4.3 1.3 0.9 70.3 56.8 1.1 1.0 6.8 3.0 3.1 1.2 64.8 38.9 1.2 1.2 3.1 2.1 1.8 1.2 49.6 9.3 1.7
***
ToPro intensity; rel. u.
10000
1000
100
10
1
DMSO
Etoposide
ICRF
Fzr1(+/+)
Fzr1(−/−)
Etoposide 25μM
Etoposide 12.5μM
Etoposide 5μM
c
Dead cells (%)
0.7 8.5 3.7 1.1 0.3 60.6 31.3 1.0 0.6 2.7 1.3 1.3 0.4 28.2 17.3 1.4 0.7 2.5 1.6 0.9 0.5 22.2 8.7 1.6
***
ToPro intensity; rel. u.
10000
1000
100
10
1
DMSO
Etoposide
ICRF
Fzr1(+/+)
Fzr1(−/−)
shScr.
shTop2α #1284
shTop2α #2837

Figure 44 Legend

Increased susceptibility to etoposide of Cdh1-deficient cells. (**a**) Quantification of the lethal effect of etoposide at the indicated doses in Cdh1-null or control cells. The percentage of live cells (negative for DAPI) is indicated. (**b**) Quantification of cell death by internalization of the dye TO-PRO using high-throughput microscopy. Cdh1-null (red) or control (black) cells were treated with etoposide (at the indicated doses) or ICRF-193 (5 μM). The percentage of dead cells is indicated for each condition [see frame in panel (**a**)]. (**c**) Similar quantification of cell death after treatment with the indicated compounds and knock down of Top2α using two different short hairpin interfering RNAs. *** indicates $p<0.001$.

the lethal effect of etoposide, and this effect was more dramatic when using sequence #2837 which is more effective knocking down Top2α (Fig. 44c and 42b). Although we cannot discard that Cdh1-null cells may display additional molecular alterations that contribute to the increased sensitivity to etoposide, upregulation of Top2α is likely to account for a significant amount of part of this phenotype. It is important to note that, due to the high levels of upregulation of Top2α in Cdh1-null cells, these hairpin molecules were not able to modulate Top2α expression down to the levels found in wild-type cells (Fig. 42b), perhaps explaining that these rescued cells still displayed some sensitivity to etoposide (Fig. 44c).

3.3. Chemical inhibition of the APC/C sensitizes cells to topoisomerase poisons

Inhibition of the APC/C is currently considered as a novel therapeutic strategy in cancer by preventing Cdc20-dependent mitotic exit (Manchado *et al.*, 2012). A small-molecule, proTAME, results in mitotic arrest in collaboration with microtubule poisons by inhibiting APC/C-Cdc20 complexes (Zeng *et al.*, 2010). proTAME targets both APC/C-Cdc20 and APC/C-Cdh1 (Zeng *et al.*, 2010) although the effect of inhibiting Cdh1 complexes has not

been analyzed so far. Thus, we first tested the effect of proTAME in the protein level of Cdh1 substrates. As shown in Fig. 45, treatment of HeLa cells with different concentrations of proTAME results in increased levels of both Eg5 and Top2α in a dosis-dependent manner. These differences are not due to mitotic arrest since the mitotic index of cells treated with 20 µM proTAME was 4.6 ± 1.1% compared to 2.1 ± 0.6% in untreated cultures. The upregulation of Top2α was also significant after immunofluorescence with specific antibodies and these results were also obtained in different cell types such as lung cancer cells (A549) and breast tumor cells (MCF7) (Fig. 46).

Figure 45

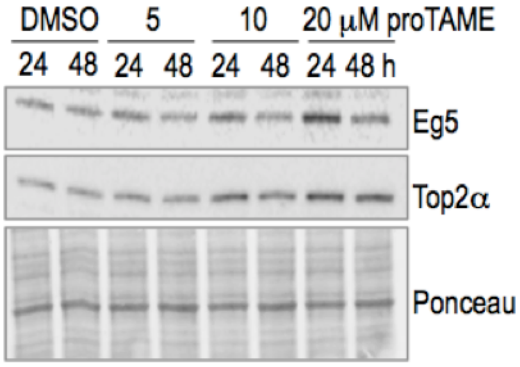

APC/C inhibitor proTAME leads to the stabilization of Top2α and Eg5. Protein levels of Eg5 and Top2α 24 or 48 h after chemical inhibition of the APC/C using proTAME at the indicated dose in HeLa cells.

Importantly, inhibition of the APC/C with proTAME sensitized HeLa cells to etoposide. Whereas single treatment with proTAME or etoposide resulted in certain levels of lethality in HeLa cells, the combination of these two compounds resulted in a significant synergism, especially when low dosis of pro-TAME was used (Fig. 47a,b). In A549 cells, treatment with 10 µM of proTAME resulted in no dramatic differences in Top2α levels (Fig. 46) and, accordingly, no differences in lethality were observed (Fig. 47c). A combination of 20 µM of proTAME and 25 µM of etoposide resulted in a significant synergism in lethality whereas higher concentrations of etoposide (100 µM) were not modulated by proTAME, suggesting that the combination of these two compounds is efficient in a specific window of moderate

Figure 41

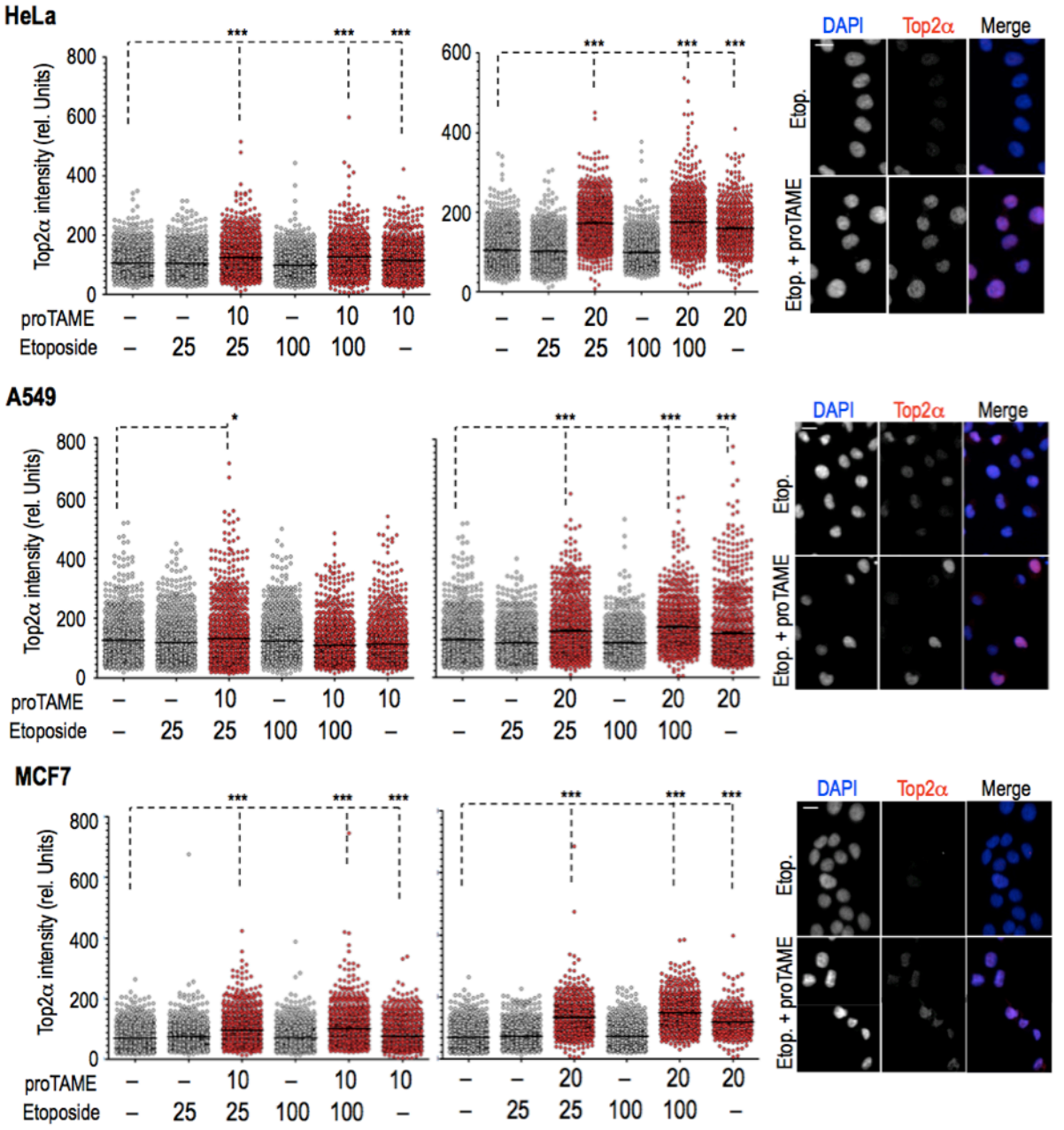

Protein levels of Top2α after inhibition of the APC/C in human cell lines. Quantification of Top2α levels in HeLa, A549 or MCF7 cells treated with the indicated dosis of proTAME or etoposide (μM). Representative images of cells treated with 25 μM etoposide or 25 μM etoposide + 20 μM proTAME are shown. Top2α is in red and DAPI in blue. Scale bars, 10 μM. At least 4000 cells per condition were quantified in these assays and only 1000 are represented in the plots for clarity. ***, p<0.001.

concentrations. Similarly, the synergism of this combination was evident using 10 µM of proTAME in MCF7 breast cancer cells, and much more dramatic when using 20 µM of this APC/C inhibitor in the presence of moderate concentrations of etoposide (Fig. 47d). These concentrations of proTAME induced a dramatic upregulation of Top2α (Fig. 46), suggesting that the therapeutic effect of this APC/C inhibitor correlates with its ability to induce Top2α accumulation.

Figure 47

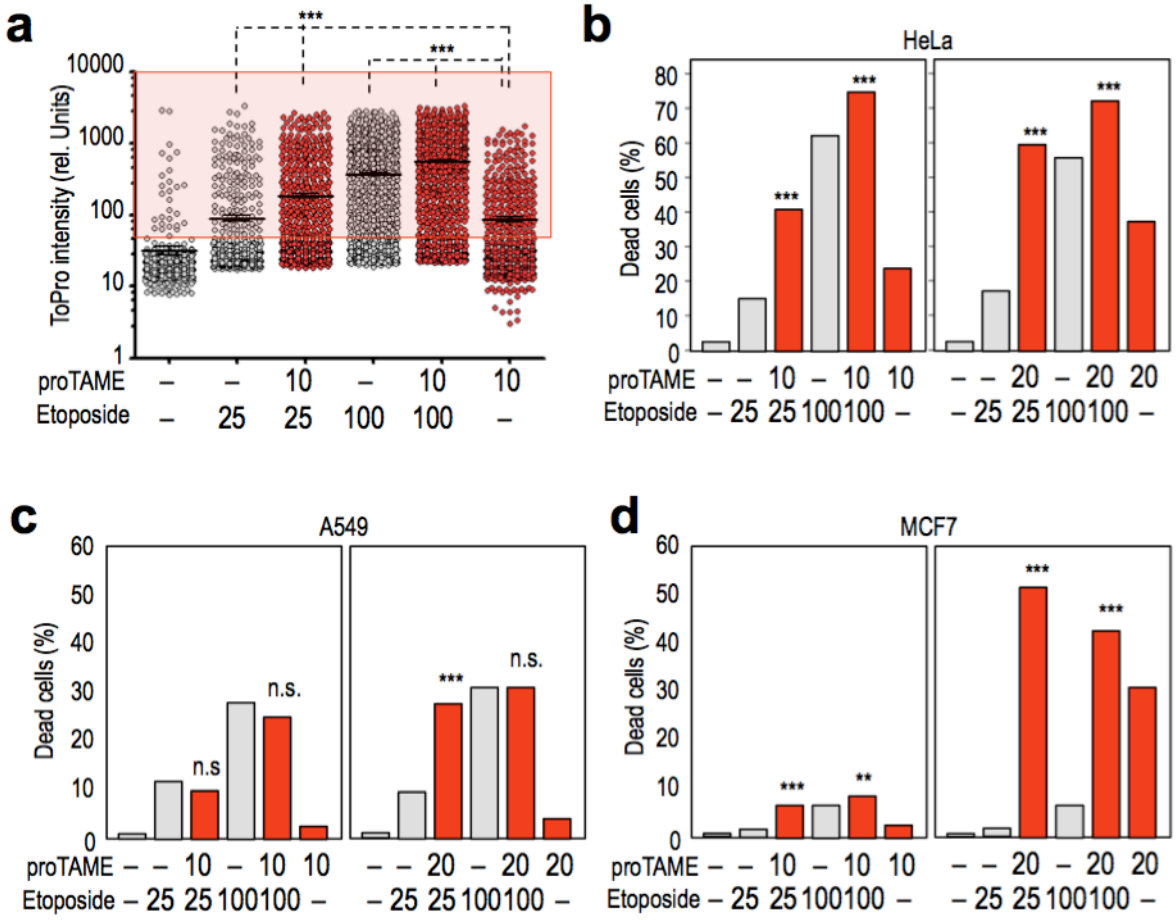

Cdh1 inhibition sensitizes human cancer cells to topoisomerase poisons. (**a**) Cellular intensity of the dye TO-PRO after treatment of HeLa cells with the indicated dose of proTAME or etoposide (µM). (**b-d**) Percentage of dead cells [as considered in the frame shown in panel (**a**)] after treatment of HeLa (**b**), A549 (**c**) or MCF7 (**d**) cells with the indicated dose of proTAME or etoposide (µM). At least 4000 cells per condition were quantified in these assays and only 1000 are represented in (**b**) and (**c**) for clarity. ***, p<0.001.

Discussion

1. Relevance of Cdh1 in the cell cycle

The APC/C is an essential E3-ubiquitin ligase involved in cell cycle regulation mostly during mitosis and the following G1 phase (Peters, 2006). In addition, this complex is involved in the control of metabolism and differentiation in various cell types (Sigrist and Lehner, 1997; Li *et al.*, 2007b; Wu *et al.*, 2007; Herrero-Mendez *et al.*, 2009; Colombo *et al.*, 2010), and recent studies have suggested a crucial role for APC/C-Cdh1 and APC/C-Cdc20 in postmitotic neurons (Konishi *et al.*, 2004; Lasorella *et al.*, 2006; Stegmuller *et al.*, 2006; Kim *et al.*, 2009; Yang *et al.*, 2009; Eguren *et al.*, 2011; Kuczera *et al.*, 2011).

Genetic ablation of Cdc20 results in a complete metaphase arrest in mammals confirming its essential role in the degradation of cyclin B and securin required for anaphase onset (Li *et al.*, 2007a; Manchado *et al.*, 2010b). Cdh1, on the other hand, is not essential for the cell cycle although lack of Cdh1 results in early entry into S-phase and reduced proliferation rate (Garcia-Higuera *et al.*, 2008; Li *et al.*, 2008; Sigl *et al.*, 2009). Genetic deletion of Cdh1 in the mouse embryo results in placental defects due to an essential role of this protein in endoreduplication (Garcia-Higuera *et al.*, 2008; Li *et al.*, 2008). The early embryonic lethality in these animals had prevented the study of the relevance of this protein in the mitotic cell cycle *in vivo* until now.

We have focused in the nervous system since multiple evidences have suggested in the past a neural role for Cdh1 (Gieffers *et al.*, 1999; Eguren *et al.*, 2011). Cdh1 depletion in neural progenitors resulted in the up-regulation of its known substrates and an initial increase in DNA replication. We and others had previously observed that Cdh1-deficient cells display an early loading of replication complexes resulting in shorter G1 and premature entry into S-phase (Engelbert *et al.*, 2008; Garcia-Higuera *et al.*, 2008). This phenotype is at least partially due to increased cyclin levels and reduced amount of cell cycle inhibitors (Figs. 13-15; see also (Garcia-Higuera *et al.*, 2008; Li *et al.*, 2008)). In fact, we have now demonstrated that the replicative stress and the proliferative defects induced by Cdh1 loss can be rescued by moderate inhibition of Cdk activity, suggesting that Cdk hyperactivation is one of the major mechanisms responsible for replicative stress in the absence of Cdh1 (Fig. 48). In Cdh1-deficient cells, there is an increase in the levels of cyclins and the Cdk activator Cdc25A as well as Skp2 and Cks1, two cofactors of the SCF E3 ubiquitin ligase. The accumulation of Skp2 and Cks1 ultimately results in increased activity of the SCF complex and, consecuently, decreased levels of the Cdk inhibitors of the Cip/Kip family (p21Cip1, p27Kip1 and p57Kip2) (Figure 48) (Bashir *et al.*, 2004; Wei *et al.*, 2004). All these events lead to an excess of Cdk activity that may favor unscheduled DNA synthesis, resulting in replicative defects and DNA damage.

In the developing cortex, the presence of DNA damage is accompanied by the accumulation of p53, G2-like arrest and apoptosis. Previously, it has been reported that the irradiation-induced checkpoint is deficient in Cdh1-deficient bone marrow cells suggesting a role for Cdh1 in the G2 checkpoint *in vivo* (Ishizawa *et al.*, 2011). In addition, this protein has been proposed to mediate DNA damage response to genotoxic stress (Bassermann *et al.*, 2008). Contrarily, our results using genetic models suggest that Cdh1 is not necessary for the G2 checkpoint, at least in neural progenitors, as the absence of the APC/C

coactivator in these cells results in an accumulation of cells arrested in G2 that have already duplicated their DNA content and centrosomes (Fig. 21).

Figure 48

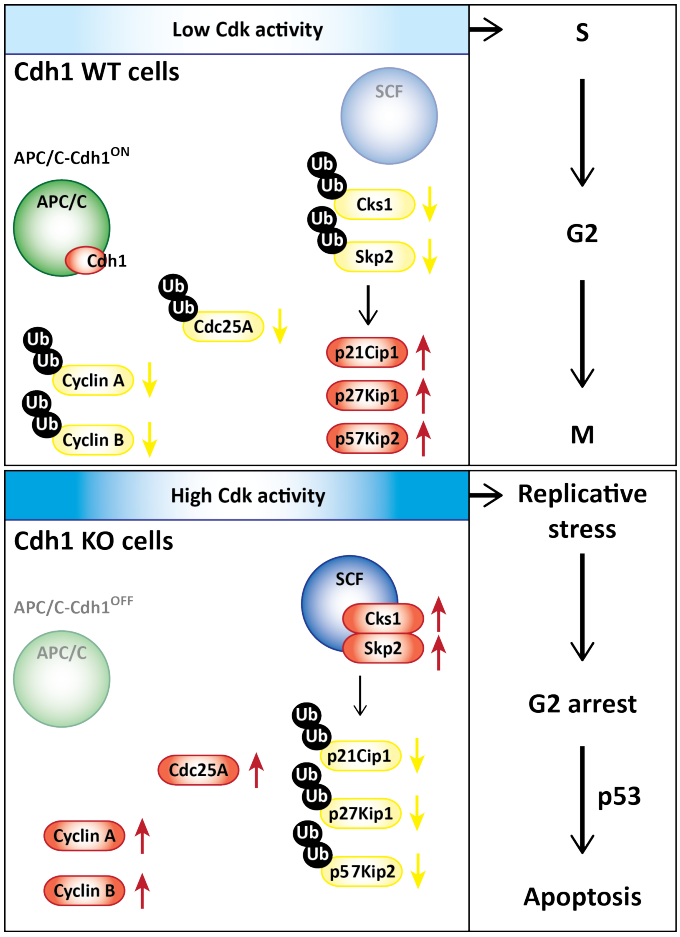

Hyperactivation of Cdk activity in Cdh1-deficient cells lead to DNA damage, G2-arrest and apoptosis. Scheme that represents how the absence of Cdh1 could lead to hyperactivation of the Cdks.

These alterations also affected the ependymal layer originated from fetal neural progenitors likely resulting in hydrocephalus, a condition that is known to occur upon compromised integrity of ependymal cells (Grondona *et al.*, 1996; Jimenez *et al.*, 2001; Morrens *et al.*, 2012). In addition, recent data suggest that increased death of neural progenitors is sufficient to induce hydrocephalus in the mouse, and that defects in these neural progenitors are crucial in the pathogenesis of neonatal hydrocephalus (Carter *et al.*, 2012). Thus, both the defects in the ependymal layer and the death of neural progenitors found in our model could be contributing to the hydrocephalus.

We therefore propose that Cdh1 deficiency results in replicative stress *in vivo* leading to a G2-like arrest and/or apoptosis of progenitor cells. In the brain, this results in a reduction in the number of neurons, tissue hypoplasia, perhaps related to microcephaly as shown for other cell cycle regulators (Malumbres, 2011), and hydrocephalus.

As suggested from *in vitro* studies with cultured cells (Engelbert *et al.*, 2008; Sigl *et al.*, 2009), p53 is not required for the proliferative defects caused by Cdh1 inhibition and double Fzr1(Δ/Δ); Nes-Cre; Tp53(–/–) brains accumulated a significant amount of replicative stress. Consequently, ablation of p53 did not rescue developmental defects caused by Cdh1 ablation. Intriguingly, p53 deficiency strongly synergized with Cdh1 loss and double mutant mice died within the first 10 weeks of life with severe brain hypoplasia and hydrocephalus. This phenotype correlated with lack of apoptosis in neural progenitors indicating that p53 is essential for the apoptotic cell death induced by Cdh1 loss (Fig. 25). These results are in agreement with the reported requirements for p53 in the apoptotic death of neural progenitors with abnormal cell cycle progression induced by p57Kip2 or Atr inactivation (Matsumoto *et al.*, 2011; Lee *et al.*, 2012). In fact, p53 loss has been shown to exacerbate the effects of DNA replication defects in several models (Murga *et al.*, 2009; Ruzankina *et al.*, 2009; Reaper *et al.*, 2011), further supporting the idea that the primary defect in Cdh1-deficient cells is related to abnormal DNA replication. This is likely to be related with the role of p53 in limiting DNA replication in the presence of damage. As proposed previously, in the absence of p53, initiation of DNA replication continues and DNA damage accumulates leading to a synthetic lethal interaction between replicative stress and p53 loss (Murga *et al.*, 2009; Reaper *et al.*, 2011). All together, these data suggest a major function for Cdh1 in protecting neural progenitors against unrestrained entry into the cell cycle, genomic damage and cell death. Thus, replicative stress in the

absence of Cdh1 is p53 independent, but p53 plays a major role preventing developmental defects by eliminating these damaged cells from the tissue.

2. Identification of new Cdh1 targets

Whereas APC/C-Cdc20 targets for degradation a few critical mitotic regulators (A- and B-cyclins, Nek2, securin), Cdh1 is more promiscuous and targets for degradation multiple cell cycle regulators from mitotic exit to G1/S transition, including Cdc20 targets as well as Cdc20 itself (Peters, 2006; Eguren *et al.*, 2011).

In the past, the identification of new Cdh1 substrates have been mostly performed through massive approaches based on transcriptional profiles or two-hybrid interaction screens in yeast (Ostapenko *et al.*, 2012). Here, we have made use of Cdh1-knockout cells and animals recently generated in our laboratory to understand major changes in protein levels in these mutant cells. By using quantitative proteomic approaches, we have identified several putative Cdh1 substrates (Table 3). We have focused in this work in two molecules (Eg5 & Top2α), which scored amongst the highest accumulated proteins in three different proteomic analyses in Cdh1-null cells or tissues. In addition, both of them are targets of chemotherapeutic drugs currently in clinical use.

Eg5, also known as Kif11, is a bipolar, homotetrameric, plus-end-directed spindle motor protein of the kinesin-5 family involved in the proper formation of a bipolar spindle. Although the APC/C-dependent control of the mammalian Eg5 kinesin has not been studied so far, earlier work in budding yeast suggested that the related Cin8p and Kip1p kinesins are degraded in an APC/C-dependent manner. Degradation of Kip1p was reported to be mediated by APC/C-Cdc20 although mutation of several putative D-boxes did not stabilize

this protein. Cdc20-dependent degradation of Kip1p seems to depend on a 17-aa sequence with no primary homology to other known domains (Gordon and Roof, 2001). Degradation of Cin8p is Cdh1-dependent although this protein also lacks a functional D-box sequence (Hildebrandt and Hoyt, 2001). Cin8p however contains a bipartite degradation signal composed of a KEN-box, located at the C-terminus of the protein similarly to Eg5 (Fig. 39), plus undefined downstream residues (Hildebrandt and Hoyt, 2001). Degradation of Cin8p is not essential for normal cell cycle progression in yeast, as we have also observed for human Eg5. However, APC/C-dependent degradation of multiple yeast kinesins including Cin8p and Kip1p, as well as two additional microtubule-associated proteins, Ase1 and Fin1, is required for the efficient disassembly of the mitotic spindle (Juang *et al.*, 1997; Shirayama *et al.*, 1998; Hildebrandt and Hoyt, 2001; Woodbury and Morgan, 2007).

In mammals, strong overexpression of Eg5 results in abnormal spindle formation with the presence of monopolar spindles and monoastral arrays of microtubules (Castillo *et al.*, 2007). This effect is much stronger that the one found in Cdh1-deficient cells (Garcia-Higuera *et al.*, 2008) suggesting that this overexpression model is not useful to evaluate the effect of the modulation of this kinesin by the APC/C. In addition, mitotic exit is only slightly delayed in Cdh1-null cells and it is difficult to attribute this defect to individual Cdh1 substrates involved in the regulation of mitosis (Aurora or Polo kinases, Tpx2, etc.) (Garcia-Higuera *et al.*, 2008).

DNA topoisomerases 2 (Top2) are enzymes that modify the topological status of DNA in order to facilitate processes such as replication or transcription and the relief of torsional stresses (Wang, 2002). These enzymes catalyze the breaking and rejoining of two strands of a double helix of DNA, allowing to pass one duplex DNA through the other (Figure 49; (Schoeffler and Berger, 2005)). There are two different isozymes with similar catalytic, but

distinct biological activity. Whereas Top2α is essential for proper cell division, Top2b is involved in brain development and differentiation (Linka *et al.*, 2007).

Figure 49

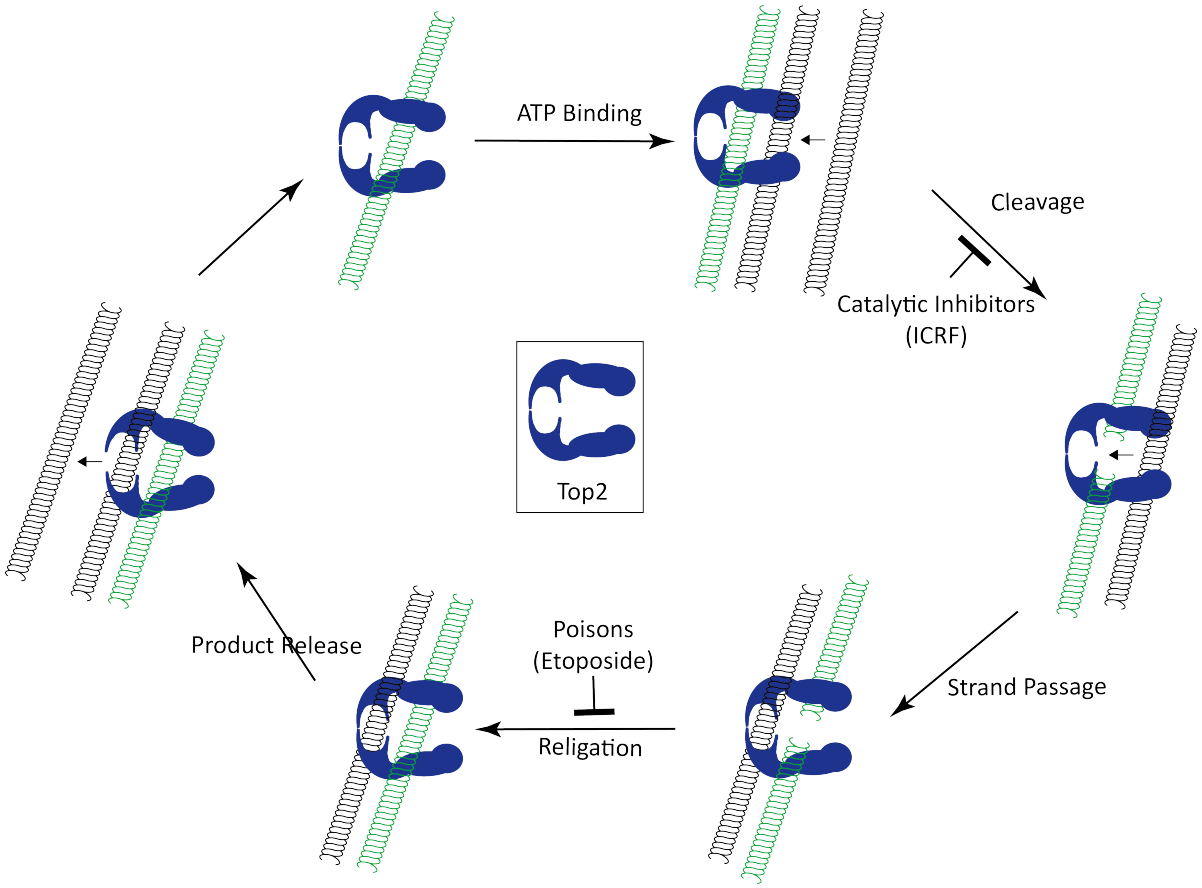

Mechanism of action of Top2 and Top2 inhibitors. Type 2 topoisomerases allow the pass of a duplex DNA (black) through another duplex DNA (green) through generating transient double strand breaks. Then, the strands are religated and the products of the reaction are released from the enzyme. The catalytic functions of Top2 are driving by the hydrolysis of ATP. Top2 inhibitors are divided in two different classes: poisons, which inhibit Top2 after the cleavage, stabilizing the enzyme-induced DNA breaks and avoiding the religation of the DNA; and catalytic inhibitors, which target the ATPase domain preventing the double strand breaks.

As mention above, the proteomic analysis of Cdh1-null cells showed that Top2α is one of the most accumulated proteins in the absence of this APC/C cofactor (Figs. 32-35). This is not a consequence of transcriptional changes due to the DNA damage present in these cells since Top2α transcripts are not altered whereas p53-responsive genes such as p21Cip1 are highly induced (Fig. 36). Top2α is known to be regulated by protein degradation although reported data suggest that it is actually degraded in a Bmi1/Ring1A-dependent manner in the presence of DNA damage (Alchanati *et al.*, 2009). Thus, the upregulation of Top2α in Cdh1-null cells is not a consequence of the damage present in these cells. Although we have not been able to observed direct degradation of Top2α in Xenopus extracts after the addition of Cdh1, this topoisomerase is ubiquitinated in a Cdh1-dependent manner, and degraded in a proteasome-dependent manner upon re-expression of Cdh1 in Cdh1-null cells (Fig. 36). Unfortunately, the Top2α KEN;D-box mutant is highly toxic in mammalian cells and we have not been able to analyze the consequences of these mutations in live cells. Thus, although the ubiquitination of Top2α is likely involved in the degradation of this protein, it is also possible that Cdh1-dependent ubiquitination may have a yet unidentified role, besides degradation.

Top2α associates with mitotic chromosomes and specifically concentrates along the central axis of each chromatid arm during prometaphase and metaphase (Earnshaw and Heck, 1985; Mo and Beck, 1999; Tavormina *et al.*, 2002). The kinetics of degradation of Top2α differs from other typical Cdh1 substrates and this protein is degraded later in G1, once daughter cells have been formed, rather than during mitotic exit [Fig. 40a,b and (Heck *et al.*, 1988; Tavormina *et al.*, 2002)]. Since Top2α is ubiquitinated, but not degraded within a few hours, after the addition of Cdh1 in Xenopus egg extracts (Fig. 38), and displays a slow kinetics of degradation during G1 [Fig. 40 and (Heck *et al.*, 1988; Tavormina *et al.*,

2002)], it is likely that degradation of this protein requires additional signals or modifications that are unknown at this moment.

In addition to the relevance in cancer treatments (see below), the control of Top2α and Eg5 by Cdh1 is likely to have important consequences in the nervous system. Whereas Top2α is the main topoisomerase isoform expressed in proliferating cells, a switch in the expression from Top2α to Top2β occurs during neuronal differentiation *in vitro* and *in vivo*. Top2α mRNA expression and protein levels decrease from the stem cell to the neuronal progenitor state and are further down-regulated strongly in postmitotic neurons (Watanabe *et al.*, 1994; Tsutsui *et al.*, 2001; Tiwari *et al.*, 2012). Futthermore, the control of Eg5 by Cdh1 may also have additional clinical implications in brain development as the activity of this kinesin is altered in human microcephaly due to a variety of mutations in the Eg5-encoding gene KIF11 (Ostergaard *et al.*, 2012). In addition, Eg5 also regulates axonal outgrowth (Myers and Baas, 2007; Nadar *et al.*, 2008) and neuronal development (Ferhat *et al.*, 1998) and migration (Falnikar *et al.*, 2011). Inhibition of Eg5 is also currently considered as a strategy to improve axon regeneration (Haque *et al.*, 2004; Lin *et al.*, 2011). Importantly, Cdh1 has also been shown to be expressed in postmitotic neurons (Gieffers *et al.*, 1999), regulates axonal growth (Konishi *et al.*, 2004), and may be involved in neurodegenerative diseases in the mammalian brain (Aulia and Tang, 2006).

We have observed that genetic ablation of Cdh1 in the nervous system results in abnormal exit from the cell cycle in neural progenitors accompanied by strong accumulation of γH2AX signal, finally leading to defective development of the nervous system and hydrocephalus. It is therefore likely that the control of Top2α and Eg5 levels by APC/C-Cdh1 may have a critical role during neuron differentiation.

3. Therapeutic implications of APC/C-Cdh1 inhibition.

The requirements for the APC/C during the cell cycle have promoted different studies to evaluate the relevance of this complex as a cancer target (Zeng *et al.*, 2010; Manchado *et al.*, 2012). The pioneer suggestion that targeting mitotic exit is a relevant therapeutic strategy (Huang *et al.*, 2009) has been confirmed using Cdc20-deficient mice (Manchado *et al.*, 2010b). Elimination of APC/C-Cdc20 activity results in metaphase arrest due to the lack of degradation of cyclin B1, and this strategy is more efficient in killing cells than current microtubule poisons such as taxanes (Huang *et al.*, 2009; Manchado *et al.*, 2010b).

The first APC/C inhibitor, proTAME, is currently under preclinical studies (Zeng *et al.*, 2010; Zeng and King, 2012), and this small-molecule APC/C inhibitor has been reported to inhibit both Cdc20 and Cdh1 complexes, although the activity on APC/C-Cdh1 has not been characterized (Zeng *et al.*, 2010). These therapeutic approaches are directed against APC/C-Cdc20 activity, and the concomitant inhibition of Cdh1 has been considered as a putative undesired effect due to the proliferative potential of overexpressed Cdh1 substrates (cyclins, Aurora or Plk1 kinases, etc). Yet, the physiological consequences of eliminating Cdh1 in mammalian tissues *in vivo* and the specific targets that mediate those Cdh1-dependent phenotypes had remained unclear.

Contrary to the original expectations, our genetic data suggest that ablation of Cdh1, at least in neural progenitors, results in replicative stress *in vivo* and a general antiproliferative response that is not p53-dependent (Fig. 50). Since depletion of Cdh1 in the complete embryo (Fzr1(–/D); Sox2-Cre mice) displayed defects in the development of multiple organs (Fig. 12), the anti-proliferative effect caused by Cdh1 ablation is likely common to many other tissues. Thus, putative APC/C inhibitors are unlikely to generate pro-proliferative

responses even in the case of unspecific inhibition of Cdh1 and with independence of the p53 status of tumor cells.

In addition, here we have shown that the inhibition of APC/C may have therapeutic use, not only by inhibiting Cdc20 leading to mitotic arrest, but also through the inhibition of Cdh1. Our work have shown the clinical relevance of targeting APC/C-Cdh1 in differente clinical settings, due to its effect on the levels of two new Cdh1 substrates, Top2α and Eg5, which we have also identified in this study (Fig. 50).

Overexpression of Eg5 in transgenic mice causes genomic instability and favors tumor development (Fig. 50; (Castillo *et al.*, 2007)). Furthermore, this protein is commonly overexpressed in human tumors and, given its function during mitotic progression, is currently under clinical evaluation as a cancer target (Rath and Kozielski, 2012; Doménech and Malumbres, 2013). The Eg5 inhibitor monastrol was identified in a pioneer screen for anti-mitotic drugs different from classical microtubule poisons (Mayer *et al.*, 1999). Treatment of cells with monastrol results in monopolar spindles and a mitotic arrest that depends on the activity of the mitotic checkpoint. This arrest is transient and mouse fibroblasts exit from mitosis without chromosome segregation in about 8 h (Fig. 41). As shown in our work, lack of Cdh1 results in partial resistance to monastrol as a significant percentage of cells is able to segregate chromosomes in the presence of this drug. This rescue does not occur after downregulation of Eg5 to levels that only slightly affect chromosome segregation in the absence of monastrol. However, we do not know if those cells that segregate in the presence of monastrol in Cdh1 deficient cells continue proliferating normally or if they eventually die. To our knowledge, the correlation between Eg5 expression and the response to Eg5 inhibitors in clinical trials has not been reported. Yet, Eg5 levels may correlate with the response to different anti-mitotic drugs combined

with classical chemotherapies (Saijo *et al.*, 2006). Therefore, further studies are needed to establish the relation between Eg5 levels and the response to Eg5 inhibitors.

Besides kinesin Eg5 we have also identified topoisomerase Top2α as a new APC/C-Cdh1 substrate with important therapeutic implications.

Figure 50

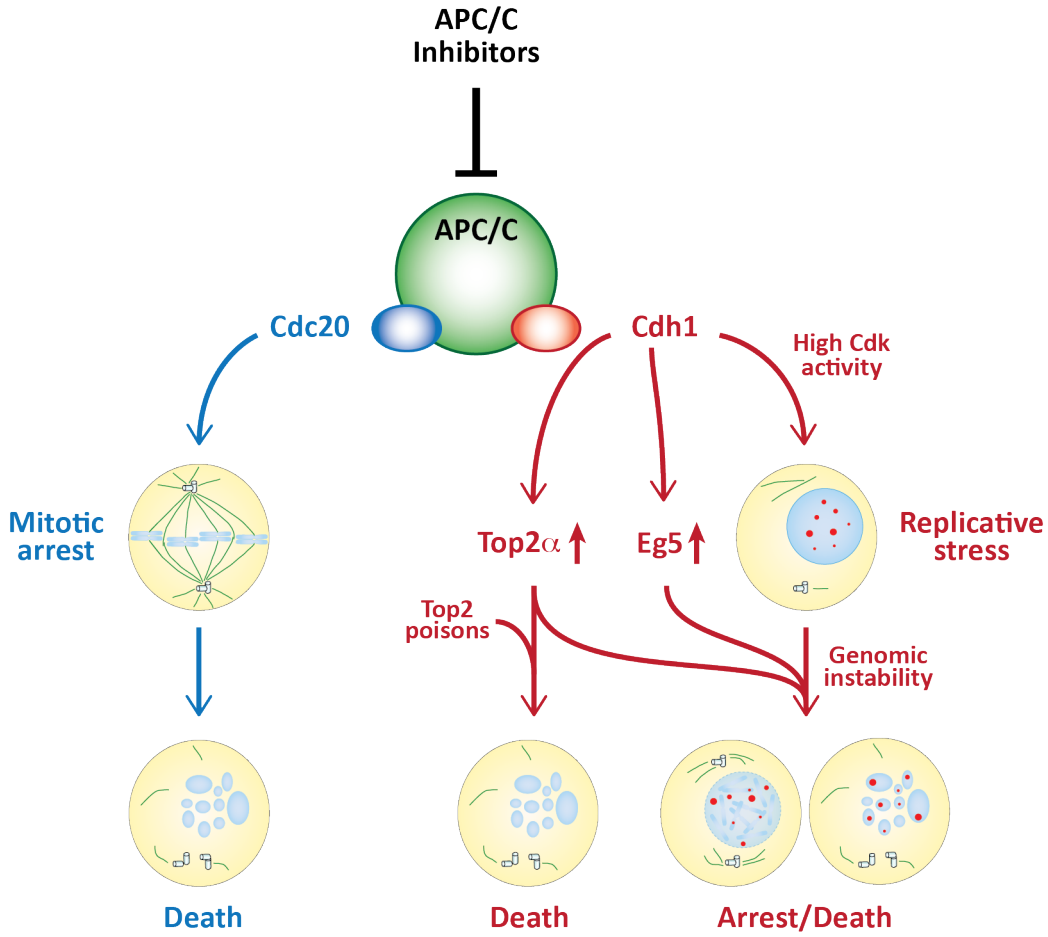

Therapeutic implications of APC/C inhibition. On one hand, APC/C-Cdh1 inhibition leads to replicative stress, arrest and cell death due to increased Cdk activity. On the other hand, APC/C-Cdh1 inhibtion sensitizes cells to Top2 posions, revealing a new synthetic lethal interaction.

Top2 poisons such as etoposide blocks the catalytic cycle after DNA is already cleaved by topoisomerase but before DNA re-ligation, thus generating Top2-DNA covalent complexes (Figure 49). These poisons therefore convert Top2 into an agent that induces cellular damage (Nitiss, 2009). We and others have shown that Cdh1-null cells display high levels of DNA damage both *in vitro* (Fig. 16, 19, 20 & 22; Sigl et al. 2009) and *in vivo* (Fig. 17, 18 & 25). As mentioned previously, the lack of Cdh1 results in increased levels of Cyclin-Cdk activity and premature entry into S-phase and this may favor increased DNA damage in these conditions (Garcia-Higuera *et al.*, 2008). The identification of Top2α as a new Cdh1 substrate highly upregulated in Cdh1-null cells suggest that Top2α might contribute to the accumulation of damage (Fig. 50).

Moreover, resistance to topoisomerase-targeting drugs in mammalian cells does not correlate with increase expression of Top2 proteins but is rather frequently associated with reduced expression of these proteins (Nitiss, 2009). In fact, overexpression of Top2α is known to correlate with susceptibility to these drugs (Coutts *et al.*, 1993; Keith *et al.*, 1993; Smith *et al.*, 1993). This is due to the correlation between the presence of topoisomerase poisons and enzyme-mediated DNA damage. Indeed, as shown in Fig. 44, the sensitivity of Cdh1-deficient cells to topoisomerase poisons such as etoposide is dramatic, and is at least partially rescued after downregulation of Top2α levels. Intersitingly, catalytic inhibitors of Top2 frequently antagonize the toxicity of Top2 poisons (Jensen and Sehested, 1997) and this is also observed in Cdh1-null cells when using ICRF-193 (Fig. 44). Thus, the accumulation of Top2α in Cdh1-null cells might both contribute to generate DNA damage in these cells and increase their sensibility to Top2 poisons.

Importantly, APC/C-Cdh1 inhibition by the small-molecule inhibitor proTAME specifically increases Top2α levels and sensitizes human cancer cells to topoisomerase poisons (Fig.

50). These results provide the first scenario to explore the relevance of inhibiting the APC/C with independence of its mitotic effect. Given the relevance of topoisomerase poisons in the clinic (Nitiss, 2009), these data may open new avenues to explore the potential benefits of new synthetic lethal interactions based on APC/C-Cdh1 substrates. Moreover, all these data suggest that a combined therapy based on targeting Cdh1 might be a better strategy than based on Cdc20. It has been shown that to achieve a mitotic arrest, a complete inhibition of APC/C-Cdc20 is required (Baumgarten *et al.*, 2009; Manchado *et al.*, 2010b), whereas our results show that a lower concentration of APC/C inhibitor (not sufficient to get a mitotic arrest) leads to an accumulation of Top2α and increased susceptibility to Top2 posions due to APC/C-Cdh1 inhibition (Figs. 46,47).

Another important issue related to therapy, is the status of Cdh1 in human tumors, which has not been explored in detail yet. Although this molecule is not mutated or downregulated in human tumors, its function is inhibited by Cdk-dependent phosphorylation (Kramer *et al.*, 2000) and Cdh1 is therefore thought to be inactive in cancer cells due to Cdk hyperactivity commonly found in malignant cells (Lehman *et al.*, 2007). As shown in this work, Cdh1-deficient cells display an increased susceptibility to topoisomerase poisons (Fig. 44) but potential resistance to Eg5 inhibitor monastrol, due to the accumulation of Top2α and Eg5, respectively. It will be therefore interesting to test in human tumors whether the functional status of Cdh1 might be useful as a biomarker for therapeutic strategies based on the use of topoisomerase poisons or mitotic drugs.

Conclusions

1. Cdh1 is not essential for cell cycle progression in mammals, it seems to be dispensable for most mammalian tissues, but it has a special relevance for the proper development of the nervous system and its absence in mice cause hydrocephalus which in most cases leads to premature death.

2. Cdh1 protects against genomic instability in neural precursors by preventing a promiscuous entry in S-phase and the accumulation of a type of DNA damage known as replication stress. Cdh1 null neural progenitors accumulate high levels of replication stress that can be alleviated by the addition of nucleosides.

3. Cdh1 depletion does not result ultimately in increased proliferation but produces replicative stress (in a p53-independent manner) and apoptosis (in a p53-dependent manner).

4. Partial inhibition of Cdk activity rescues the increased DNA damage and proliferation defects present in the absence of Cdh1, suggesting that Cdks hyperactivation is the ultimate cause of replication stress.

5. Proteomics screens for novel Cdh1 targets showed that APC/C-Cdh1 modulates Eg5 and Top2α protein levels, contributing to the genomic instability present in the Cdh1-null cells.

6. The upregulation of kinesin Eg5 in Cdh1-deficient cells leads to increased resistance to the Eg5 inhibitor monastrol.

7. The accumulation of the topoisomerase Top2α sensitizes Cdh1-depleted cells to topoisomerase poisons, one of the most used drugs in cancer therapy.

8. APC/C inhibition in human cancer cells by the small molecule proTAME enhances their susceptibility to the topoisomerase poison etoposide, unveiling a new synthetic lethal interaction.

9. APC/C inhibition may have therapeutic use, not only by inhibiting Cdc20 leading to mitotic arrest and cell death, but also by accumulating Cdh1 substrates (such as Eg5 and Top2α) resulting in genomic instability and differential responses (increased resistance or susceptibility) to particular/specific antitumoral therapeutic agents.

References

Acquaviva, C., and Pines, J. (2006). The anaphase-promoting complex/cyclosome: APC/C. J Cell Sci *119*, 2401-2404.

Alchanati, I., Teicher, C., Cohen, G., Shemesh, V., Barr, H.M., Nakache, P., Ben-Avraham, D., Idelevich, A., Angel, I., Livnah, N., Tuvia, S., Reiss, Y., Taglicht, D., and Erez, O. (2009). The E3 ubiquitin-ligase Bmi1/Ring1A controls the proteasomal degradation of Top2alpha cleavage complex - a potentially new drug target. PLoS One *4*, e8104.

Almeida, A., Bolanos, J.P., and Moncada, S. (2010). E3 ubiquitin ligase APC/C-Cdh1 accounts for the Warburg effect by linking glycolysis to cell proliferation. Proc Natl Acad Sci U S A *107*, 738-741.

Almeida, A., Bolanos, J.P., and Moreno, S. (2005). Cdh1/Hct1-APC is essential for the survival of postmitotic neurons. J Neurosci *25*, 8115-8121.

Aulia, S., and Tang, B.L. (2006). Cdh1-APC/C, cyclin B-Cdc2, and Alzheimer's disease pathology. Biochem Biophys Res Commun *339*, 1-6.

Bashir, T., Dorrello, N.V., Amador, V., Guardavaccaro, D., and Pagano, M. (2004). Control of the SCF(Skp2-Cks1) ubiquitin ligase by the APC/C(Cdh1) ubiquitin ligase. Nature *428*, 190-193.

Bassermann, F., Eichner, R., and Pagano, M. (2013). The ubiquitin proteasome system - Implications for cell cycle control and the targeted treatment of cancer. Biochim Biophys Acta.

Bassermann, F., Frescas, D., Guardavaccaro, D., Busino, L., Peschiaroli, A., and Pagano, M. (2008). The Cdc14B-Cdh1-Plk1 axis controls the G2 DNA-damage-response checkpoint. Cell *134*, 256-267.

Baumgarten, A.J., Felthaus, J., and Wasch, R. (2009). Strong inducible knockdown of APC/CCdc20 does not cause mitotic arrest in human somatic cells. Cell Cycle *8*, 643-646.

Bester, A.C., Roniger, M., Oren, Y.S., Im, M.M., Sarni, D., Chaoat, M., Bensimon, A., Zamir, G., Shewach, D.S., and Kerem, B. (2011). Nucleotide deficiency promotes genomic instability in early stages of cancer development. Cell *145*, 435-446.

Bevins, R.A., and Besheer, J. (2006). Object recognition in rats and mice: a one-trial non-matching-to-sample learning task to study 'recognition memory'. Nat Protoc *1*, 1306-1311.

Blow, J.J., and Dutta, A. (2005). Preventing re-replication of chromosomal DNA. Nat Rev Mol Cell Biol *6*, 476-486.

Brandeis, M., and Hunt, T. (1996). The proteolysis of mitotic cyclins in mammalian cells persists from the end of mitosis until the onset of S phase. Embo J *15*, 5280-5289.

Brandeis, M., Rosewell, I., Carrington, M., Crompton, T., Jacobs, M.A., Kirk, J., Gannon, J., and Hunt, T. (1998). Cyclin B2-null mice develop normally and are fertile whereas cyclin B1-null mice die in utero. Proc Natl Acad Sci U S A *95*, 4344-4349.

Burton, J.L., and Solomon, M.J. (2007). Mad3p, a pseudosubstrate inhibitor of APCCdc20 in the spindle assembly checkpoint. Genes Dev *21*, 655-667.

Buschhorn, B.A., Petzold, G., Galova, M., Dube, P., Kraft, C., Herzog, F., Stark, H., and Peters, J.M. (2011). Substrate binding on the APC/C occurs between the coactivator Cdh1 and the processivity factor Doc1. Nat Struct Mol Biol *18*, 6-13.

Cardozo, T., and Pagano, M. (2004). The SCF ubiquitin ligase: insights into a molecular machine. Nat Rev Mol Cell Biol *5*, 739-751.

Carmena, M., and Earnshaw, W.C. (2003). The cellular geography of aurora kinases. Nat Rev Mol Cell Biol *4*, 842-854.

Carroll, C.W., Enquist-Newman, M., and Morgan, D.O. (2005). The APC subunit Doc1 promotes recognition of the substrate destruction box. Curr Biol *15*, 11-18.

Carter, C.S., Vogel, T.W., Zhang, Q., Seo, S., Swiderski, R.E., Moninger, T.O., Cassell, M.D., Thedens, D.R., Keppler-Noreuil, K.M., Nopoulos, P., Nishimura, D.Y., Searby, C.C., Bugge, K., and Sheffield, V.C. (2012). Abnormal development of NG2+PDGFR-alpha+ neural progenitor cells leads to neonatal hydrocephalus in a ciliopathy mouse model. Nat Med *18*, 1797-1804.

Carter, S.L., Eklund, A.C., Kohane, I.S., Harris, L.N., and Szallasi, Z. (2006). A signature of chromosomal instability inferred from gene expression profiles predicts clinical outcome in multiple human cancers. Nat Genet *38*, 1043-1048.

Castillo, A., Morse, H.C., 3rd, Godfrey, V.L., Naeem, R., and Justice, M.J. (2007). Overexpression of Eg5 causes genomic instability and tumor formation in mice. Cancer Res *67*, 10138-10147.

Cebolla, A., Vinardell, J.M., Kiss, E., Olah, B., Roudier, F., Kondorosi, A., and Kondorosi, E. (1999). The mitotic inhibitor ccs52 is required for endoreduplication and ploidy-dependent cell enlargement in plants. Embo J *18*, 4476-4484.

Chabes, A.L., Pfleger, C.M., Kirschner, M.W., and Thelander, L. (2003). Mouse ribonucleotide reductase R2 protein: a new target for anaphase-promoting complex-Cdh1-mediated proteolysis. Proc Natl Acad Sci U S A *100*, 3925-3929.

Chao, W.C., Kulkarni, K., Zhang, Z., Kong, E.H., and Barford, D. (2012). Structure of the mitotic checkpoint complex. Nature *484*, 208-213.

Colombo, S.L., Palacios-Callender, M., Frakich, N., De Leon, J., Schmitt, C.A., Boorn, L., Davis, N., and Moncada, S. (2010). Anaphase-promoting complex/cyclosome-Cdh1 coordinates glycolysis and glutaminolysis with transition to S phase in human T lymphocytes. Proc Natl Acad Sci U S A *107*, 18868-18873.

Coppock, D.L., and Pardee, A.B. (1987). Control of thymidine kinase mRNA during the cell cycle. Mol Cell Biol *7*, 2925-2932.

Coutts, J., Plumb, J.A., Brown, R., and Keith, W.N. (1993). Expression of topoisomerase II alpha and beta in an adenocarcinoma cell line carrying amplified topoisomerase II alpha and retinoic acid receptor alpha genes. Br J Cancer *68*, 793-800.

Cox, J., and Mann, M. (2008). MaxQuant enables high peptide identification rates, individualized p.p.b.-range mass accuracies and proteome-wide protein quantification. Nat Biotechnol *26*, 1367-1372.

da Fonseca, P.C., Kong, E.H., Zhang, Z., Schreiber, A., Williams, M.A., Morris, E.P., and Barford, D. (2011). Structures of APC/C(Cdh1) with substrates identify Cdh1 and Apc10 as the D-box co-receptor. Nature *470*, 274-278.

DeBerardinis, R.J., Mancuso, A., Daikhin, E., Nissim, I., Yudkoff, M., Wehrli, S., and Thompson, C.B. (2007). Beyond aerobic glycolysis: transformed cells can engage in glutamine metabolism that exceeds the requirement for protein and nucleotide synthesis. Proc Natl Acad Sci U S A *104*, 19345-19350.

Diffley, J.F. (2004). Regulation of early events in chromosome replication. Curr Biol *14*, R778-786.

Earnshaw, W.C., and Heck, M.M. (1985). Localization of topoisomerase II in mitotic chromosomes. J Cell Biol *100*, 1716-1725.

Edgar, B.A., and Orr-Weaver, T.L. (2001). Endoreplication cell cycles: more for less. Cell *105*, 297-306.

Eguren, M., Manchado, E., and Malumbres, M. (2011). Non-mitotic functions of the Anaphase-Promoting Complex. Semin Cell Dev Biol *22*, 572-578.

Elias, J.E., and Gygi, S.P. (2007). Target-decoy search strategy for increased confidence in large-scale protein identifications by mass spectrometry. Nat Methods *4*, 207-214.

Engelbert, D., Schnerch, D., Baumgarten, A., and Wasch, R. (2008). The ubiquitin ligase APC(Cdh1) is required to maintain genome integrity in primary human cells. Oncogene *27*, 907-917.

Ernoult, E., Gamelin, E., and Guette, C. (2008). Improved proteome coverage by using iTRAQ labelling and peptide OFFGEL fractionation. Proteome Sci *6*, 27.

Falnikar, A., Tole, S., and Baas, P.W. (2011). Kinesin-5, a mitotic microtubule-associated motor protein, modulates neuronal migration. Mol Biol Cell *22*, 1561-1574.

Fay, D.S., Keenan, S., and Han, M. (2002). fzr-1 and lin-35/Rb function redundantly to control cell proliferation in C. elegans as revealed by a nonbiased synthetic screen. Genes Dev *16*, 503-517.

Ferhat, L., Cook, C., Chauviere, M., Harper, M., Kress, M., Lyons, G.E., and Baas, P.W. (1998). Expression of the mitotic motor protein Eg5 in postmitotic neurons: implications for neuronal development. J Neurosci *18*, 7822-7835.

Ferron, S., Mira, H., Franco, S., Cano-Jaimez, M., Bellmunt, E., Ramirez, C., Farinas, I., and Blasco, M.A. (2004). Telomere shortening and chromosomal instability abrogates

proliferation of adult but not embryonic neural stem cells. Development *131*, 4059-4070.

Fu, A.K., Hung, K.W., Fu, W.Y., Shen, C., Chen, Y., Xia, J., Lai, K.O., and Ip, N.Y. (2011). APC(Cdh1) mediates EphA4-dependent downregulation of AMPA receptors in homeostatic plasticity. Nat Neurosci *14*, 181-189.

Garcia-Higuera, I., Manchado, E., Dubus, P., Canamero, M., Mendez, J., Moreno, S., and Malumbres, M. (2008). Genomic stability and tumour suppression by the APC/C cofactor Cdh1. Nat Cell Biol *10*, 802-811.

Gieffers, C., Peters, B.H., Kramer, E.R., Dotti, C.G., and Peters, J.M. (1999). Expression of the CDH1-associated form of the anaphase-promoting complex in postmitotic neurons. Proc Natl Acad Sci U S A *96*, 11317-11322.

Glotzer, M., Murray, A.W., and Kirschner, M.W. (1991). Cyclin is degraded by the ubiquitin pathway. Nature *349*, 132-138.

Gordon, D.M., and Roof, D.M. (2001). Degradation of the kinesin Kip1p at anaphase onset is mediated by the anaphase-promoting complex and Cdc20p. Proc Natl Acad Sci U S A *98*, 12515-12520.

Grondona, J.M., Perez-Martin, M., Cifuentes, M., Perez, J., Jimenez, A.J., Perez-Figares, J.M., and Fernandez-Llebrez, P. (1996). Ependymal denudation, aqueductal obliteration and hydrocephalus after a single injection of neuraminidase into the lateral ventricle of adult rats. J Neuropathol Exp Neurol *55*, 999-1008.

Haque, S.A., Hasaka, T.P., Brooks, A.D., Lobanov, P.V., and Baas, P.W. (2004). Monastrol, a prototype anti-cancer drug that inhibits a mitotic kinesin, induces rapid bursts of axonal outgrowth from cultured postmitotic neurons. Cell Motil Cytoskeleton *58*, 10-16.

Harper, J.W., Burton, J.L., and Solomon, M.J. (2002). The anaphase-promoting complex: it's not just for mitosis any more. Genes Dev *16*, 2179-2206.

Havens, C.G., Ho, A., Yoshioka, N., and Dowdy, S.F. (2006). Regulation of late G1/S phase transition and APC Cdh1 by reactive oxygen species. Mol Cell Biol *26*, 4701-4711.

Hayashi, S., Lewis, P., Pevny, L., and McMahon, A.P. (2002). Efficient gene modulation in mouse epiblast using a Sox2Cre transgenic mouse strain. Mech. Dev. *119 (suppl 1)*, S97–S101.

Heck, M.M., Hittelman, W.N., and Earnshaw, W.C. (1988). Differential expression of DNA topoisomerases I and II during the eukaryotic cell cycle. Proc Natl Acad Sci U S A *85*, 1086-1090.

Herrero-Mendez, A., Almeida, A., Fernandez, E., Maestre, C., Moncada, S., and Bolanos, J.P. (2009). The bioenergetic and antioxidant status of neurons is controlled by continuous degradation of a key glycolytic enzyme by APC/C-Cdh1. Nat Cell Biol *11*, 747-752.

Herzog, F., Primorac, I., Dube, P., Lenart, P., Sander, B., Mechtler, K., Stark, H., and Peters, J.M. (2009). Structure of the anaphase-promoting complex/cyclosome interacting with a mitotic checkpoint complex. Science *323*, 1477-1481.

Hildebrandt, E.R., and Hoyt, M.A. (2001). Cell cycle-dependent degradation of the Saccharomyces cerevisiae spindle motor Cin8p requires APC(Cdh1) and a bipartite destruction sequence. Mol Biol Cell *12*, 3402-3416.

Hong, K.U., Park, Y.S., Seong, Y.S., Kang, D., Bae, C.D., and Park, J. (2007). Functional importance of the anaphase-promoting complex-Cdh1-mediated degradation of TMAP/CKAP2 in regulation of spindle function and cytokinesis. Mol Cell Biol *27*, 3667-3681.

Huang, H.C., Shi, J., Orth, J.D., and Mitchison, T.J. (2009). Evidence that mitotic exit is a better cancer therapeutic target than spindle assembly. Cancer Cell *16*, 347-358.

Ikeuchi, Y., Stegmuller, J., Netherton, S., Huynh, M.A., Masu, M., Frank, D., Bonni, S., and Bonni, A. (2009). A SnoN-Ccd1 pathway promotes axonal morphogenesis in the mammalian brain. J Neurosci *29*, 4312-4321.

Irniger, S., and Nasmyth, K. (1997). The anaphase-promoting complex is required in G1 arrested yeast cells to inhibit B-type cyclin accumulation and to prevent uncontrolled entry into S-phase. J Cell Sci *110 (Pt 13)*, 1523-1531.

Ishizawa, J., Kuninaka, S., Sugihara, E., Naoe, H., Kobayashi, Y., Chiyoda, T., Ueki, A., Araki, K., Yamamura, K., Matsuzaki, Y., Nakajima, H., Ikeda, Y., Okamoto, S., and Saya, H. (2011). The cell cycle regulator Cdh1 controls the pool sizes of hematopoietic stem cells and mature lineage progenitors by protecting from genotoxic stress. Cancer Sci *102*, 967-974.

Jacks, T., Remington, L., Williams, B.O., Schmitt, E.M., Halachmi, S., Bronson, R.T., and Weinberg, R.A. (1994). Tumor spectrum analysis in p53-mutant mice. Curr Biol *4*, 1-7.

Jeng, J.C., Lin, Y.M., Lin, C.H., and Shih, H.M. (2009). Cdh1 controls the stability of TACC3. Cell Cycle *8*, 3529-3536.

Jensen, P.B., and Sehested, M. (1997). DNA topoisomerase II rescue by catalytic inhibitors: a new strategy to improve the antitumor selectivity of etoposide. Biochem Pharmacol *54*, 755-759.

Jimenez, A.J., Tome, M., Paez, P., Wagner, C., Rodriguez, S., Fernandez-Llebrez, P., Rodriguez, E.M., and Perez-Figares, J.M. (2001). A programmed ependymal denudation precedes congenital hydrocephalus in the hyh mutant mouse. J Neuropathol Exp Neurol *60*, 1105-1119.

Juang, Y.L., Huang, J., Peters, J.M., McLaughlin, M.E., Tai, C.Y., and Pellman, D. (1997). APC-mediated proteolysis of Ase1 and the morphogenesis of the mitotic spindle. Science *275*, 1311-1314.

Juo, P., and Kaplan, J.M. (2004). The anaphase-promoting complex regulates the abundance of GLR-1 glutamate receptors in the ventral nerve cord of C. elegans. Curr Biol *14*, 2057-2062.

Ke, P.Y., and Chang, Z.F. (2004). Mitotic degradation of human thymidine kinase 1 is dependent on the anaphase-promoting complex/cyclosome-CDH1-mediated pathway. Mol Cell Biol *24*, 514-526.

Ke, P.Y., Kuo, Y.Y., Hu, C.M., and Chang, Z.F. (2005). Control of dTTP pool size by anaphase promoting complex/cyclosome is essential for the maintenance of genetic stability. Genes Dev *19*, 1920-1933.

Keith, W.N., Douglas, F., Wishart, G.C., McCallum, H.M., George, W.D., Kaye, S.B., and Brown, R. (1993). Co-amplification of erbB2, topoisomerase II alpha and retinoic acid receptor alpha genes in breast cancer and allelic loss at topoisomerase I on chromosome 20. Eur J Cancer *29A*, 1469-1475.

Kim, A.H., Puram, S.V., Bilimoria, P.M., Ikeuchi, Y., Keough, S., Wong, M., Rowitch, D., and Bonni, A. (2009). A centrosomal Cdc20-APC pathway controls dendrite morphogenesis in postmitotic neurons. Cell *136*, 322-336.

Kim, S., and Yu, H. (2011). Mutual regulation between the spindle checkpoint and APC/C. Semin Cell Dev Biol *22*, 551-558.

Kimata, Y., Baxter, J.E., Fry, A.M., and Yamano, H. (2008). A role for the Fizzy/Cdc20 family of proteins in activation of the APC/C distinct from substrate recruitment. Mol Cell *32*, 576-583.

King, E.M., van der Sar, S.J., and Hardwick, K.G. (2007). Mad3 KEN boxes mediate both Cdc20 and Mad3 turnover, and are critical for the spindle checkpoint. PLoS One *2*, e342.

King, R.W., Glotzer, M., and Kirschner, M.W. (1996). Mutagenic analysis of the destruction signal of mitotic cyclins and structural characterization of ubiquitinated intermediates. Mol Biol Cell *7*, 1343-1357.

Kitamura, K., Maekawa, H., and Shimoda, C. (1998). Fission yeast Ste9, a homolog of Hct1/Cdh1 and Fizzy-related, is a novel negative regulator of cell cycle progression during G1-phase. Mol Biol Cell *9*, 1065-1080.

Konishi, Y., Stegmuller, J., Matsuda, T., Bonni, S., and Bonni, A. (2004). Cdh1-APC controls axonal growth and patterning in the mammalian brain. Science *303*, 1026-1030.

Kraft, C., Vodermaier, H.C., Maurer-Stroh, S., Eisenhaber, F., and Peters, J.M. (2005). The WD40 propeller domain of Cdh1 functions as a destruction box receptor for APC/C substrates. Mol Cell *18*, 543-553.

Kramer, E.R., Scheuringer, N., Podtelejnikov, A.V., Mann, M., and Peters, J.M. (2000). Mitotic regulation of the APC activator proteins CDC20 and CDH1. Mol Biol Cell *11*, 1555-1569.

Kuczera, T., Stilling, R.M., Hsia, H.E., Bahari-Javan, S., Irniger, S., Nasmyth, K., Sananbenesi, F., and Fischer, A. (2011). The anaphase promoting complex is required for memory function in mice. Learn Mem *18*, 49-57.

Labit, H., Fujimitsu, K., Bayin, N.S., Takaki, T., Gannon, J., and Yamano, H. (2012). Dephosphorylation of Cdc20 is required for its C-box-dependent activation of the APC/C. EMBO J *31*, 3351-3362.

Lasorella, A., Stegmuller, J., Guardavaccaro, D., Liu, G., Carro, M.S., Rothschild, G., de la Torre-Ubieta, L., Pagano, M., Bonni, A., and Iavarone, A. (2006). Degradation of Id2 by the anaphase-promoting complex couples cell cycle exit and axonal growth. Nature *442*, 471-474.

Lee, Y., Shull, E.R., Frappart, P.O., Katyal, S., Enriquez-Rios, V., Zhao, J., Russell, H.R., Brown, E.J., and McKinnon, P.J. (2012). ATR maintains select progenitors during nervous system development. EMBO J *31*, 1177-1189.

Lehman, N.L., Tibshirani, R., Hsu, J.Y., Natkunam, Y., Harris, B.T., West, R.B., Masek, M.A., Montgomery, K., van de Rijn, M., and Jackson, P.K. (2007). Oncogenic regulators and substrates of the anaphase promoting complex/cyclosome are frequently overexpressed in malignant tumors. Am J Pathol *170*, 1793-1805.

Li, M., Shin, Y.H., Hou, L., Huang, X., Wei, Z., Klann, E., and Zhang, P. (2008). The adaptor protein of the anaphase promoting complex Cdh1 is essential in maintaining replicative lifespan and in learning and memory. Nat Cell Biol *10*, 1083-1089.

Li, M., York, J.P., and Zhang, P. (2007a). Loss of Cdc20 causes a securin-dependent metaphase arrest in two-cell mouse embryos. Mol Cell Biol *27*, 3481-3488.

Li, W., Wu, G., and Wan, Y. (2007b). The dual effects of Cdh1/APC in myogenesis. FASEB J *21*, 3606-3617.

Lin, S., Liu, M., Son, Y.J., Timothy Himes, B., Snow, D.M., Yu, W., and Baas, P.W. (2011). Inhibition of Kinesin-5, a microtubule-based motor protein, as a strategy for enhancing regeneration of adult axons. Traffic *12*, 269-286.

Lindon, C., and Pines, J. (2004). Ordered proteolysis in anaphase inactivates Plk1 to contribute to proper mitotic exit in human cells. J Cell Biol *164*, 233-241.

Linka, R.M., Porter, A.C., Volkov, A., Mielke, C., Boege, F., and Christensen, M.O. (2007). C-terminal regions of topoisomerase IIalpha and IIbeta determine isoform-specific functioning of the enzymes in vivo. Nucleic Acids Res *35*, 3810-3822.

Listovsky, T., Oren, Y.S., Yudkovsky, Y., Mahbubani, H.M., Weiss, A.M., Lebendiker, M., and Brandeis, M. (2004). Mammalian Cdh1/Fzr mediates its own degradation. EMBO J *23*, 1619-1626.

Malumbres, M. (2011). Physiological relevance of cell cycle kinases. Physiol Rev *91*, 973-1007.

Malumbres, M., and Barbacid, M. (2001). To cycle or not to cycle: a critical decision in cancer. Nat Rev Cancer *1*, 222-231.

Malumbres, M., and Barbacid, M. (2009). Cell cycle, CDKs and cancer: a changing paradigm. Nat Rev Cancer *9*, 153-166.

Malumbres, M., Sotillo, R., Santamaria, D., Galan, J., Cerezo, A., Ortega, S., Dubus, P., and Barbacid, M. (2004). Mammalian cells cycle without the D-type cyclin-dependent kinases Cdk4 and Cdk6. Cell *118*, 493-504.

Malureanu, L.A., Jeganathan, K.B., Hamada, M., Wasilewski, L., Davenport, J., and van Deursen, J.M. (2009). BubR1 N terminus acts as a soluble inhibitor of cyclin B degradation by APC/C(Cdc20) in interphase. Dev Cell *16*, 118-131.

Manchado, E., Eguren, M., and Malumbres, M. (2010a). The anaphase-promoting complex/cyclosome (APC/C): cell-cycle-dependent and -independent functions. Biochem Soc Trans *38*, 65-71.

Manchado, E., Guillamot, M., de Carcer, G., Eguren, M., Trickey, M., Garcia-Higuera, I., Moreno, S., Yamano, H., Canamero, M., and Malumbres, M. (2010b). Targeting mitotic exit leads to tumor regression in vivo: Modulation by Cdk1, Mastl, and the PP2A/B55alpha,delta phosphatase. Cancer Cell *18*, 641-654.

Manchado, E., Guillamot, M., and Malumbres, M. (2012). Killing cells by targeting mitosis. Cell Death Differ *19*, 369-377.

Matsumoto, A., Susaki, E., Onoyama, I., Nakayama, K., Hoshino, M., and Nakayama, K.I. (2011). Deregulation of the p57-E2F1-p53 axis results in nonobstructive hydrocephalus and cerebellar malformation in mice. Mol Cell Biol *31*, 4176-4192.

Mayer, T.U., Kapoor, T.M., Haggarty, S.J., King, R.W., Schreiber, S.L., and Mitchison, T.J. (1999). Small molecule inhibitor of mitotic spindle bipolarity identified in a phenotype-based screen. Science *286*, 971-974.

McGarry, T.J., and Kirschner, M.W. (1998). Geminin, an inhibitor of DNA replication, is degraded during mitosis. Cell *93*, 1043-1053.

Miller, J.J., Summers, M.K., Hansen, D.V., Nachury, M.V., Lehman, N.L., Loktev, A., and Jackson, P.K. (2006). Emi1 stably binds and inhibits the anaphase-promoting complex/cyclosome as a pseudosubstrate inhibitor. Genes Dev *20*, 2410-2420.

Mirzadeh, Z., Merkle, F.T., Soriano-Navarro, M., Garcia-Verdugo, J.M., and Alvarez-Buylla, A. (2008). Neural stem cells confer unique pinwheel architecture to the ventricular surface in neurogenic regions of the adult brain. Cell Stem Cell *3*, 265-278.

Mo, Y.Y., and Beck, W.T. (1999). Association of human DNA topoisomerase IIalpha with mitotic chromosomes in mammalian cells is independent of its catalytic activity. Exp Cell Res *252*, 50-62.

Morrens, J., Van Den Broeck, W., and Kempermann, G. (2012). Glial cells in adult neurogenesis. Glia *60*, 159-174.

Murga, M., Bunting, S., Montana, M.F., Soria, R., Mulero, F., Canamero, M., Lee, Y., McKinnon, P.J., Nussenzweig, A., and Fernandez-Capetillo, O. (2009). A mouse model of ATR-Seckel shows embryonic replicative stress and accelerated aging. Nat Genet *41*, 891-898.

Murray, A.W., Solomon, M.J., and Kirschner, M.W. (1989). The role of cyclin synthesis and degradation in the control of maturation promoting factor activity. Nature *339*, 280-286.

Musacchio, A., and Salmon, E.D. (2007). The spindle-assembly checkpoint in space and time. Nat Rev Mol Cell Biol *8*, 379-393.

Myers, K.A., and Baas, P.W. (2007). Kinesin-5 regulates the growth of the axon by acting as a brake on its microtubule array. J Cell Biol *178*, 1081-1091.

Nadar, V.C., Ketschek, A., Myers, K.A., Gallo, G., and Baas, P.W. (2008). Kinesin-5 is essential for growth-cone turning. Curr Biol *18*, 1972-1977.

Narbonne-Reveau, K., Senger, S., Pal, M., Herr, A., Richardson, H.E., Asano, M., Deak, P., and Lilly, M.A. (2008). APC/CFzr/Cdh1 promotes cell cycle progression during the Drosophila endocycle. Development *135*, 1451-1461.

Nitiss, J.L. (2009). Targeting DNA topoisomerase II in cancer chemotherapy. Nat Rev Cancer *9*, 338-350.

Olsen, J.V., de Godoy, L.M., Li, G., Macek, B., Mortensen, P., Pesch, R., Makarov, A., Lange, O., Horning, S., and Mann, M. (2005). Parts per million mass accuracy on an Orbitrap mass spectrometer via lock mass injection into a C-trap. Mol Cell Proteomics *4*, 2010-2021.

Ong, S.E., Blagoev, B., Kratchmarova, I., Kristensen, D.B., Steen, H., Pandey, A., and Mann, M. (2002). Stable isotope labeling by amino acids in cell culture, SILAC, as a simple and accurate approach to expression proteomics. Mol Cell Proteomics *1*, 376-386.

Ostapenko, D., Burton, J.L., and Solomon, M.J. (2012). Identification of anaphase promoting complex substrates in S. cerevisiae. PLoS One *7*, e45895.

Ostergaard, P., Simpson, M.A., Mendola, A., Vasudevan, P., Connell, F.C., van Impel, A., Moore, A.T., Loeys, B.L., Ghalamkarpour, A., Onoufriadis, A., Martinez-Corral, I., Devery, S., Leroy, J.G., van Laer, L., Singer, A., Bialer, M.G., McEntagart, M., Quarrell, O., Brice, G., Trembath, R.C., Schulte-Merker, S., Makinen, T., Vikkula, M., Mortimer, P.S., Mansour, S., and Jeffery, S. (2012). Mutations in KIF11 cause autosomal-dominant microcephaly variably associated with congenital lymphedema and chorioretinopathy. Am J Hum Genet *90*, 356-362.

Passmore, L.A., McCormack, E.A., Au, S.W., Paul, A., Willison, K.R., Harper, J.W., and Barford, D. (2003). Doc1 mediates the activity of the anaphase-promoting complex by contributing to substrate recognition. EMBO J *22*, 786-796.

Pastrana, E., Silva-Vargas, V., and Doetsch, F. (2011). Eyes wide open: a critical review of sphere-formation as an assay for stem cells. Cell Stem Cell *8*, 486-498.

Perez de Castro, I., de Carcer, G., and Malumbres, M. (2007). A census of mitotic cancer genes: new insights into tumor cell biology and cancer therapy. Carcinogenesis *28*, 899-912.

Perkins, D.N., Pappin, D.J., Creasy, D.M., and Cottrell, J.S. (1999). Probability-based protein identification by searching sequence databases using mass spectrometry data. Electrophoresis *20*, 3551-3567.

Peters, J.M. (2006). The anaphase promoting complex/cyclosome: a machine designed to destroy. Nat Rev Mol Cell Biol *7*, 644-656.

Pfleger, C.M., and Kirschner, M.W. (2000). The KEN box: an APC recognition signal distinct from the D box targeted by Cdh1. Genes Dev *14*, 655-665.

Rape, M., and Kirschner, M.W. (2004). Autonomous regulation of the anaphase-promoting complex couples mitosis to S-phase entry. Nature *432*, 588-595.

Reaper, P.M., Griffiths, M.R., Long, J.M., Charrier, J.D., Maccormick, S., Charlton, P.A., Golec, J.M., and Pollard, J.R. (2011). Selective killing of ATM- or p53-deficient cancer cells through inhibition of ATR. Nat Chem Biol *7*, 428-430.

Reimann, J.D., Gardner, B.E., Margottin-Goguet, F., and Jackson, P.K. (2001). Emi1 regulates the anaphase-promoting complex by a different mechanism than Mad2 proteins. Genes Dev *15*, 3278-3285.

Ross, P.L., Huang, Y.N., Marchese, J.N., Williamson, B., Parker, K., Hattan, S., Khainovski, N., Pillai, S., Dey, S., Daniels, S., Purkayastha, S., Juhasz, P., Martin, S., Bartlet-Jones, M., He, F., Jacobson, A., and Pappin, D.J. (2004). Multiplexed protein quantitation in Saccharomyces cerevisiae using amine-reactive isobaric tagging reagents. Mol Cell Proteomics *3*, 1154-1169.

Ruzankina, Y., Schoppy, D.W., Asare, A., Clark, C.E., Vonderheide, R.H., and Brown, E.J. (2009). Tissue regenerative delays and synthetic lethality in adult mice after combined deletion of Atr and Trp53. Nat Genet *41*, 1144-1149.

Saijo, T., Ishii, G., Ochiai, A., Yoh, K., Goto, K., Nagai, K., Kato, H., Nishiwaki, Y., and Saijo, N. (2006). Eg5 expression is closely correlated with the response of advanced non-small cell lung cancer to antimitotic agents combined with platinum chemotherapy. Lung Cancer *54*, 217-225.

Schaeffer, V., Althauser, C., Shcherbata, H.R., Deng, W.M., and Ruohola-Baker, H. (2004). Notch-dependent Fizzy-related/Hec1/Cdh1 expression is required for the mitotic-to-endocycle transition in Drosophila follicle cells. Curr Biol *14*, 630-636.

Schoeffler, A.J., and Berger, J.M. (2005). Recent advances in understanding structure-function relationships in the type II topoisomerase mechanism. Biochem Soc Trans *33*, 1465-1470.

Schreiber, A., Stengel, F., Zhang, Z., Enchev, R.I., Kong, E.H., Morris, E.P., Robinson, C.V., da Fonseca, P.C., and Barford, D. (2011). Structural basis for the subunit assembly of the anaphase-promoting complex. Nature *470*, 227-232.

Schwab, M., Lutum, A.S., and Seufert, W. (1997). Yeast Hct1 is a regulator of Clb2 cyclin proteolysis. Cell *90*, 683-693.

Sczaniecka, M., Feoktistova, A., May, K.M., Chen, J.S., Blyth, J., Gould, K.L., and Hardwick, K.G. (2008). The spindle checkpoint functions of Mad3 and Mad2 depend on a Mad3 KEN box-mediated interaction with Cdc20-anaphase-promoting complex (APC/C). J Biol Chem *283*, 23039-23047.

Seki, A., and Fang, G. (2007). CKAP2 is a spindle-associated protein degraded by APC/C-Cdh1 during mitotic exit. J Biol Chem *282*, 15103-15113.

Shcherbata, H.R., Althauser, C., Findley, S.D., and Ruohola-Baker, H. (2004). The mitotic-to-endocycle switch in Drosophila follicle cells is executed by Notch-dependent regulation of G1/S, G2/M and M/G1 cell-cycle transitions. Development *131*, 3169-3181.

Sherley, J.L., and Kelly, T.J. (1988). Regulation of human thymidine kinase during the cell cycle. J Biol Chem *263*, 8350-8358.

Shevchenko, A., Tomas, H., Havlis, J., Olsen, J.V., and Mann, M. (2006). In-gel digestion for mass spectrometric characterization of proteins and proteomes. Nat Protoc *1*, 2856-2860.

Shirayama, M., Zachariae, W., Ciosk, R., and Nasmyth, K. (1998). The Polo-like kinase Cdc5p and the WD-repeat protein Cdc20p/fizzy are regulators and substrates of the anaphase promoting complex in Saccharomyces cerevisiae. EMBO J *17*, 1336-1349.

Sigl, R., Wandke, C., Rauch, V., Kirk, J., Hunt, T., and Geley, S. (2009). Loss of the mammalian APC/C activator FZR1 shortens G1 and lengthens S phase but has little effect on exit from mitosis. J Cell Sci *122*, 4208-4217.

Sigrist, S.J., and Lehner, C.F. (1997). Drosophila fizzy-related down-regulates mitotic cyclins and is required for cell proliferation arrest and entry into endocycles. Cell *90*, 671-681.

Skaar, J.R., and Pagano, M. (2009). Control of cell growth by the SCF and APC/C ubiquitin ligases. Curr Opin Cell Biol *21*, 816-824.

Smith, K., Houlbrook, S., Greenall, M., Carmichael, J., and Harris, A.L. (1993). Topoisomerase II alpha co-amplification with erbB2 in human primary breast cancer and breast cancer cell lines: relationship to m-AMSA and mitoxantrone sensitivity. Oncogene *8*, 933-938.

Spassky, N., Merkle, F.T., Flames, N., Tramontin, A.D., Garcia-Verdugo, J.M., and Alvarez-Buylla, A. (2005). Adult ependymal cells are postmitotic and are derived from radial glial cells during embryogenesis. J Neurosci *25*, 10-18.

Srinivas, S., Watanabe, T., Lin, C.S., William, C.M., Tanabe, Y., Jessell, T.M., and Costantini, F. (2001). Cre reporter strains produced by targeted insertion of EYFP and ECFP into the ROSA26 locus. BMC Dev Biol *1*, 4.

Stegmuller, J., Huynh, M.A., Yuan, Z., Konishi, Y., and Bonni, A. (2008). TGFbeta-Smad2 signaling regulates the Cdh1-APC/SnoN pathway of axonal morphogenesis. J Neurosci *28*, 1961-1969.

Stegmuller, J., Konishi, Y., Huynh, M.A., Yuan, Z., Dibacco, S., and Bonni, A. (2006). Cell-intrinsic regulation of axonal morphogenesis by the Cdh1-APC target SnoN. Neuron *50*, 389-400.

Stroschein, S.L., Bonni, S., Wrana, J.L., and Luo, K. (2001). Smad3 recruits the anaphase-promoting complex for ubiquitination and degradation of SnoN. Genes Dev *15*, 2822-2836.

Tavormina, P.A., Come, M.G., Hudson, J.R., Mo, Y.Y., Beck, W.T., and Gorbsky, G.J. (2002). Rapid exchange of mammalian topoisomerase II alpha at kinetochores and chromosome arms in mitosis. J Cell Biol *158*, 23-29.

Thornton, B.R., and Toczyski, D.P. (2006). Precise destruction: an emerging picture of the APC. Genes Dev *20*, 3069-3078.

Tiwari, V.K., Burger, L., Nikoletopoulou, V., Deogracias, R., Thakurela, S., Wirbelauer, C., Kaut, J., Terranova, R., Hoerner, L., Mielke, C., Boege, F., Murr, R., Peters, A.H., Barde, Y.A., and Schubeler, D. (2012). Target genes of Topoisomerase IIbeta regulate neuronal survival and are defined by their chromatin state. Proc Natl Acad Sci U S A *109*, E934-943.

Trickey, M., Fujimitsu, K., and Yamano, H. (2013). Anaphase-promoting complex/cyclosome-mediated proteolysis of Ams2 in the G1 phase ensures the coupling of histone gene expression to DNA replication in fission yeast. J Biol Chem *288*, 928-937.

Tronche, F., Kellendonk, C., Kretz, O., Gass, P., Anlag, K., Orban, P.C., Bock, R., Klein, R., and Schutz, G. (1999). Disruption of the glucocorticoid receptor gene in the nervous system results in reduced anxiety. Nat Genet *23*, 99-103.

Tsutsui, K., Sano, K., Kikuchi, A., and Tokunaga, A. (2001). Involvement of DNA topoisomerase IIbeta in neuronal differentiation. J Biol Chem *276*, 5769-5778.

Ullah, Z., Kohn, M.J., Yagi, R., Vassilev, L.T., and DePamphilis, M.L. (2008). Differentiation of trophoblast stem cells into giant cells is triggered by p57/Kip2 inhibition of CDK1 activity. Genes Dev *22*, 3024-3036.

Van Hooser, A., Goodrich, D.W., Allis, C.D., Brinkley, B.R., and Mancini, M.A. (1998). Histone H3 phosphorylation is required for the initiation, but not maintenance, of mammalian chromosome condensation. J Cell Sci *111 (Pt 23)*, 3497-3506.

van Roessel, P., Elliott, D.A., Robinson, I.M., Prokop, A., and Brand, A.H. (2004). Independent regulation of synaptic size and activity by the anaphase-promoting complex. Cell *119*, 707-718.

Visintin, R., Prinz, S., and Amon, A. (1997). CDC20 and CDH1: a family of substrate-specific activators of APC-dependent proteolysis. Science *278*, 460-463.

Wan, Y., Liu, X., and Kirschner, M.W. (2001). The anaphase-promoting complex mediates TGF-beta signaling by targeting SnoN for destruction. Mol Cell *8*, 1027-1039.

Wang, J.C. (2002). Cellular roles of DNA topoisomerases: a molecular perspective. Nat Rev Mol Cell Biol *3*, 430-440.

Wasch, R., and Cross, F.R. (2002). APC-dependent proteolysis of the mitotic cyclin Clb2 is essential for mitotic exit. Nature *418*, 556-562.

Wasch, R., and Engelbert, D. (2005). Anaphase-promoting complex-dependent proteolysis of cell cycle regulators and genomic instability of cancer cells. Oncogene *24*, 1-10.

Watanabe, M., Tsutsui, K., and Inoue, Y. (1994). Differential expressions of the topoisomerase II alpha and II beta mRNAs in developing rat brain. Neurosci Res *19*, 51-57.

Wei, W., Ayad, N.G., Wan, Y., Zhang, G.J., Kirschner, M.W., and Kaelin, W.G., Jr. (2004). Degradation of the SCF component Skp2 in cell-cycle phase G1 by the anaphase-promoting complex. Nature *428*, 194-198.

Williamson, A., Wickliffe, K.E., Mellone, B.G., Song, L., Karpen, G.H., and Rape, M. (2009). Identification of a physiological E2 module for the human anaphase-promoting complex. Proc Natl Acad Sci U S A *106*, 18213-18218.

Wirth, K.G., Ricci, R., Gimenez-Abian, J.F., Taghybeeglu, S., Kudo, N.R., Jochum, W., Vasseur-Cognet, M., and Nasmyth, K. (2004). Loss of the anaphase-promoting complex in quiescent cells causes unscheduled hepatocyte proliferation. Genes Dev *18*, 88-98.

Wisniewski, J.R., Zougman, A., Nagaraj, N., and Mann, M. (2009). Universal sample preparation method for proteome analysis. Nat Methods *6*, 359-362.

Wohlschlegel, J.A., Dwyer, B.T., Dhar, S.K., Cvetic, C., Walter, J.C., and Dutta, A. (2000). Inhibition of eukaryotic DNA replication by geminin binding to Cdt1. Science *290*, 2309-2312.

Woodbury, E.L., and Morgan, D.O. (2007). Cdk and APC activities limit the spindle-stabilizing function of Fin1 to anaphase. Nat Cell Biol *9*, 106-112.

Wu, G., Glickstein, S., Liu, W., Fujita, T., Li, W., Yang, Q., Duvoisin, R., and Wan, Y. (2007). The anaphase-promoting complex coordinates initiation of lens differentiation. Mol Biol Cell *18*, 1018-1029.

Yamaguchi, S., Murakami, H., and Okayama, H. (1997). A WD repeat protein controls the cell cycle and differentiation by negatively regulating Cdc2/B-type cyclin complexes. Mol Biol Cell *8*, 2475-2486.

Yamano, H., Gannon, J., and Hunt, T. (1996). The role of proteolysis in cell cycle progression in Schizosaccharomyces pombe. EMBO J *15*, 5268-5279.

Yang, Y., Kim, A.H., Yamada, T., Wu, B., Bilimoria, P.M., Ikeuchi, Y., de la Iglesia, N., Shen, J., and Bonni, A. (2009). A Cdc20-APC ubiquitin signaling pathway regulates presynaptic differentiation. Science *326*, 575-578.

Yu, H. (2007). Cdc20: a WD40 activator for a cell cycle degradation machine. Mol Cell *27*, 3-16.

Zachariae, W., Schwab, M., Nasmyth, K., and Seufert, W. (1998). Control of cyclin ubiquitination by CDK-regulated binding of Hct1 to the anaphase promoting complex. Science *282*, 1721-1724.

Zeng, X., and King, R.W. (2012). An APC/C inhibitor stabilizes cyclin B1 by prematurely terminating ubiquitination. Nat Chem Biol *8*, 383-392.

Zeng, X., Sigoillot, F., Gaur, S., Choi, S., Pfaff, K.L., Oh, D.C., Hathaway, N., Dimova, N., Cuny, G.D., and King, R.W. (2010). Pharmacologic inhibition of the anaphase-promoting complex induces a spindle checkpoint-dependent mitotic arrest in the absence of spindle damage. Cancer Cell *18*, 382-395.

Zhao, W.M., and Fang, G. (2005). Anillin is a substrate of anaphase-promoting complex/cyclosome (APC/C) that controls spatial contractility of myosin during late cytokinesis. J Biol Chem *280*, 33516-33524.

Zielke, N., Querings, S., Rottig, C., Lehner, C., and Sprenger, F. (2008). The anaphase-promoting complex/cyclosome (APC/C) is required for rereplication control in endoreplication cycles. Genes Dev *22*, 1690-1703.